ISTITUTO NAZIONALE DI FISICA NUCLEARE
Laboratori Nazionali di Frascati

FRASCATI PHYSICS SERIES

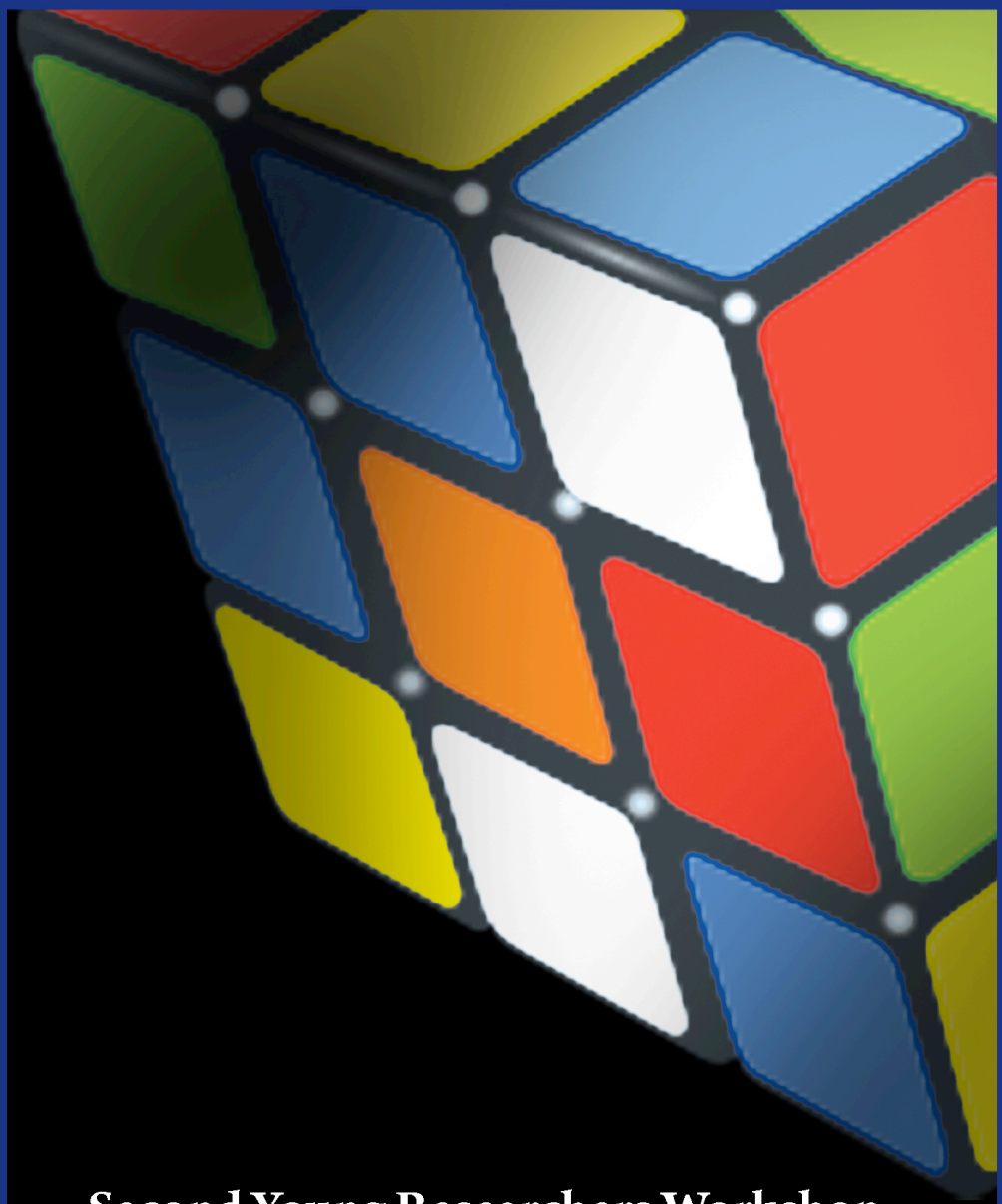

# Second Young Researchers Workshop
# "Physics Challenges in the LHC Era"
# 2010

Editor:
Enrico Nardi

# Second Young Researchers Workshop
# "Physics Challenges in the LHC Era"
# 2010

# FRASCATI PHYSICS SERIES

Series Editor
*Danilo Babusci*

Technical Editor
*Luigina Invidia*

*Cover by Claudio Federici*

Volume LI

*Istituto Nazionale di Fisica Nucleare – Laboratori Nazionali di Frascati*
*Divisione Ricerca*
*SIDS – Servizio Informazione e Documentazione Scientifica*
*Ufficio Biblioteca e Pubblicazioni*
*P.O. Box 13, I–00044 Frascati Roma Italy*
*email: sis.publications@lnf.infn.it*

FRASCATI PHYSICS SERIES

**Second Young Researchers Workshop**
**"Physics Challenges in the LHC Era"**
**2010**



ISBN 978–88–86409–60–5

FRASCATI PHYSICS SERIES

Volume LI

# Second Young Researchers Workshop "Physics Challenges in the LHC Era" 2010

Editor
*Enrico Nardi*

Frascati, May 10th and May 13th, 2010

*International Advisory Committee*

| | |
|---|---|
| G. Altarelli | *Università Roma Tre* |
| W. Buchmuller | *DESY* |
| F. Ceradini | *Università Roma Tre* |
| A. Di Ciaccio | *Università Roma Tor Vergata* |
| J. Ellis | *CERN* |
| B. Grinstein | *University of California San Diego* |
| R. Fiore | *Università della Calabria* |

*Local Organizing Committee*

| | |
|---|---|
| M. Antonelli | *INFN Frascati,* |
| D. Aristizabal | *INFN Frascati & Université de Liège* |
| O. Cata | *INFN Frascati* |
| V. Del Duca | *INFN Frascati* |
| R. Faccini | *Università Roma La Sapienza & INFN Roma* |
| G. Isidori | *INFN Frascati* |
| J. F. Kamenik | *INFN Frascati & JSI* |
| E. Nardi | *INFN Frascati (School Director)* |
| M. Palutan | *INFN Frascati* |
| T. Spadaro | *INFN Frascati* |

## PREFACE

The second Young Researcher Workshop “Physics Challenges in the LHC Era” was held in the Frascati Laboratories during May $10^{th}$ and $13^{th}$ 2010, in conjunction with the 15th edition of the Frascati Spring School ”Bruno Touschek”.

The Frascati Young Researcher Workshop provides an opportunity for the students attending the Spring School to complement the scientific program by giving short lectures to their colleagues on their specific research topics. The Workshop also constitutes an important step in the scientific formation of our students: they learn how to organize a presentation on a specialistic subject that should be understandable for a general audience of young physicists in the training stage, and how to condense the results of their work within a fifteen minutes talk. They get a training in preparing a write up of their speech for the Workshop Proceedings, and they also experience how to interact with the Scientific Editor and with the Editorial Office of the Frascati Physics Series. Eventually, they also learn how to prepare a submission of their preprint to the arXive database. Helping to develop these skills is an integral part of the scientific formation the Frascati Spring School is aiming to.

The second edition of the Young Researcher Workshop confirmed the success of the first edition. We received a number of applications larger than what could be allotted within the two afternoons of the Workshop, and regrettedly we could not satisfy all the requests to give a talk. The resulting scientific program of the workshop was rich and quite interesting, covering a large variety of actual topics both in theoretical and experimental particle physics.

These proceedings, that collect the joint efforts of the speakers of the Young Researchers Workshop, testify the remarkably high professional level of all the contributions, and give a benchmark for the scientific level required to participate in future editions of the Workshop. They can also provide useful guidelines for structuring the presentations of our future young lecturers.

Too many people contributed to the success of the Young Researcher Workshop "Physics Challenges in the LHC Era" and of the joint XV Frascati Spring

School "Bruno Touschek" to give here a complete list. However, a special acknowledgment must be given to the Workshop secretariat staff and backbones of the Frascati Spring School Maddalena Legramante, Silvia Colasanti and Angela Mantella. To Claudio Federici, that put a special effort in realizing the graphics of the Workshop and School posters, to Luigina Invidia for the technical editing of these proceedings, and to the Director of the Frascati Laboratories Mario Calvetti for his support.

Frascati, July 2010 Enrico Nardi

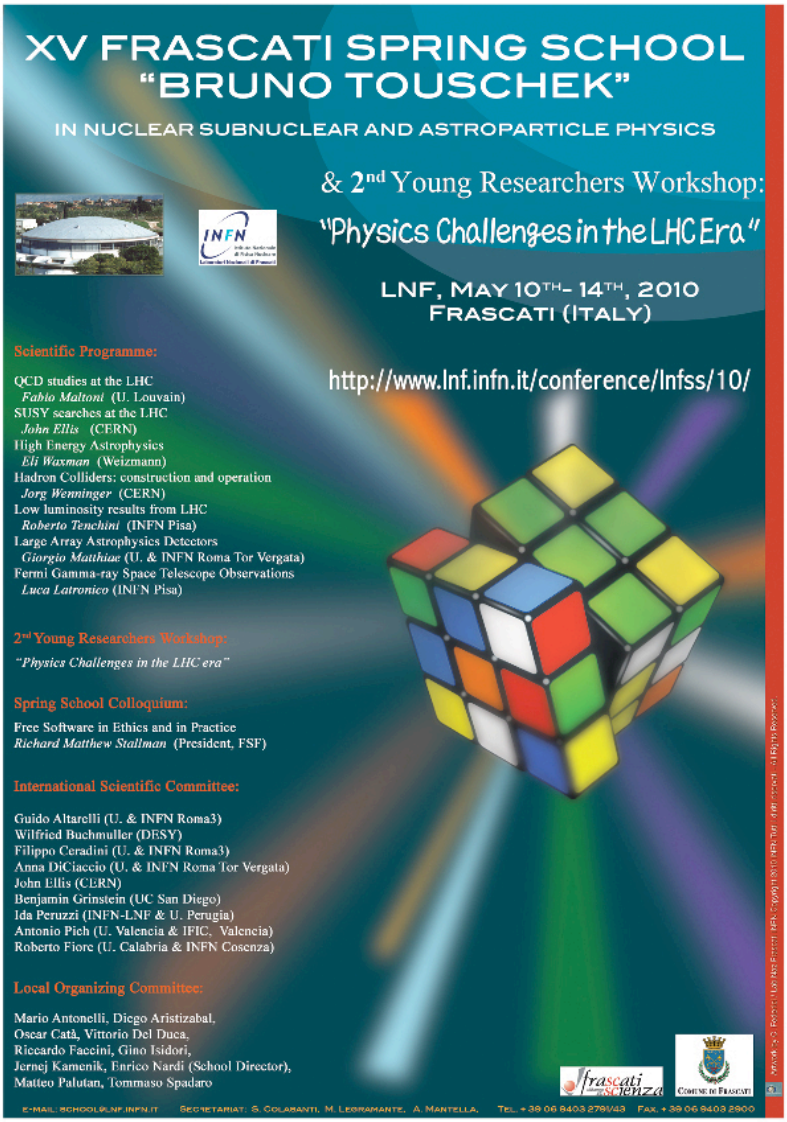


*Artwork by Claudio Federici*

**CONTENTS**

Frascati Physics Series Vol. LI (2010), pp. 1-6
2nd Young Researchers Workshop: Physics Challenges in the LHC Era
Frascati, May 10 and 13, 2010

# MINIMAL $Z'$ MODELS AND THE EARLY LHC

Ennio Salvioni
*Dipartimento di Fisica, Università di Padova and INFN, Sezione di Padova*
*Via Marzolo 8, I-35131 Padova, Italy*

**Abstract**

We consider a class of minimal extensions of the Standard Model with an extra massive neutral gauge boson $Z'$. They include both family-universal models, where the extra $U(1)$ is associated with $(B - L)$, and non-universal models where the $Z'$ is coupled to a non-trivial linear combination of $B$ and the lepton flavours. After giving an estimate of the range of parameters compatible with a Grand Unified Theory, we present the current experimental bounds, discussing the interplay between electroweak precision tests and direct searches at the Tevatron. Finally, we assess the discovery potential of the early LHC.

## 1 Introduction

Extra neutral gauge bosons, known in the literature as $Z'$, appear in many proposals for Beyond-the-Standard Model (BSM) physics; for a review, see for

instance [1]. Here we focus on *minimal* $Z'$, previously studied in [2], which stand out both for their simplicity, and because they could arise in several of the above mentioned BSM scenarios, such as, *e.g.*, Grand Unified Theories (GUTs) and string compactifications.

## 2 Theory

Following [3], we consider a minimal extension of the SM gauge group that includes an additional Abelian factor, labeled $U(1)_X$, commuting with $SU(3)_c \times SU(2)_L \times U(1)_Y$. The fermion content of the SM is augmented by one right-handed neutrino per family. We require anomaly cancellation, as this allows us to write a renormalizable Lagrangian. If family-universality is imposed, then the anomaly cancellation conditions yield a unique solution: $X = (B - L)$, where $B$ and $L$ are baryon and lepton number respectively [1]. However, if the requirement of family-universality is relaxed, it can be shown that the following set of family-dependent charges satisfy the anomaly cancellation conditions: $X = \sum_{a=e,\,\mu,\,\tau} (\lambda_a/3)(B - 3L_a)$ , where $L_a$ are the lepton flavours, and $\lambda_a$ are arbitrary coefficients. We will consider a specific example of such *non-universal* $Z'$ in the following.

In the basis of mass eigenstates for vectors, and with canonical kinetic terms, the neutral current Lagrangian reads

$$\mathcal{L}_{NC} = e J^{\mu}_{em} A_{\mu} + g_Z \left( Z_{\mu} J^{\mu}_{Z} + Z'_{\mu} J^{\mu}_{Z'} \right) , \tag{1}$$

where $A_\mu$ is the photon field coupled to the electromagnetic current, while $(Z_\mu,\, Z'_\mu)$ are the massive states, which couple to the currents $(J^\mu_Z,\, J^\mu_{Z'})$ respectively, obtained from $J^\mu_{Z^0} = \sum_f \left[ T_{3L}(f) - \sin^2\theta_W\, Q(f) \right] \overline{f} \gamma^\mu f$ and $J^\mu_{Z'^0} = \sum_f \left[ g_Y\, Y(f) + g_X\, X(f) \right] \overline{f} \gamma^\mu f$ via a rotation of the $Z - Z'$ mixing angle $\theta'$. The explicit expression of the latter reads $\tan\theta' = -(g_Y/g_Z)\, M^2_{Z^0}/(M^2_{Z'} - M^2_{Z^0})$. Thus, under our minimal assumptions, only three parameters beyond the SM ones are sufficient to describe the $Z'$ phenomenology: the physical mass of the extra vector, $M_{Z'}$, and the two coupling constants $(g_Y, g_X)$. In the following discussion, we normalize these couplings to the SM $Z^0$ coupling, namely $\widetilde{g}_{Y,X} = g_{Y,X}/g_Z$.

[1] The most general solution to the anomaly cancellation conditions is $X = a\, Y + b\, (B - L)$, with $a$, $b$ arbitrary coefficients. However, the $Y$ component can be absorbed in the kinetic mixing in the class of models we consider.

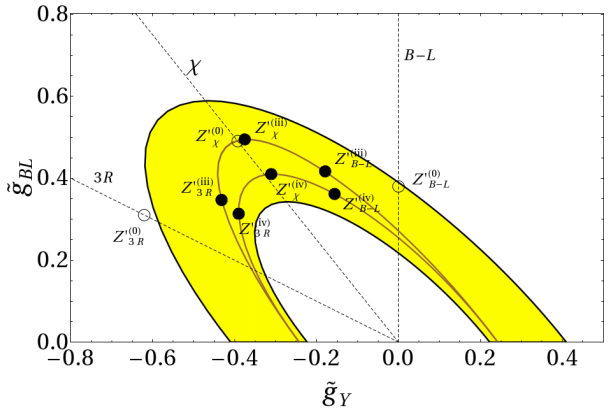


Figure 1: Estimate of the GUT-favoured region for the universal case, $X = (B-L)$. The yellow band represents the region of couplings compatible with a GUT, whereas dots and lines correspond to specific benchmark models or full supersymmetric GUT models, see [3] for details.

## 3 GUT-favoured region of parameters

Because GUTs are one of the motivations for considering minimal $Z'$, it is interesting to give an estimate of the constraints that a GUT would imply on the weak-scale couplings $(\widetilde{g}_Y, \widetilde{g}_X)$. For choosing the boundary conditions at unification scale $M_U$, we normalize all charges as in $SO(10)$, and take $M_U = 10^{16}$ GeV. We allow the $Z'$ coupling at unification scale to vary within the interval $1/100 < g^2_{Z'}(M_U)/(4\pi) < 1/20$, and using the RGE of the model we obtain the GUT-favoured region of weak-scale couplings, shown in fig.1 for the universal case $X = (B-L)$. Since the boundary conditions at scale $M_U$ are symmetric under the reflection $\widetilde{g}_Y \to -\widetilde{g}_Y$, it is evident from fig. 2 that mixing effects in the RGE (due to the non-orthogonality of the generators $Y$ and $(B-L)$) are important. The GUT-favoured regions for non-universal models, computed along similar lines, can be found in [3].

## 4 Bounds from present data

The measurements providing constraints on minimal $Z'$ can be divided into two classes: electroweak precision tests and direct searches at the Tevatron.

### 4.1 Electroweak precision tests

Measurements performed at LEP1 and at low energy mainly constrain $Z - Z'$ mixing, whereas data collected at LEP2 (above the $Z$ pole) constrain effective four-fermion operators. To compute the bounds from EWPT on minimal $Z'$, we integrate out the heavy vector and use the effective Lagrangian thus obtained to perform a global fit to the data. The results are shown in fig. 1, for the universal '$\chi$ model', corresponding to a particular direction in the $(\widetilde{g}_Y, \widetilde{g}_X)$ plane often considered in the literature.

### 4.2 Tevatron direct searches

The CDF and D0 collaborations have derived, from the non-observation of discrepancies with the SM expectations, upper limits on $\sigma(\overline{p}p \to Z') \times Br(Z' \to \ell^+\ell^-)$ $(\ell = e, \mu)$, [4]. To extract bounds on minimal $Z'$, we compute the same quantity at NLO in QCD, and compare it with the limits published by the experimental collaborations. The comparison between bounds from EWPT and from the Tevatron is most clear if we plot them in (coupling *vs.* mass), for a chosen direction in the $(\widetilde{g}_Y, \widetilde{g}_{BL})$ plane, as it is done in fig. 2 for the $\chi$ model. We see that bounds from EWPT have a linear behaviour, because all the effects due to the $Z'$ in the low-energy effective Lagrangian depend on the ratio $g_{Z'}/M_{Z'}$, whereas bounds from the Tevatron become negligible above a kinematic limit, which is of the order of 1 TeV. Thus for low masses the Tevatron data give the strongest limits, while above a certain value of $M_{Z'}$ (which is of the order of 500 GeV for the $\chi$ model), bounds from EWPT are stronger. In particular, for models compatible with GUTs the strongest bounds are those given by EWPT.

## 5 Early LHC reach

The present schedule foresees that in 2010/2011 the LHC will run at 7 TeV in the center of mass, collecting up to 1 fb$^{-1}$ of integrated luminosity $L$. Therefore, it is interesting to ask whether there are any minimal $Z'$ which are both allowed by present constraints and accessible for discovery in such early phase. To answer this question, we have performed a NLO analysis similar to the one used in extracting bounds from Tevatron data, requiring the $Z'$ signal to be at least a $5\sigma$ fluctuation over the SM-Drell Yan background. The results are

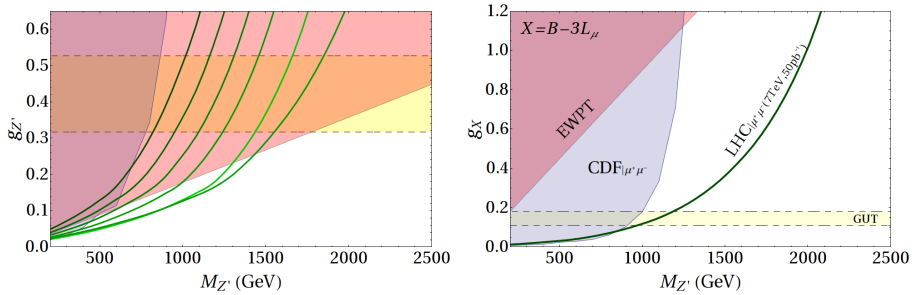


Figure 2: (left) Comparison of bounds from EWPT (red), Tevatron (blue), and discovery reach of the early LHC (green curves, from left to right: 50, 100, 200, 400 and 1000 pb$^{-1}$ at 7 TeV, and 400 pb$^{-1}$ at 10 TeV) for the $\chi$ model. (right) Present bounds and discovery prospects of the LHC at 7 TeV and 50 pb$^{-1}$ for the *muonphilic* model with $\widetilde{g}_Y = 0$. For $g_X > 0.3$, both the bounds from the Tevatron and the LHC reach are indeed weaker, because of finite-width effects not included in the figure, but the general message is unaffected. The yellow bands correspond to the GUT-favored region, see Section 3.

displayed for the $\chi$ model in fig. 2, where a comparison with present bounds is made. We see that for $L \sim 100$ pb$^{-1}$ (the luminosity approximately foreseen at the end of 2010), no discovery is possible. On the other hand, for $L \sim 1$ fb$^{-1}$ some unexplored regions become accessible; however, $Z'$ compatible with GUTs are still out of reach, and more energy and luminosity will be needed to test them.

### 5.1 The *muonphilic* model

We have seen that universal models are strongly constrained by present data. On the other hand, when we consider non-universal couplings to leptons, the bounds can be significantly altered. In particular, let us consider the case where $X = B - 3L_\mu$, which we called 'muonphilic $Z'$'. Let us further assume that kinetic mixing is negligible, *i.e.* $\widetilde{g}_Y \approx 0$. In this case, the $Z'$ has no coupling to the first and third leptonic families, in particular it has no coupling to the electron. As a consequence, bounds from EWPT are strongly relaxed, the only surviving constraints coming from $(g-2)_\mu$ and $\nu$-$N$ scattering (NuTeV). On the other hand, the Tevatron reach is limited, as already noted in Section 4, to $M_{Z'} \leq 1$ TeV: therefore the LHC has access to a wide region of unexplored

parameter space already with a very low integrated luminosity at 7 TeV, as shown in fig. 2.

## 6 Summary

We have discussed the present experimental bounds and the early LHC reach on minimal $Z'$ models, showing that present constraints cannot be neglected when assessing the discovery potential of the early LHC. In particular, we have found that exploration of universal models, coupled to $(B - L)$, may need more energy and luminosity than those foreseen for 2010/2011, in particular for values of the couplings compatible with GUTs. On the other hand, some non-universal models which are weakly constrained by present data, such as the *muonphilic* $Z'$, could be discovered at the LHC with very low integrated luminosity.

## 7 Acknowledgements

I am indebted to my collaborators F. Zwirner, G. Villadoro, and A. Strumia. I would also like to thank the organizers of the $2^{nd}$ Young Researchers Workshop *Physics Challenges in the LHC Era* for giving me the possibility to present this work.

## References

1. P. Langacker, Rev. Mod. Phys. **81** (2008) 1199, arXiv:0801.1345 [hep-ph].
2. T. Appelquist, B. A. Dobrescu and A. R. Hopper, Phys. Rev. D **68** (2003) 035012, arXiv:hep-ph/0212073.
3. E. Salvioni, G. Villadoro and F. Zwirner, JHEP **0911** (2009) 068, arXiv:0909.1320 [hep-ph]; E. Salvioni, A. Strumia, G. Villadoro and F. Zwirner, JHEP **1003** (2010) 010, arXiv:0911.1450 [hep-ph].
4. T. Aaltonen *et al.* [CDF Collaboration], Phys. Rev. Lett. **102** (2009) 031801, arXiv:0810.2059 [hep-ex]; T. Aaltonen *et al.* [CDF Collaboration], Phys. Rev. Lett. **102** (2009) 091805, arXiv:0811.0053 [hep-ex]; [D0 collaboration], D0 note 5923-CONF (July 2009), http://www-d0.fnal.gov/Run2Physics/WWW/results/np.htm.

Frascati Physics Series Vol. LI (2010), pp. 7-12
2nd Young Researchers Workshop: Physics Challenges in the LHC Era
Frascati, May 10 and 13, 2010

# MODEL INDEPENDENT ANALYSIS OF FCNC TOP QUARK DECAYS

Jure Drobnak
*Jozef Stefan Institute, Jamova cesta 39, 1000 Ljubljana, Slovenia*

Svjetlana Fajfer and Jernej F. Kamenik
*Jozef Stefan Institute, Jamova cesta 39, 1000 Ljubljana, Slovenia*

**Abstract**

We study flavor changing neutral current decays of the top quark, $t \to cZ$ and $t \to c\gamma$. These decays are highly suppressed in the standard model. Numerous extensions of the standard model however, still allow significant enhancement of the branching ratios for such processes. Using model independent effective Lagrangian approach, we perform a full next-to-leading order QCD analysis and the impact it may have on the observability of such FCNC processes. We also study $t \to c\ell^+\ell^-$ decays and observables that could help to discriminate among variety of new physics scenarios.

## 1 Introduction

The standard model (SM) predicts highly suppressed flavour changing neutral current (FCNC) processes of the top quark ($t \to cV$, $V = Z, \gamma, g$) while new

physics beyond the SM (NP) in many cases lifts this suppression (for a recent review c.f. [1]).

Top quark FCNCs can be probed both in production and in decays. Present experimental upper bounds on branching ratios are at a precent level [2, 3, 4]. The LHC will be producing about $80,000$ $t\bar{t}$ events per day at the luminosity $L = 10^{33}\text{cm}^{-2}\text{s}^{-1}$ and will be able to access rare top decay branching ratios at the $10^{-5}$ level with $10\text{fb}^{-1}$ [5].

We present two of our recent works in treating FCNC top quark decay in a model independent way. First [6] is dedicated to the two-body final state decays, where we perform a full next-to-leading order (NLO) QCD analysis. We study operator renormalization effects as well as finite matrix element corrections. The second [7] is dedicated to the three-body final state decays $t \to c\ell^+\ell^-$ where the $Z$ boson or the virtual photon emerging from the FCNC vertex is considered to further decay into a lepton pair. Exploring this decay channel offers the advantage to consider more observables – in particular angular asymmetries among the final lepton and jet directions. Our goal is to discriminate different types of FCNC couplings.

## 2 Effective Lagrangian

In writing the effective top FCNC Lagrangian we follow roughly the notation of ref. [1, 8]. Hermitian conjugate and chirality flipped operators are implicitly contained in the Lagrangian

$$\mathcal{L}_{\text{eff}}^{tc} = \frac{v}{\Lambda^2} \sum_{V=g,\gamma,Z} b_{LR}^V \mathcal{O}_{LR}^V + \frac{v^2}{\Lambda^2} a_L^Z \mathcal{O}_L^Z + (L \leftrightarrow R) + \text{h.c.}\,, \tag{1}$$

where $\mathcal{O}_{LR,RL}^V = g_V V_{\mu\nu}^a \bar{q}_{L,R} T^a \sigma^{\mu\nu} t_{R,L}$, $\mathcal{O}_{L,R}^Z = g_Z Z_\mu \bar{q}_{L,R} \gamma^\mu t_{L,R}$, $q = c(u)$, $q_{R,L} = (1 \pm \gamma_5)q/2$, $\sigma_{\mu\nu} = i[\gamma_\mu, \gamma_\nu]/2$, $g_Z = 2e/\sin 2\theta_W$, $g_\gamma = e$, $g_g = \sqrt{\alpha_s 4\pi}$. Furthermore $V(A,Z)_{\mu\nu} = \partial_\mu V_\nu - \partial_\nu V_\mu$, $G_{\mu\nu}^a = \partial_\mu G_\nu^a - \partial_\nu G_\mu^a + g f_{abc} G_\mu^b G_\nu^c$, and $T^a$ are the Gell-Mann matrices in the case of the gluon and 1 for the $\gamma, Z$. Finally $v = 246$ GeV is the electroweak condensate and $\Lambda$ is the effective scale of NP. The lepton couplings to the $Z, \gamma$ bosons in the $t \to c\ell^+\ell^-$ analysis are considered to be SM-like.

## 3 NLO QCD corrections to $t \to cZ, \gamma$

### 3.1 Renormalization effects

QCD virtual corrections to effective operators in eq.(1) involve ultra violet (UV) divergencies. These are cancelled exactly in the matching procedure to the underlying NP theory. The remaining logarithmic dependence on the matching scale can be resumed using renormalization group (RG) methods. The effective couplings are evolved from the high scale $\Lambda$ down to the top quark mass scale $\mu_t$.

We investigate the values of $b^{\gamma,Z}$[1] at the top mass scale $\mu_t \simeq 200$ GeV induced solely by the mixing of the gluonic dipole contribution produced at the UV scale $\Lambda$. We find that for $\Lambda$ above 2 TeV these contributions are around 10% of $b^g(\Lambda)$ for $b^\gamma$, but much smaller (below 1 %) for $b^Z$.

### 3.2 Matrix element corrections

To consistently describe rare top decays at NLO in $\alpha_s$ one has to take into account finite QCD loop corrections evaluated at the top mass scale as well as single gluon bremsstrahlung corrections, which cancel the associated infrared divergencies in the decay rates. In ref. [9] we give these results in a complete analytical form. In the case of the photon we also investigate the influence of the experimentally motivated kinematical cuts on the photon energy $E_\gamma^{\rm cut}$ and the angle between the photon and the $c$-jet $\delta r = 1 - \mathbf{p}_\gamma \cdot \mathbf{p}_j / E_\gamma E_j$. We analyze the change of decay rates and branching ratios when going from leading order (LO) to NLO in QCD, where branching ratio for the top quark is defined as $\mathrm{Br}(t \to cZ, \gamma) = \Gamma(t \to cZ, \gamma)/\Gamma(t \to bW)$. The results for the $Z$ case are summarized in tab.1. The change in the decay width is of the order 10%. Due to the cancellation of NLO corrections to $t \to cZ$ decay rates and the main decay channel rate, the change in branching ratios are only at a promile level for $b^g = 0$. However, setting $b^g$ to be equal to $a^Z$ or $b^Z$, the change is increased by an order of magnitude and reaches a few percent. The results for the photon case are summarized by fig.1. We observe a significant dependence of the relative change of Br on the kinematical cuts. It can reach $10 - 15\%$

[1] Chirality assignments are implicit so $b^i$ stands for $b^i_{LR}$ or $b^i_{RL}$, for $i = Z, \gamma, g$.

Table 1: *Ratios between NLO and LO decay rates and branching ratios given for certain values and relations between FCNC coefficients for $t \to cZ$. SM inputs used are: $m_t = 172.3$ GeV, $m_Z = 91.2$ GeV, $\sin^2\theta_W = 0.231$.*

| | $b^Z = 0$ $b^g = 0$ | $a^Z = 0$ $b^g = 0$ | $a^Z = b^Z$ $b^g = 0$ | $b^Z = 0$ $a^Z = b^g$ | $a^Z = 0$ $b^Z = b^g$ |
|---|---|---|---|---|---|
| $\Gamma^{\rm NLO}/\Gamma^{\rm LO}$ | 0.92 | 0.91 | 0.92 | 0.95 | 0.94 |
| ${\rm Br}^{\rm NLO}/{\rm Br}^{\rm LO}$ | 1.001 | 0.999 | 1.003 | 1.032 | 1.022 |

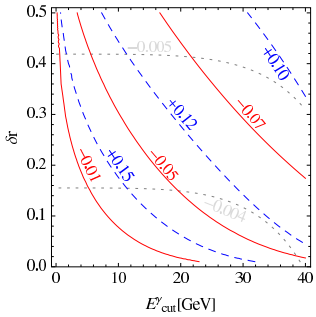


Figure 1: *Relative size of $\alpha_s$ corrections to the ${\rm Br}(t \to c\gamma)$ at representative ranges of $\delta r$ and $E_\gamma^{\rm cut}$. Contours of constant correction values are plotted for $b^g = 0$ (gray, dotted), $b^g = b^\gamma$ (red) and $b^g = -b^\gamma$ (blue, dashed).*

when $b^g \sim b^\gamma$. Consequently, a bound on ${\rm Br}(t \to c\gamma)$ can, depending on the experimental cuts, probe both $b^{g,\gamma}$ couplings.

## 4 Angular asymmetries in $t \to c\ell^+\ell^-$

We define two angles $\theta_j$ and $\theta_l$. The first one is defined in the $\ell^+\ell^-$ rest-frame $z_j = \cos\theta_j$ and measures the relative direction between the positively charged lepton and the light quark jet. Conversely, in the rest-frame of the positive lepton and the quark jet, we can define $z_\ell = \cos\theta_\ell$ to measure the relative directions between the two leptons. In terms of these variables, we can define two asymmetries ($i = j, \ell$) as

$$A_i = \frac{\Gamma_{z_i>0} - \Gamma_{z_i<0}}{\Gamma_{z_i>0} + \Gamma_{z_i<0}}\,, \tag{2}$$

where we have denoted $\Gamma_{z_i<0}$, $\Gamma_{z_i>0}$ as the integrated decay rates with an upper or lower cut on one of the $z_i$ variables. We can then identify $A_j \equiv A_{\rm FB}$ as the commonly known forward-backward asymmetry and define $A_l \equiv A_{\rm LR}$ as the left-right asymmetry.

In [7] we present analytical formulae for the two asymmetries and explore the possible ranges and correlations between the two asymmetries. Fixing the total decay rate we scan over the FCNC coupling parameter space plotting points in $(A_{\rm FB}, A_{\rm LR})$ plane. Two such plots are shown in fig.2.

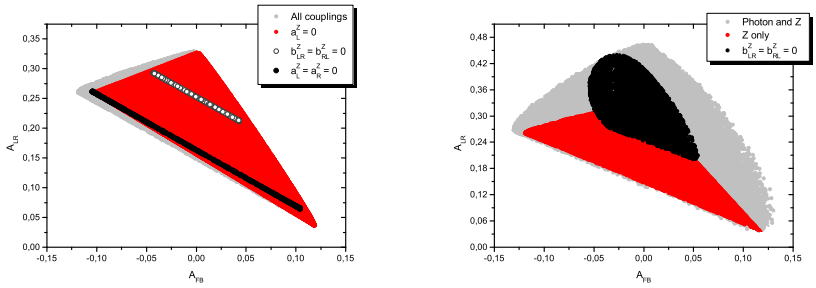


Figure 2: *Left: The correlation of $A_{\rm FB}$ and $A_{\rm LR}$ in Z mediated transition. Right: The correlation of $A_{\rm FB}$ and $A_{\rm LR}$ in Z and $\gamma$ mediated transition.*

We see that $A_{\rm FB}$ cannot exceed $\sim 10$ % even when the interference of $t \to cZ$ and $t \to c\gamma$ is considered. This interference can, however, increase $A_{\rm LR}$ by more then 10 %.

## 5 Conclusions

We have found that especially in the $t \to c\gamma$ decay we can expect the effects of NLO QCD corrections to be significant. Furthermore effects of the kinematical cuts of the nontrivial photon spectrum should be taken into account. We have found two angular asymmetries that can be used in $t \to c\ell^+\ell^-$ decay to discriminate between different couplings governing the FCNC decay.

## References


1. J. A. Aguilar-Saavedra, Acta Phys. Polon. B **35**, 2695 (2004) [arXiv:hep-ph/0409342].

2. T. Aaltonen *et al.* [CDF Collaboration], Phys. Rev. Lett. **101**, 192002 (2008) [arXiv:0805.2109 [hep-ex]].

3. S. Chekanov *et al.* [ZEUS Collaboration], Phys. Lett. B **559**, 153 (2003) [arXiv:hep-ex/0302010].

4. T. Aaltonen *et al.* [CDF Collaboration], Phys. Rev. Lett. **102** (2009) 151801 [arXiv:0812.3400 [hep-ex]].

5. J. Carvalho *et al.* [ATLAS Collaboration], Eur. Phys. J. C **52**, 999 (2007) [arXiv:0712.1127 [hep-ex]].

6. J. Drobnak, S. Fajfer and J. F. Kamenik, arXiv:1004.0620 [hep-ph].

7. J. Drobnak, S. Fajfer and J. F. Kamenik, JHEP **0903** (2009) 077 [arXiv:0812.0294 [hep-ph]].

8. J. A. Aguilar-Saavedra, Nucl. Phys. B **812**, 181 (2009) [arXiv:0811.3842 [hep-ph]].

9. J. Drobnak, S. Fajfer and J. F. Kamenik, in preparation.

Frascati Physics Series Vol. LI (2010), pp. 13-18
2nd Young Researchers Workshop: Physics Challenges in the LHC Era
Frascati, May 10 and 13, 2010

# HIGGS BOSONS IN $t\bar{t}$ PRODUCTION

Roberto Barceló
*CAFPE and Departamento de Física Teórica y del Cosmos,*
*Universidad de Granada, E-18071 Granada, Spain.*

**Abstract**

The top quark has a large Yukawa coupling with the Higgs boson. In the usual extensions of the standard model the Higgs sector includes extra scalars, which also tend to couple strongly with the top quark. Unlike the Higgs, these fields have a *natural* mass above $2m_t$, so they could introduce anomalies in $t\bar{t}$ production at the LHC. We study their effect on the $t\bar{t}$ invariant mass distribution at $\sqrt{s} = 7$ TeV. We focus on the bosons ($H$,$A$) of the minimal SUSY model and on the scalar field ($r$) associated to the new scale $f$ in Little Higgs (LH) models. We show that in all cases the interference with the standard amplitude dominates over the narrow-width contribution. As a consequence, the mass difference between $H$ and $A$ or the contribution of an extra $T$-quark loop in LH models become important effects in order to determine if these fields are observable there. We find that a 1 fb$^{-1}$ luminosity could probe the region $\tan\beta \leq 3$ of SUSY and $v/(\sqrt{2}f) \geq 0.3$ in LH models.

## 1 Introduction

The main objective of the LHC is to reveal the nature of the mechanism breaking the electroweak symmetry. This requires not only a determination of the Higgs mass and couplings, but also a search for additional particles that may be related to new dynamics or symmetries present at the TeV scale. The top-quark sector appears then as a promising place to start the search, as it is there where the EW symmetry is broken the most. Generically, the large top-quark Yukawa coupling with the Higgs boson ($h$) also implies large couplings with the extra physics. For example, in SUSY extensions $h$ comes together with neutral scalar ($H$) and pseudoscalar ($A$) fields [1]. Or in Little Higgs (LH) models, a global symmetry in the Higgs and the top-quark sectors introduces a scalar singlet and an extra $T$ quark [2, 3]. In all cases these scalar fields have large Yukawa couplings that could imply a sizeable production rate in hadron collisions and a dominant decay channel into $t\bar{t}$.

## 2 Top quarks from scalar Higgs bosons

The potential to observe new physics in $m_{t\bar{t}}$ at hadron colliders has been discussed in previous literature [4, 5]. In general, any heavy $s$–channel resonance with a significant branching ratio to $t\bar{t}$ will introduce distortions. In the diagram depicted in fig.1 the intermediate scalar is produced at one loop, but the gauge and Yukawa couplings are all strong.

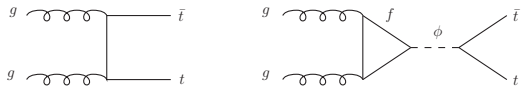


Figure 1: *Diagrams that interfere in $t\bar{t}$ production.*

In [6] we give the expressions for the leading-order differential cross section for $gg \to t\bar{t}$ through a scalar and a pseudoscalar, $\phi$. To have an observable effect it is essential that the width $\Gamma_\phi$ is small. This is precisely the reason why the effect on $m_{t\bar{t}}$ of a very heavy standard Higgs $h$ would be irrelevant. A 500 GeV Higgs boson would couple strongly to the top quark, but even stronger to

itself. Its decay into would-be Goldstone bosons would then dominate, implying a total decay width of around 60 GeV.

To have a smaller width and a larger effect the mass of the resonance must *not* be EW. In particular, SUSY or LH models provide a new scale and massive Higgses with no need for large scalar self-couplings.

## 3 SUSY neutral bosons

SUSY incorporates two Higgs doublets, and after EWSB there are two neutral bosons ($H$ and $A$) in addition to the light Higgs. The mass of these two fields is not EW, so they are *naturally* heavy enough to decay in $t\bar{t}$. Their mass difference depends on the $\mu$ parameter and the stop masses and trilinears in addition to $\tan\beta$ [7]. Varying these parameters, for $m_A = 500$ GeV we obtain typical values of $m_H - m_A$ between $-2$ and $+10$ GeV.

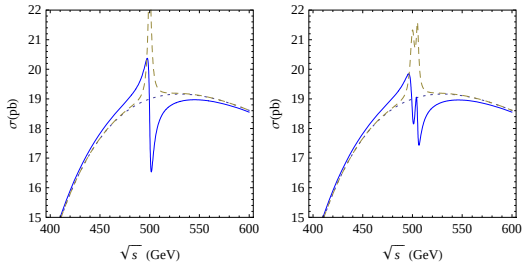


Figure 2: $\sigma(gg \to t\bar{t})$ *for* $\tan\beta = 2$ *and SUSY bosons of mass* $m_A = m_H = 500$ *GeV (left) or* $m_A = 500$, $m_H = 505$ *GeV (right). Dashes provide the narrow-width approximation and dots the standard model cross section.*

In fig.2-left we observe an average 5.5% excess and 8.1% deficit in the 5 GeV intervals before and after $\sqrt{s} = 500$ GeV, respectively. There the position of the peaks and dips caused by $H$ and $A$ overlap *constructively*. In contrast, in fig.2-right their mass difference implies a partial cancellation between the dip caused by $A$ and the peak of $H$.

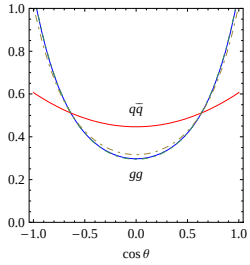


Figure 3: *Standard angular distribution for the t quarks from $q\bar{q}$ and gg collisions at $\sqrt{s} = 500$ GeV. We include (dashes) the distribution from gg at the peak and the dip of fig.2-left.*

From fig.3 we argue that different cuts could be applied to reduce the background for $t\bar{t}$ production at the LHC or even to optimize the contribution from $gg$ versus $q\bar{q}$, but not to enhance the relative effect of the scalars on $\sigma(gg \to t\bar{t})$.

## 4 Little Higgs boson

In LH models the Higgs appears as a pseudo-Goldstone boson of a global symmetry broken spontaneously at the scale $f > v/\sqrt{2} = 174$ GeV. The global symmetry introduces an extra $T$ quark and a massive scalar singlet $r$, the *Higgs* of the symmetry broken at $f$. Once the electroweak VEV is included the doublet and singlet Higgses mix [8, 9].

The extra Higgs $r$ is somehow similar to the heavier scalar in a doublet plus singlet model, with the doublet component growing with $s_\theta = v/(\sqrt{2}f)$. If $s_\theta$ is sizeable so is its coupling to the top quark. The coupling to the extra $T$ quark is stronger, but if $r$ is lighter than $2m_T$ then its main decay mode will be into $t\bar{t}$. Therefore, $r$ is a naturally heavy ($m_r \approx f$) but narrow scalar resonance with large couplings to quarks and an order one braching ratio to $t\bar{t}$.

In [6] we examine this case in detail. The results are similar to the ones obtained for SUSY bosons of the same mass.

## 5 Signal at the LHC

Let us now estimate the invariant mass distribution of $t\bar{t}$ events ($m_{t\bar{t}}$) in $pp$ collisions at the LHC. We will take a center of mass energy of 7 TeV and 1 fb$^{-1}$ luminosity and we will not apply any cuts . At these energies the cross section $pp \to t\bar{t}$ is dominated by $gg$ fusion (90%).

In fig.4 we observe a 5% excess followed by a 9% deficit, with smaller deviations as $m_{t\bar{t}}$ separates from the mass of the extra Higgs bosons. In fig.5 we find that changing the binning is important in order to optimize the effect.

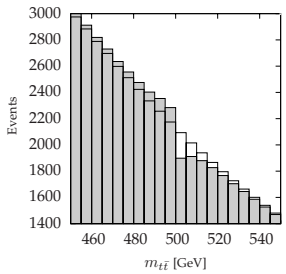


Figure 4: *Number of $t\bar{t}$ events in pp collisions at 7 TeV and 1 fb$^{-1}$ for $m_A = m_H = 500$ GeV and $\tan\beta = 2$ distributed in 5 GeV bins.*

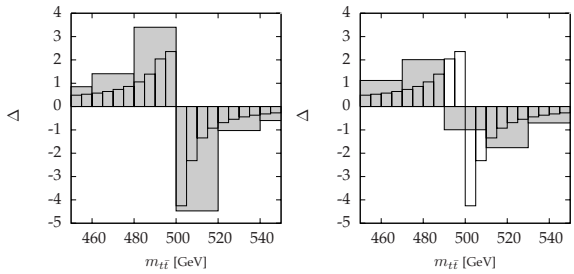


Figure 5: *Deviation $\Delta = (N - N_{SM})/\sqrt{N_{SM}}$ in the number of events respect to the standard prediction for two different binning ($m_A = m_H = 500$ GeV and $\tan\beta = 2$).*

## 6 Summary and discussion

In models with an extended Higgs sector the extra bosons tend to have large couplings with the top quark that imply a sizeable one-loop production rate at hadron colliders. If the mass of these bosons is not EW but comes from a new scale (*e.g.*, the SUSY or the global symmetry-breaking scales), then they may decay predominantly into $t\bar{t}$. We have studied their effect on the $t\bar{t}$ invariant mass distribution at 7 TeV and 1 fb$^{-1}$. We have considered the deviations due to the neutral bosons $A$ and $H$ of the MSSM, and to the scalar $r$ associated to the scale $f$ in LH models. In all cases the interference dominates, invalidating the narrow-width approximation.

## References


1. A. Djouadi, Phys. Rept. **459** (2008) 1 [arXiv:hep-ph/0503173].
2. M. Schmaltz and D. Tucker-Smith, Ann. Rev. Nucl. Part. Sci. **55** (2005) 229.
3. M. Perelstein, Prog. Part. Nucl. Phys. **58** (2007) 247.
4. D. Dicus, A. Stange and S. Willenbrock, Phys. Lett. B **333** (1994) 126 [arXiv:hep-ph/9404359].
5. R. Frederix and F. Maltoni, JHEP **0901** (2009) 047 [arXiv:0712.2355 [hep-ph]].
6. R. Barcelo and M. Masip, Phys. Rev. D **81** (2010) 075019 [arXiv:1001.5456 [hep-ph]].
7. W. de Boer, R. Ehret and D. I. Kazakov, Z. Phys. C **67** (1995) 647 [arXiv:hep-ph/9405342].
8. R. Barcelo and M. Masip, Phys. Rev. D **78** (2008) 095012 [arXiv:0809.3124 [hep-ph]].
9. R. Barcelo, M. Masip and M. Moreno-Torres, Nucl. Phys. B **782** (2007) 159 [arXiv:hep-ph/0701040].

Frascati Physics Series Vol. LI (2010), pp. 19-24
2nd Young Researchers Workshop: Physics Challenges in the LHC Era
Frascati, May 10 and 13, 2010

# INCREASING THE LIGHTEST HIGGS MASS BOUND OF THE MSSM

Paolo Lodone
*Scuola Normale Superiore and INFN,*
*Piazza dei Cavalieri 7, 56126 Pisa, Italy*

**Abstract**

In the MSSM the Higgs boson mass at tree level cannot exceed the $Z$ boson mass. One could then ask himself: should we throw away low energy Supersymmetry if we don't see the Higgs boson at the LHC? To answer this question it makes sense to consider extensions of the MSSM in which the Higgs boson can be relatively heavier. An additional motivation for looking in this direction comes from flavour physics, since a heavier Higgs boson would relax the naturalness bound on the masses of the sfermions of the first two generations, allowing them to be heavier and thus in better agreement with the absence of any signal so far. We consider three possibile models from a bottom-up point of view, and briefly discuss the phenomenological consequences.

## 1 Introduction

The main virtues of Low Energy Supersymmetry are: (i) naturalness, (ii) compatibility with Electroweak Precision Tests (EWPT), (iii) perturbativity, and (iv) manifest unification. However, after the LEP2 bound $m_h > 114.4$ GeV on the lightest Higgs boson mass, the minimal model (MSSM) has a serious problem in dealing with (i) because $m_h$ cannot exceed $m_Z$ at tree level. This motivates adding extra $F$ terms, like in the Next to Minimal Supersymmetric Standard Model (NMSSM) [1], or extra $D$ terms if the Higgs shares new gauge interactions [2] [3], or both. The usual approach is imposing that the new couplings do not become strong before $M_{GUT}$. For this reason it is typically difficoult to go beyond $m_h = 150$ GeV. Should we then throw away low energy (not finetuned) Supersymmetry if the lightest Higgs boson is not found below 150 GeV? To answer this question one should notice that the request of *manifest* (iv) could be highly too restrictive: there are explicit examples [4] in which some couplings become strong at an intermediate scale without spoiling unification. Thus we stick to a bottom-up point of view, as in [5]. We call $\Lambda$ the scale of semiperturbativity, at which some expansion parameter becomes equal to 1, and $M$ the scale at which the soft breaking terms are generated, allowing both to be relatively low. We tolerate a finetuning of 10 %, according to the usual criterion [6]. In a minimalistic approach, we make a comparative study (see [7] for details) of the simplest possible extensions of the MSSM which meet the goal: adding a $U(1)$ or $SU(2)$ gauge interaction [3], or a gauge singlet with large coupling to the Higgses [5]. The only constraints come from naturalness and EWPT. In other words, we prefer to retain (i)-(iii) at low energies at the price of (iv), instead of insisting on (iv) at the price of (i).

## 2 Comparative study of the three models

Refering to [7] for details, the lightest Higgs boson mass bound is, respectively:

$$(m_h^{(tree)})^2 \leq m_Z^2 \cos^2 2\beta \qquad \text{(MSSM)}$$

$$(m_h^{(tree)})^2 \leq (m_Z^2 + g_x^2 v^2/(2 + \tfrac{M_X^2}{M_\phi^2})) \cos^2 2\beta \qquad (U(1)_x)$$

$$(m_h^{(tree)})^2 \leq m_Z^2 \tfrac{g'^2+\eta g^2}{g'^2+g^2} \cos^2 2\beta, \quad , \quad \eta = (1 + \tfrac{g_I^2 M_\Sigma^2}{g^2 M_X^2})/(1 + \tfrac{M_\Sigma^2}{M_X^2}) \qquad (SU(2))$$

$$(m_h^{(tree)})^2 \leq m_Z^2 (\cos^2 2\beta + \tfrac{2\lambda^2}{g^2+g'^2} \sin^2 2\beta) \qquad (\lambda\text{SUSY})$$

where $g_x$, $g_I$ and $\lambda$ are new gauge and Yukawa couplings, $M_X$ is the mass of the new heavy vectors, and $M_\phi$, $M_\Sigma$ are new soft masses.

First of all there must be compatibility with the EWPT. In the $U(1)$ case, from the analysis [8] one can deduce $M_X \gtrsim 5$ TeV. For the $SU(2)$ model we impose $M_X/(5\text{ TeV}) \gtrsim g_X/g$, where $g_X$ is the coupling of the triplet of heavy vectors. The case of $\lambda$SUSY is thoroughly studied in [5] and shown to be compatible with data for low $\tan\beta$ ($\leq 3$).

On the other hand there are constraints from the naturalness of the breaking scale of the new gauge groups and of the Fermi scale. For the former we fix some ratios among parameters so that there is a tuning of no more than 10 % at tree level, for the latter the amount of tuning can be shown to be given, in the interesting cases, by:

$$\delta m_{H_u}^2 \leq \frac{(m_h^{(tree)})^2}{2} \times \Delta \tag{1}$$

where $1/\Delta$ is the finetuning as defined by [6], and we accept $\Delta = 10$ at most. From these conditions one obtains respectively lower bounds on the ratios $M_X/M_{\phi,\Sigma}$ and upper bounds on the soft masses $M_\phi$ and $M_\Sigma$.

Putting all together one obtains the upper bound on $m_h$ at tree level which is shown in Figure 1.

## 3 Phenomenological consequences

A unified discussion of the phenomenological consequences of this models is presented in [9]. Let us briefly mention some important points:

- *Collider signatures*: At least at the early stages of the LHC, taking Tevatron into account, the most interesting signals come from gluino pair production. An effective way to characterize these signals is to consider the semi-inclusive branching ratios:

  $$BR(\tilde{g} \to q_1 \overline{q}_2 \chi) \tag{2}$$

  where $q_{1,2}$ stand for third generation quarks and $\chi$ stands for LSP plus $W$ and/or $Z$ bosons, real or virtuals. The final state would then be:

  $$pp \to \tilde{g}\tilde{g} \to \overline{q}\,\overline{q}\,q\,q + \chi\,\chi \tag{3}$$

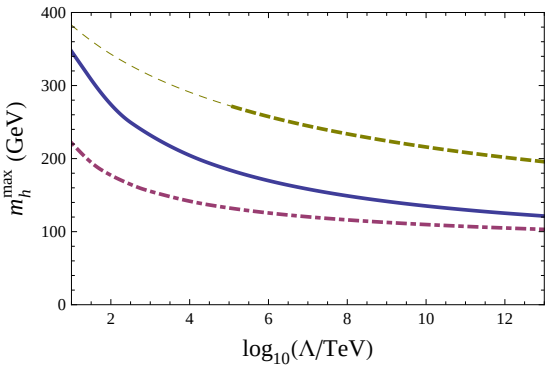


Figure 1: *Tree level bound on $m_h$ as a function of the scale $\Lambda$ at which $g_I$ or $\lambda$ or $g_X$ equals $\sqrt{4\pi}$; for $SU(2)$ (dashed), $\lambda SUSY$ (solid), and $U(1)$ (dotdashed). For $\lambda SUSY$ one needs $\tan\beta \lesssim 3$, in the other cases $\tan\beta \gg 1$ and 10% finetuning at tree level in the scalar potential which determines the new breaking scale. In the $SU(2)$ case naturalness disfavours $m_h \geq 270$ GeV.*

with $q$ = top or bottom quarks. A particularly interesting signal are the equal sign dileptons from semi-leptonic decays.

An additional very much non-MSSM like signal would be the appearence of the 'golden mode' $h \to ZZ$.

- *Relic Dark Matter abundance*: As is well known [10], after the LEP2 bounds for the LSP to reproduce the observed dark matter abundance one needs special relations among the parameters, which take the name of "well temperament". For example for large $SU(2)$ gaugino mass $M_2 \gg M_1$ one needs $M_1 \approx \mu$, which looks like a finetuning problem. It is interesting to notice that these special relations are significantly distorted in these models, mainly because of the increased lightest Higgs boson mass.

- *Flavour physics*: Without degeneracy nor alignement the bounds that the masses of the squarks of the first two generations would have to satisfy are in the range of hundreds of TeV. Assuming an amount of degeneracy and alignement of the order of the Cabibbo angle and $\delta^{RR} \gg \delta^{LL}, \delta^{LR}$ or vice versa, one can see that even the strongest bounds can be satisfied if

Table 1: *Summary of the "performance" of the three models, see text.*

| Model | $m_h^{max}$ / $m_Z$ | Price to pay |
|---|---|---|
| $U(1)$ | 2 | (1),(2),(3) |
| $SU(2)$ | 2 | (3) |
| $SU(2)$ | 3 | (2),(3),(4) |
| $\lambda$SUSY | 2 | – |
| $\lambda$SUSY | 3 | (1) |

$m_{\tilde{q}_{1,2}} \gtrsim 10-20$ TeV. In the MSSM this would introduce an unacceptable finetuning on the Fermi scale. On the contrary, if the lightest Higgs boson mass is significantly increased at tree level, there can be room for these values compatibly with naturalness. From this respect, the most promising possibility is $\lambda$SUSY.

## 4 Conclusions

From a bottom-up point of view, the lightest Higgs boson mass can be significantly raised at tree level. Constraints come from the interplay between naturalness and experimental constraints. The maximum possible $m_h$ that one can obtain is shown in Figure 1 as a function of the scale of semiperturbativity. In the $SU(2)$ case it seems difficoult to be consistent with both the EWPT and naturalness if $m_h$ is beyond 270 GeV. The prices that one may have to pay are the following: (1) low semiperturbativity scale $\Lambda$; (2) low "messenger" scale $M$ at which the soft terms are generated; (3) presence of different scales of soft masses; (4) need for extra positive contributions to $T$. With low scale we mean $\lesssim 100$ TeV, with (3) we mean that, besides the usual soft masses of order of hundreds of GeV, one may need some new soft masses of order 10 TeV. The "performance" of the three models is summarized in Table 1. A unified viewpoint on the Higgs mass and the flavor problem for this kind of models and other phenomenological consequences are discussed in [9].

## 5 Acknowledgments

I thank Enrico Bertuzzo, Marco Farina, and especially Riccardo Barbieri.

## References


1. P. Fayet, Nucl. Phys. B **90**, 104 (1975).
   J. R. Ellis *et al*, Phys. Rev. D **39**, 844 (1989).
   M. Drees, Int. J. Mod. Phys. A **4**, 3635 (1989).

2. H. E. Haber and M. Sher, Phys. Rev. D **35**, 2206 (1987).
   J. R. Espinosa and M. Quiros, Phys. Lett. B **279**, 92 (1992).
   J. R. Espinosa and M. Quiros, Phys. Rev. Lett. **81**, 516 (1998) arXiv:hep-ph/9804235.

3. P. Batra *et al*, JHEP **0402**, 043 (2004) arXiv:hep-ph/0309149.

4. R. Harnik *et al*, Phys. Rev. D **70**, 015002 (2004) arXiv:hep-ph/0311349.
   S. Chang *et al*, Phys. Rev. D **71**, 015003 (2005) arXiv:hep-ph/0405267.
   A. Birkedal *et al*, Phys. Rev. D **71**, 015006 (2005) arXiv:hep-ph/0408329.

5. R. Barbieri *et al*, Phys. Rev. D **75**, 035007 (2007) arXiv:hep-ph/0607332.

6. R. Barbieri and G. F. Giudice, Nucl. Phys. B **306**, 63 (1988).

7. P. Lodone, JHEP **1005** (2010) 068 arXiv:1004.1271.

8. E. Salvioni *et al*, arXiv:0911.1450; .
   E. Salvioni *et al*, JHEP **0911**, 068 (2009) arXiv:0909.1320.

9. R. Barbieri *et al*, arXiv:1004.2256.

10. N. Arkani-Hamed *et al*, Nucl. Phys. B **741** (2006) 108, arXiv:0601041.

Frascati Physics Series Vol. LI (2010), pp. 25-30
2nd Young Researchers Workshop: Physics Challenges in the LHC Era
Frascati, May 10 and 13, 2010

# STUDY OF W+JETS BACKGROUND TO TOP QUARK PAIR PRODUCTION CROSS SECTION IN ATLAS AT THE LHC

Maria Ilaria Besana
*Università degli Studi di Milano and INFN Milano*

**Abstract**

The measurement of top quark pair production cross section in p-p collisions at center-of-mass energy of 7 TeV is one of the first measurements that will be made by ATLAS at the LHC. The most promising channel is the semileptonic final state, where one of the top decays into a W decaying into hadrons and the other top into a W decaying leptonically. The dominant background to this channel of top quark pairs is given by direct p-p production of W+jets. Monte Carlo predictions for the rate of this background have large uncertainties; however it will be important to know it with precision in order to make an accurate measurement of top quark pair production cross section. In the following, a data-driven technique developed in order to reduce this uncertainty is presented and first results on real data are discussed.

## 1 Introduction

The top quark discovery at Fermilab in 1995 completed the three generation structure of the Standard Model (SM) and opened the new field of top quark physics. After QCD jets, W and Z bosons, the production of top quarks is the dominant process in p-p collisions at multi-TeV energies. The LHC would be a top quark factory: top quark pair production cross section at LHC is expected to be enhanced by a factor 20 with respect to Tevatron even at 7 TeV. Top quark physics is a rich subject. Top quark events are indeed very useful for detector commissioning and they can provide a consistency test of Standard Model. The knowledge of top quark production cross section is also crucial, because it can be a significant background to events predicted by some models beyond the Standard Model.

This report will concentrate on the measurement of top quark pair production cross section in the early stage of data taking, i.e. with the amount of data expected to be collected in 2010. Event selection cuts and expected numbers of candidate events with an integrated luminosity of 10 $\text{pb}^{-1}$ are reported in Section 2. A data-driven technique for the estimation of the dominant background process, W+jets, is discussed in Section 3. Finally first results on 7 TeV data collected by ATLAS detector are reported in Section 4.

## 2 Selection of top quark pairs events

In Standard Model, top quarks decay takes place almost exclusively through the $t \to Wb$ decay mode. A W-boson decays in about 1/3 of the cases into a charged lepton and a neutrino. All three lepton flavors are produced at an approximately equal rate. In the remaining 2/3 of the cases, the $\text{W}^+$-boson decays into an up-type quark and a down-type anti-quark pair [1]. Since the CKM matrix suppresses decays involving b-quarks as $|V_{cb}|^2 \simeq 1.7\ 10^{-5}$, W-boson decay can be considered as a clean source of light quarks (u,d, s,c). Top quark pairs decay modes are then classified into:

- fully leptonic, if both W's decay leptonically,
- fully hadronic, if both W's decay into hadrons,
- semileptonic, if a W decays into leptons and the other one into hadrons.

[1] Charge coniugate states are implicitly included through the paper.

Table 1: *Expected number of selected events at 7 TeV with an integrated luminosity of 10 $pb^{-1}$ both of signal and main backgrounds.*

| Sample | Electron channel | Muon channel |
|---|---|---|
| top quark pairs | 53 | 65 |
| W+jets | 29 | 40 |
| single top | 5 | 5 |
| other backgrounds | 6 | 6 |

Semileptonic channel is very interesting, because of good branching ratio (45%) and clear experimental signature. The final state is indeed characterized by one energetic lepton, at least four energetic jets (initial and final state gluon radiation often increases the number of final state jets) and missing transverse energy ($E_{\mathrm{T}}^{\mathrm{miss}}$), because of the neutrino. Finally invariant mass of three of these jets is equal to top quark mass. Top quark pairs events in semileptonic channel are selected requiring exactly one lepton (electron or muon [2]) with transverse momentum $p_{\mathrm{T}} > 20$ GeV and absolute value of pseudorapidity $|\eta| < 2.5$, $E_{\mathrm{T}}^{\mathrm{miss}} > 20$ GeV and at least 4 jets with transverse momentum $p_{\mathrm{T}} > 20$ GeV and $|\eta| < 2.5$. Finally we require that 3 of these jets have transverse momentum $p_{\mathrm{T}} > 40$ GeV. Electrons and jets are measured using calorimeters and inner tracker. Missing transverse energy is a complex quantity, because of the use of information from the whole detector. It is calculated from the sum of energy of all particles seen in the detector:

$$E_{\mathrm{T}}^{\mathrm{miss}} = \sqrt{(E_{\mathrm{x}}^{\mathrm{miss}})^2 + (E_{\mathrm{y}}^{\mathrm{miss}})^2} \qquad E_{\mathrm{i}}^{\mathrm{miss}} = -\Sigma E_{\mathrm{i}} \quad \text{with} \quad i = x, y \quad (1)$$

### 2.1 Expected number of selected events with an integrated luminosity of 10 $\mathrm{pb}^{-1}$

The signal and major backgrounds have been estimated from Monte Carlo simulations which include a full simulation of the ATLAS detector. Table 1 summarises the expected numbers of signal and background events for the electron and muon channel analysis, namely the direct W+jets production from p-p collisions, single top production and other backgrounds as Z+jets production, dibosons production and top quark pair decaying fully hadronically.

The dominant expected background is W+jets direct production from p-p collision and it is very dangerous. W+jets events can have indeed the

[2]Single lepton channel with tau lepton needs a dedicated analysis.

same experimental signature of top quark pairs events. The cross section for associated production of W and 4 hadronic jets is non negligible at the LHC ($\simeq$350 pb at 7 TeV). W+jets cross section has a big uncertainty, up to 100% for W+4jets. There is not indeed NLO calculation for the cross section of this process and Monte Carlo predictions are based on parameters estimated for energy 4 times lower than the LHC one. Finally, it is very difficult to measure it directly from data because of big top quark contamination. Estimation of this background is however crucial in order to have a precise measurement of top quark pair production cross section. A data-driven technique, described in the next section, has been developed for this purpose.

## 3 Data-driven technique for W+jets background estimation

W+jets can be estimated with a data-driven technique based on the fact that W to Z ratio is predicted with a much smaller uncertainty [1) 2)] than W+jets cross section. Since the jet multiplicity distribution for Z events can be measured with data, this observation can be used to reduce the Monte Carlo uncertainty on the fraction of W+jets present in the selected sample of candidate top events. The idea is to extrapolate from a control region (CR) with one jet into the top signal region (SR) with four or more jets and estimate the number of W+jets background events using the formula:

$$W^{\mathrm{SR}} = C_{\mathrm{MC}} * \frac{Z^{\mathrm{SR}}}{Z^{\mathrm{CR}}} * W^{\mathrm{CR}} \qquad \text{where } C_{\mathrm{MC}} = \left(\frac{Z^{\mathrm{CR}}}{W^{\mathrm{CR}}}\right)_{\mathrm{MC}} \tag{2}$$

where $W^{\mathrm{CR}}$ and $Z^{\mathrm{CR}}$ represent the number of W and Z candidates reconstructed in the low jet multiplicity control region. $Z^{\mathrm{SR}}$ is the number of candidate Z events which pass the same selection criteria as those imposed in the top-antitop analysis (top quark signal region). $C_{\mathrm{MC}}$ is a coefficient determined from Monte Carlo, which takes into account mass difference between W and Z bosons. $Z \to ee$ ($Z \to \mu\mu$) candidate events are selected (after the trigger) by requiring two electrons (muons) of opposite charge, with an invariant mass between 80 GeV and 100 GeV. $Z^{\mathrm{SR}}$ sample is selected by applying the default baseline analysis selection, i.e. requiring three jets with $p_{\mathrm{T}}$ above 40 GeV, a fourth with $p_{\mathrm{T}}$ greater than 20 GeV and $|\eta| < 2.5$. Events in control region are selected asking exactly one jet of transverse momentum $p_{\mathrm{T}}$ >20 GeV and $|\eta| < 2.5$.

### 3.1 Main sources of uncertainty

There are three main sources of uncertainty for this method. The first one is the uncertainty on $C_{\mathrm{MC}}$. This has been estimated comparing different Monte Carlo generators and varying their parameters and was found to be 12% both in electron and muon channel. Another source of uncertainty comes from background contamination to $W^{\mathrm{CR}}$. The dominant background is QCD di-jets production. Estimation of its contribution from data is ongoing. At present a conservative assumption was done that it will be possible to estimate it with an accuracy of 50%. Its contribution on W+jets background estimation uncertainty is 16% in electron channel and 13% in muon channel. Finally statistical uncertainty is dominated by the number of expected Z events in signal region. It is reduced combining electron and muon channels for Z events , since $Z^{\mathrm{SR}}/Z^{\mathrm{CR}}$ is independent from lepton flavor. The number of W events in top quark signal region can be estimated as:

$$W^{\mathrm{SR}} = C_{\mathrm{MC}} * \frac{Z^{\mathrm{SR}} \to ee + Z^{\mathrm{SR}} \to \mu\mu}{Z^{\mathrm{CR}} \to ee + Z^{\mathrm{CR}} \to \mu\mu} * W^{\mathrm{CR}} \tag{3}$$

Taking into account all these sources of uncertainty, W+jets background uncertainty will be reduced to 50% with first 10 $pb^{-1}$; this is a significant improvement with respect to Monte Carlo predictions. The contribution of the W+jets background uncertainty to the uncertainty on top quark cross section measurement will be 25%. After an integrated luminosity of 100 $pb^{-1}$, the uncertainty on W+jets background estimation will be reduced to 20%.

## 4 Analysis on real data

ATLAS detector started to take collision data at 7 TeV on March 30th, 2010. At the time of this report (June 2010) with data corrisponding to integrated luminosities of 6.7 $\mathrm{nb}^{-1}$ and 6.4 $\mathrm{nb}^{-1}$ in the electron and muon channels respectively, 17 $W \to e\nu$ and 40 $W \to \mu\nu$ candidates were selected. One $Z \to ee$ and two $Z \to \mu\mu$ candidates were also observed, resulting from total integrated luminosities of 6.7 $\mathrm{nb}^{-1}$ and 7.9 $\mathrm{nb}^{-1}$, respectively. W and Z candidate events were selected as reported in Section 3. An higher cut on $E_{\mathrm{T}}^{\mathrm{miss}}$ was applied for W candidates selection in order to suppress QCD background contamination (25 GeV instead of 20 GeV). No requirements on associated jets were applied. Figures 1 shows transverse mass ($m_{\mathrm{T}}$) of W candidates and compares it to signal and background Monte Carlo samples. It is clear the presence of signal over the background. Analysis on real data is ongoing. With a luminosity of

few $\mathrm{nb}^{-1}$, W/Z ratio can be studied at low jet multiplicity and QCD di-jets contamination to $W^{\mathrm{CR}}$ sample can be estimated

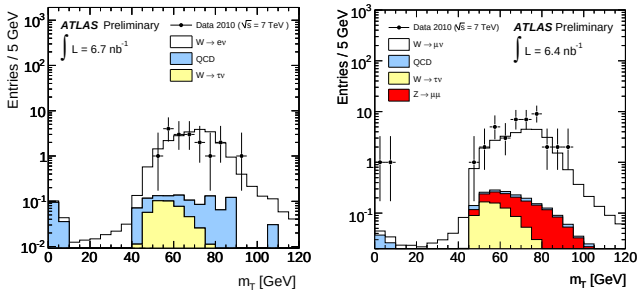


(a) (b)

Figure 1: *Transverse mass of W candidates in electron (a) and muon (b) channel. Expectation from Monte Carlo are compared with data.*

## 5 Conclusions

It is crucial for the measurement of the top quark cross section to reduce the uncertainty on the expected number of W+jets background events. The data-driven technique presented here allows to reduce this uncertainty by a factor two even with first 10 $\mathrm{pb}^{-1}$. Selection cut optimization is ongoing in order to reduce the systematic uncertainty coming from QCD di-jets contamination to $W^{\mathrm{CR}}$ and statistical uncertainty coming from the number of Z events in signal region.

## References


1. F. A. Berends, W. T. Giele, H. Kuijf, R. Kleiss, W. J. Stirling, Physics Letters B 224, (1989) 237.

2. E. Abouzaid, H. Frisch, Phys. Rev. D 68 (2003) 033014.

Frascati Physics Series Vol. LI (2010), pp. 31-36
2nd Young Researchers Workshop: Physics Challenges in the LHC Era
Frascati, May 10 and 13, 2010

# MONITORING THE Mrk421 FLARING ACTIVITY BY THE ARGO-YBJ EXPERIMENT

Roberto Iuppa
*INFN, Sezione Roma Tor Vergata*
*Dipartimento di Fisica,* Università di Roma Tor Vergata
on behalf of the ARGO-YBJ collaboration

**Abstract**

ARGO-YBJ is an extensive air shower detector exploiting the full coverage approach at high altitude (4300 m a.s.l.), designed for gamma-ray astronomy and cosmic-ray physics in the 300 GeV - 30 TeV energy range. One of the most intense gamma-ray sources detected by ARGO-YBJ is Mrk421. It is a blazar close to the Earth (redshift: $z = 0.031$), intensively studied because of its highly varying flaring activity. During the last four years, three major flaring periods have been observed by ARGO-YBJ, in July 2006, in June 2008 and in February 2010. Thsee flares show interesting spectral features, mostly as far as the relation between the X-ray and the gamma-ray emissions is concerned. The status of the observation of Mrk421 is reported.

## 1 Introduction

In 1992 the blazar Markarian 421 (Mrk421) became the first extragalactic source observed at gamma-ray energy $E > 500\text{GeV}$ [1]. It is classified as a radio-loud active galactic nucleus (AGN), a subclass of BL Lacertae objects (BL Lac), characterized by a non-thermal spectrum extending up to high energies and by rapid flux variability at nearly all wavelengths. So far, Mrk421 is the closest BL Lac detected above 100 GeV ($z = 0.031$), making it the most studied TeV-emitting AGN and the main benchmark for each model on the emission processes in AGNs and the attenuation of TeV gamma rays propagating through extragalactic space.

The flaring activity of Mrk421 spans over twelve decades of energy (from optical to TeV) and has been observed with variability timescales ranging from minutes to months. Such physical properties require data merging from different experiments in order to get observations as complete as possible.

TeV detection is especially challenging, because of the low emission rate and the short duration of most flares. Nonetheless, many efforts have been spent to observe Mrk421 at TeV energies, because these measurements provide important indications on the source properties and the radiation processes. Recently, several multiwavelength campaigns have revealed a strong correlation of gamma rays with X-rays, that can be easily interpreted in terms of the Synchrotron Self-Compton model [2] [3]. Altough significant variations of the TeV spectrum slope during different activity phases still remain unexplained, some hints have been found of the correlation between the spectral hardness and the flux intensity [4].

Since the emission flux at Very High Energy (VHE, above 100 GeV) is rather low, detections must be carried out with ground-based experiments, with large effective area. In addition, the strong variability of the flaring phenomena demands high duty-cycle and large field of view.

The ARGO-YBJ experiment, located at the Yangbajing Cosmic Ray Laboratory (Tibet, 4300 m a.s.l., $30^\circ\,0'38''N, 90^\circ\,3'50''E$), since 2007 December has been performing a continuous monitoring of the sky in the declination band from $-10^\circ$ to $70^\circ$. The detector was taking data also during summer 2006, and the ARGO-YBJ dataset represents a unique chance to report on the Mrk421 activity during the last four years.

## 2 The ARGO-YBJ experiment

The ARGO-YBJ detector, located at the Yangbajing Cosmic Ray Laboratory (Tibet, P.R. China, 4300 m a.s.l.), is the only experiment exploiting the *full coverage* approach at very high altitude. The detector is composed of a central carpet $\sim$74$\times$78 m$^2$, made of a single layer of Resistive Plate Chambers (RPCs) with $\sim$92% of active area, enclosed by a partially instrumented guard ring that extends the detector surface up to $\sim$100$\times$110 m$^2$, for a total active surface of $\sim$6700 m$^2$. The apparatus has a modular structure, described in [5].

The spatial coordinates and the arrival time of any detected particle are used to reconstruct the position of the shower core and the arrival direction of the primary [6].

The ARGO-YBJ experiment started recording data with the whole central carpet in June 2006. Since 2007 November the full detector has been in stable data taking (trigger particle multiplicity $N_{trig}$ =20) with a duty cycle $\sim$ 90%. The trigger rate is about 3.6 kHz.

## 3 Signal maps

Showers induced by VHE photons coming from Mrk421 are collected when the source zenith angle with respect to Yangbajing is less than 40°. Extending the analysis beyond such limit would slightly increase the exposure time, but a general worsening of the angular resolution should be faced and the energy resolution would be poorer. Since the ratio signal/noise within 1° from the source is about $10^{-4} \div 10^{-5}$, a reliable method of background estimation is needed. The ARGO-YBJ successfully applied different background estimation techniques, each of them giving results consistent with the others.

In order to resolve the primary photons energy, the dataset is divided into multiplicity ranges, according to how many pads the induced shower fires on the central carpet. Fig. 1 reports the cumulative signal detected by ARGO until February 2010, obtained with showers having multiplicity greater than 60. As anticipated in the introduction, the importance of Mrk421 rests basically in the strong variability of its emission. During the last four years, several flares lasting up to tens of days occurred. A short description of the results concerning each flare follows.

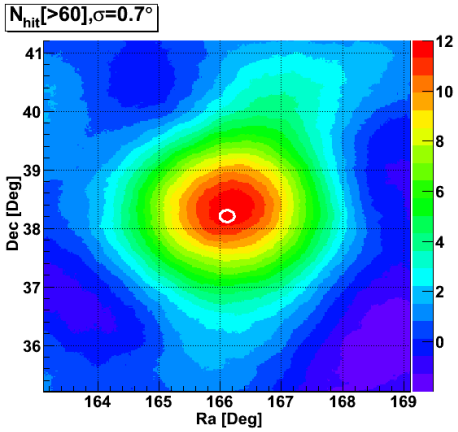


Figure 1: *Showers excess observed by ARGO-YBJ from Mrk421 (nominal position: white circle). It is obtained with events firing more than 60 pads within the central carpet. The angular resolution is about* $0.7^\circ$ *degrees and the reached significance is about 12 s.d. (see the color scale).*

### 3.1 The July 2006 flare

It was a long flare, starting in mid-June and lasting up to the first days of September. The most active phase was observed in July, with a strong correlation with X-rays emission. The detection significance was 6 s.d. and the mode energy 500 GeV. The emission corresponded to $3 \div 4$ times the Crab flux intensity at the same energies.

### 3.2 The June 2008 flare

It was the first flare observed by ARGO-YBJ in stable data taking. Two flaring episodes were reported, in June 3-8 and 9-15. The second flare was not observed at TeV energies by any Cherenkov telescope, hampered by the moonlight, but ARGO-YBJ was able to collect data, contributing to the multiwavelength campaign [7] that was organized on purpose. The results are summarized in fig. 2.

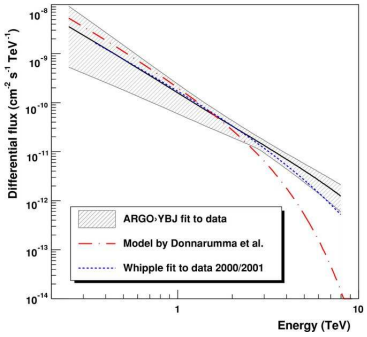


Figure 2: *Energy spectrum of Mrk421 emission as measured by ARGO-YBJ. It is compared with recent theoretical predictions and previous measurements* [8].

### 3.3 The February 2010 flare

On February, $16^{th}$ 2010, it took ARGO-YBJ only 6 hours to detect a 5 s.d. significant signal from Mrk421. Positive detections occurred in the following three days too. It was the first time an array-like EAS experiment reached such sensitivities in $\gamma$-ray astronomy. Altough further analyses are needed to take conclusions, the energy spectrum looked exceptionally softer, thus feeding the discussion in [4].

## 4 Correlations with X-ray emission

Fig. 3 illustrates the correlation between the TeV emission from Mrk421 obvserved by ARGO-YBJ and the X-rays fluxes reported by satellites in the same time. Both plots report the cumulative event rate from ARGO-YBJ as a function of time (red points). Integral fluxes in soft (left plot) and hard X-ray (right plot) are also reported (black lines). There is evidence that the VHE signal is more correlated with the hard X component than with the soft X. Deeper studies are in progress to understand the implications of such observations on the emission models.

## 5 Conclusions

ARG0-YBJ successfully monitored the VHE emission of Mrk421 over the last four years. In this period, three major flaring phases were observed, down to daily timescale, completing the experimental dataset available to the scientific

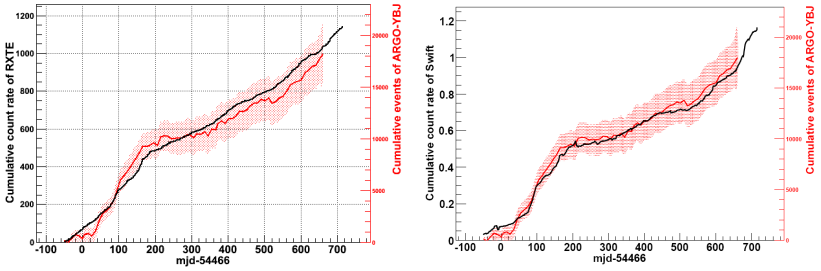


Figure 3: *Cumulative event rate from Mrk421 measured by ARGO-YBJ as a function of the time. In the left plot a comparison with the soft X-ray emission* ($2 \div 12 keV$) *is reported (http://heasarc.nasa.gov/docs/swift/swiftsc.html). In the right plot a comparison with the hard X-ray emission* ($15 \div 50 keV$) *is reported (http://heasarc.gsfc.nasa.gov/docs/xte/XTE.html).*

community. Some hints on a possible correlation of the TeV emission with the hard X-ray emission were found. Further analyses are in progress.

## 6 Acknowledgements

This work is supported in China by NSFC (Contract No. 10120130794), the Chinese Ministry of Science and Technology, the Chinese Academy of Sciences, the Key Laboratory of Particle Astrophysics, CAS, and in Italy by the Istituto Nazionale di Fisica Nucleare (INFN) and the Ministero dellIstruzione, dellUniversita e della Ricerca (MIUR).

## References

1. Punch, M., et al., *Nature* **358** (1992) 477.
2. Fossati, G., et al., *ApJ* **677** (2008) 906.
3. Wagner, R. M. *PoS (BLAZARS2008)* **63** (2008) 013 (arXiv:0809.2843).
4. Krennrich, F., et al.,*ApJ* **575** (2002) L9.
5. G. Aielli et al., *NIM* **A562** (2006) 92.
6. G. Di Sciascio et al., *Proc. 30th ICRC* (2007) (preprint: arXiv:0710.1945).
7. G. Aielli et al., *ApJ Letters* **714** (2010) 208.
8. Donnarumma, I., et al., *ApJ* **691** (2009) L13.

Frascati Physics Series Vol. LI (2010), pp. 37-42
2nd Young Researchers Workshop: Physics Challenges in the LHC Era
Frascati, May 10 and 13, 2010

# STUDY OF THE DECOHERENCE OF ENTANGLED KAONS BY THE INTERACTION WITH THERMAL PHOTONS

Izabela Balwierz
*Jagiellonian University, Institute of Physics, Krakow, Poland*

Wojciech Wislicki
*A. Soltan Institute for Nuclear Studies, Warszawa, Poland*

Pawel Moskal
*Jagiellonian University, Institute of Physics, Krakow, Poland*

**Abstract**

The KLOE-2 detector is a powerful tool to study the temporal evolution of quantum entangled pairs of kaons. The accuracy of such studies may in principle be limited by the interaction of neutral kaons with thermal photons present inside the detector. Therefore, it is crucial to estimate the probability of this effect and its influence on the interference patterns. In this paper we introduce the phenomenology of the interaction of photons with neutral kaons and present and discuss the obtained quantitative results.

## 1 The interaction frequency between thermal photons and neutral kaons

Interaction between $K^0$ meson and thermal photons may remain undetected inside the KLOE-2 detector and constitute the background process where quantum coherence is destroyed.

To estimate the probability of this interaction, we assume in the calculations that photons are in a room temperature and $K^0$ is moving with respect to the laboratory frame with the energy obtained in the $\phi \to K^0\bar{K}^0$ decay.

Meson $K^0$ is electrically neutral but it has inner electromagnetic structure so it can interact with photons. We are interested in interactions in which $K^0$ is observed in a final state. The main process is the inverse Compton effect, that is photon scattering on kaon in which photon's energy increases and kaon's decreases. The total number of photons scattered on a kaon in time unit is given by:

$$\frac{dN}{dt} = \frac{1}{\gamma}\frac{dN^*}{dt^*} = \frac{c}{\gamma}\int dn^*\sigma^*_{\gamma K}(k^*), \tag{1}$$

where $\gamma$ is the Lorentz factor, $c$ the velocity of light and $\sigma_{\gamma K}$ denotes the cross section for $\gamma K^0$ Compton scattering. Superscript „$*$" indicates the rest frame of $K^0$ meson. We denote by $dn$ number of photons in unit of volume in the $dk$ energy interval, given by:

$$dn = \frac{1}{4\pi^3}\cdot\frac{k^2 dk d\phi \sin\theta d\theta}{e^{\frac{k}{k_B T}} - 1}. \tag{2}$$

The above formula was obtained assuming that the photon distribution is given by the Planck's law of black-body radiation in the temperature T. Here $\theta$ stands for the polar angle between the incoming photon and the velocity of kaon, and $k_B$ is the Boltzmann constant.

The cross section $\sigma_{\gamma K}$ for the $\gamma K^0$ Compton scattering can be obtained from the cross section for the radiative scattering of the kaon in electromagnetic fields of nuclei, known as the Primakoff effect, and is given by [1]:

$$\frac{d\sigma^*_{\gamma K}(k^*,\theta^*)}{d\cos\theta^*} = \frac{2\pi\alpha_f}{m_K}\frac{k^{*2}\Big(\alpha_K(1+\cos^2\theta^*) + 2\beta_K\cos\theta^*\Big)}{\Big(1+\frac{k^*}{m_K}(1-\cos\theta^*)\Big)^3}, \tag{3}$$

where $m_K$ is the $K^0$ mass and $\alpha_f$ the fine-structure constant. The $\alpha_K$ and $\beta_K$ stand for the electric and magnetic polarizability of $K^0$. These quantities characterize susceptibility of the $K^0$ to the electromagnetic field. Taking into account the Lorentz transformation of the photon energy from the laboratory frame to the rest frame of $K^0$:

$$k^* = \gamma k(1-\beta\cos\theta)) \tag{4}$$

and the Lorentz invariance of $dn/k$, one gets the transformation of the density of photons:

$$dn^* = dn(1 - \beta\cos\theta)\gamma, \tag{5}$$

where $\beta$ is the velocity of $K^0$ with respect to the laboratory frame. Using consecutively equations (5), (2) and (4) and knowing that $\int_0^{2\pi} d\phi = 2\pi$, the formula for the interaction frequency (1) reads (where $u = \cos\theta$):

$$\frac{dN}{dt} = \frac{c}{2\pi^2}\int_0^\infty dk \frac{k^2}{e^{\frac{k}{k_B T}} - 1}\int_{-1}^1 du \cdot (1 - \beta u) \cdot \sigma^*_{\gamma K}(\gamma k(1 - \beta u)). \tag{6}$$

## 2 Units and values of parameters

Numerical values of parameters $\alpha_K$ and $\beta_K$ used in equations in the last paragraph are equal to $\alpha_K = 2.4 \cdot 10^{-49}$ m$^3$ and $\beta_K = 10.3 \cdot 10^{-49}$ m$^3$ [2]. Values for $\alpha_f, m_K, k_B$ and $c$ are taken from Particle Data Group [3]. Temperature is assumed to be 300K.

In natural units, the conversion eV $\rightarrow$ m should be done in the following way: eV $= (197.33 \cdot 10^{-9}$ m$)^{-1}$, so the unit of (6) is:

$$\left[\frac{dN}{dt}\right] = \mathrm{m}^4 \cdot \mathrm{eV}^4 \cdot \frac{1}{\mathrm{s}} = 6.595 \cdot 10^{26}\frac{1}{\mathrm{s}}. \tag{7}$$

In the case of the $\phi \rightarrow K^0\bar{K}^0$ decay the kinetic energy of kaons in the laboratory frame is equal to ca. $E = 12$ MeV, corresponding to:

$$\gamma = \tfrac{E+m_K}{m_K} = 1.02412, \qquad \beta = \sqrt{1 - \tfrac{1}{\gamma^2}} = 0.21573.$$

## 3 Calculation of the cross section for inverse Compton scattering of $\gamma$ on $K^0$

The total cross section $\sigma_{\gamma K}$ may be obtained by integrating (3) over the $\cos\theta^*$. In order to simplify the calculations we will introduce the notation $\cos\theta^* = x$ and $u = -m - k^* + k^*x$:

$$\begin{aligned}\sigma^*_{\gamma K}(k^*, u) &= 2\pi\alpha_f m^2\Big(\alpha_K \int \frac{-k^{*2} - (m + k^*)^2 - u^2 - 2u(m + k^*)}{k^* u^3} du + \\ &+ 2\beta_K \int \frac{-m - k^* - u}{u^3} du\Big).\end{aligned} \tag{8}$$

After calculating $\sigma^*_{\gamma K}(k^*, u)$ and replacing $u = -m - k^* + k^* x$, we integrate it over $x$ in the interval $[-1, 1]$. As a result we get:

$$\begin{aligned}\sigma^*_{\gamma K}(k^*) &= \sigma^*_{\gamma K}(k^*, x\,|^1_{-1}) = \frac{2\pi\alpha_f}{k^*(m+2k^*)^2}\Big(2k^*(2(\alpha_K+\beta_K)k^{*3} + \\ &- 3\alpha_K m^2 k^* - \alpha_K m^3) + \alpha_K m^2(2k^*+m)^2(\ln\frac{m+2k^*}{m})\Big). \quad (9)\end{aligned}$$

## 4 Calculation of interaction frequency

Now we put equation (9) from the previous section into formula for $\frac{dN}{dt}$ (6). The integrand for $\frac{dN}{dt}$, multiplied by the unit conversion constant (7), is shown in Figure 1.

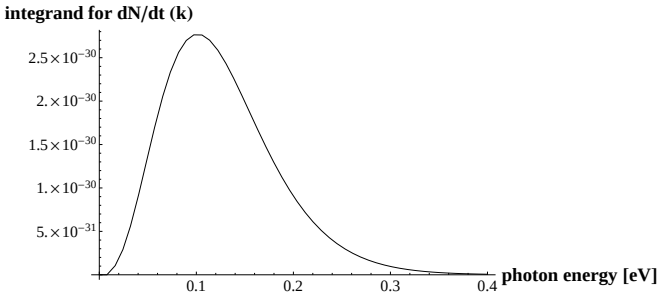


Figure 1: *Integrand for* $\frac{dN}{dt}(k)$

Finally integrating numerically $\frac{dN}{dt}$ over $k$ we obtain:

$$\frac{dN}{dt} = 3.7 \cdot 10^{-31}\frac{1}{s}$$

### 4.1 Numerical stability

Integral calculated in this chapter is quite sensitive to the numerical accuracy and have to be treated with caution. The graph below shows the value of the whole integral $\frac{dN}{dt}$ (6) with respect to the numerical precision (number of significant digits). One can see from it, that when we reach sufficient precision, the result stabilizes.

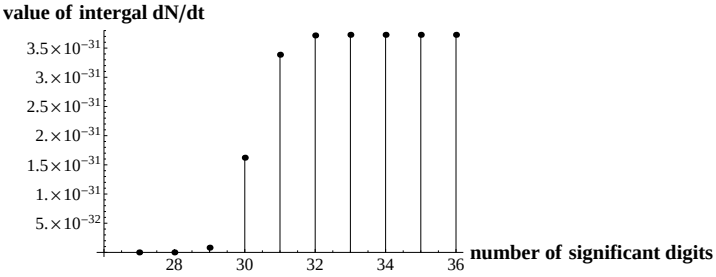


Figure 2: *Value of integral dN/dt*

## 4.2 Investigation on systematic errors

Although the interaction probability is small, the systematic error on it was estimated. Obvious sources of systematics are uncertainty of $\alpha_K$ and $\beta_K$ and variation of temperature.

The first one was estimated using values of $\alpha_K$ and $\beta_K$, derived using different methods in papers [4] and [5]. The result obtained in this paragraph was calculated using kaon polarizabilities taken from the paper [2]. Points on the graph 3a correspond to the different combinations of $\alpha_K$ and $\beta_K$. Figure 3b illustrates how the result changes due to the room temperature variations in the range of 20K around value of 300K.

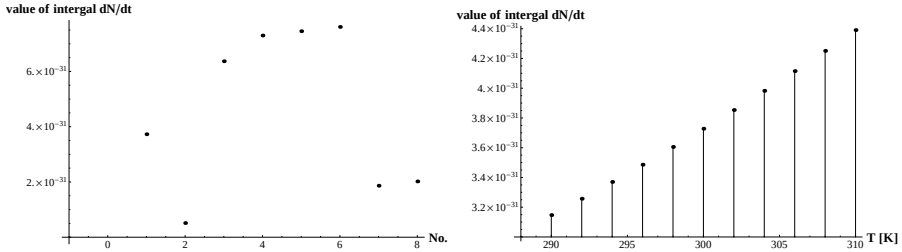


Figure 3: *a) Values of integral for different $\alpha_K$ and $\beta_K$ parameters. b) Values of integral as a function of temperature.*

Depending on the assumed values of $\alpha_K$, $\beta_K$ and temperature, the $\frac{dN}{dt}$ varies from about $5{\cdot}10^{-32}$ to $7.5{\cdot}10^{-31}$ so by more than one order of magnitude. However, as we will see in the next paragraph, this difference is not significant for the parameters of decoherence of kaon pairs at KLOE-2 detector.

## 5 Physical interpretation

Kaon is moving with velocity equal to ca. $v = 0.6 \cdot 10^8 \frac{\mathrm{m}}{\mathrm{s}}$ with respect to the laboratory frame. From the place of its creation to the calorimeter it moves through about 2.5m so it needs for it about $4.2 \cdot 10^{-8}$s. Because the frequency of the Compton interaction is $3.7 \cdot 10^{-31} \frac{1}{\mathrm{s}}$ so probability of the interaction is:

$$P = 1.5 \cdot 10^{-38}$$

This background stays small with respect to the statistical uncertainty of decoherence parameters expected in KLOE-2 [6].

## 6 Acknowledgements

We acknowledge support by Polish Ministry of Science and Higher Education through the Grant No. 0469/B/H03/2009/37.

## References

1. M.A. Moinester, V. Steiner, e-Print: arXiv:hep-ex/9801008v3, 7 (1998).
2. D. Ebert, M.K. Volkovy, T. Feldmann, Intern. Journal of Modern Phys. A **12**, 4408 (1997).
3. Particle Data Group: http://pdg.lbl.gov
4. J. Christensen, W. Wilcox, F.X. Lee, L. Zhou, Phys. Rev. D **72**, 9-10 (2005).
5. M. A. Ivanov, T. Mizutani, Phys. Rev. D **45**, 1590 (1992).
6. G. Amelino-Camelia *et al.*, e-Print: arXiv:1003.3868v3 [hep-ex], 14 (2010).

Frascati Physics Series Vol. LI (2010), pp. 43-48
2nd Young Researchers Workshop: Physics Challenges in the LHC Era
Frascati, May 10 and 13, 2010

# INVESTIGATIONS OF THE TIME INTERVAL DISTRIBUTIONS BETWEEN THE DECAYS OF QUANTUM ENTANGLED NEUTRAL KAONS

Tomasz Twaróg
*Jagiellonian University, Institute of Physics, Kraków, Poland*

**Abstract**

One of the physics issues to be investigated in KLOE-2 experiment [1)] is the time evolution of quantum entangled neutral kaons. Studies of kaons' decay times distributions enable us to test $CPT$ symmetry and quantum mechanics (QM). In this article it is shown how these distributions can be obtained on the basis of QM. It is also discussed how $CPT$ and QM violations can manifest themselves in the interference patterns of entangled kaons which will be measured by means of the KLOE-2 detector setup.

## 1 Introduction

Neutral kaons were particles for which $CP$ [2)] and $T$ [3)] violations were first observed. Then it should not come as a surprise that they are promising candidates in the search of $CPT$ noninvariance. At the same time neutral kaons enable us to test QM, for instance through decoherence tests.

## 2 Hamiltonian

Neutral kaon's time evolution can be described as:

$$|K(t)\rangle = a(t)\left|K^0\right\rangle + b(t)\left|\bar{K}^0\right\rangle + \sum_j c_j(t)\left|f_j\right\rangle, \tag{1}$$

where the sum is over all final states $|f_j\rangle$ a kaon may decay to and functions $a$ and $b$ obey the Schrödinger-like equation with effective Hamiltonian $\mathbf{H}$: [4)]

$$i\frac{\partial}{\partial t}\begin{pmatrix} a(t) \\ b(t) \end{pmatrix} = \mathbf{H}\frac{\partial}{\partial t}\begin{pmatrix} a(t) \\ b(t) \end{pmatrix}. \tag{2}$$

$\mathbf{H}$ can be divided into its hermitian and antihermitian parts:

$$\mathbf{H} = \mathbf{M} - \frac{i}{2}\mathbf{\Gamma} = \begin{pmatrix} M_{11} & M_{12} \\ M_{12}^* & M_{22} \end{pmatrix} - \frac{i}{2}\begin{pmatrix} \Gamma_{11} & \Gamma_{12} \\ \Gamma_{12}^* & \Gamma_{22} \end{pmatrix}, \tag{3}$$

where $\mathbf{M}$ and $\mathbf{\Gamma}$ are hermitian and are called mass and decay matrices. The eigenvectors of $\mathbf{H}$ are found to be: [4)]

$$\begin{aligned} |K_S\rangle &= \frac{1}{\sqrt{2\left(1+|\epsilon_S^2|\right)}}\cdot\left[(1+\epsilon_S)\left|K^0\right\rangle + (1-\epsilon_S)\left|\bar{K}^0\right\rangle\right], \\ |K_L\rangle &= \frac{1}{\sqrt{2\left(1+|\epsilon_L^2|\right)}}\cdot\left[(1+\epsilon_L)\left|K^0\right\rangle - (1-\epsilon_L)\left|\bar{K}^0\right\rangle\right]. \end{aligned} \tag{4}$$

Here $\epsilon_S$ and $\epsilon_L$ are two small parameters measuring CP violation. One can define another two variables:

$$\bar{\epsilon} \stackrel{def}{=\!=} \frac{\epsilon_S + \epsilon_L}{2}, \qquad \delta \stackrel{def}{=\!=} \frac{\epsilon_S - \epsilon_L}{2}. \tag{5}$$

Parameter $\bar{\epsilon}$ measures average $CP$ violation for $K_L$ and $K_S$, while $\delta$ is a $CPT$-violating parameter.

## 3 Final states amplitudes and double decay rate

At KLOE, neutral kaons are produced in $\Phi$ meson decay, $J^{PC} = 1^{--}$. To conserve the eigenvalues of $P$ and $C$, the (normalized) initial state of the two kaons, written in the $\Phi$ rest frame, has to be:

$$|i\rangle = \frac{1}{\sqrt{2}}\{\left|K^0(-\vec{p})\right\rangle\left|\bar{K}^0(+\vec{p})\right\rangle - \left|\bar{K}^0(-\vec{p})\right\rangle\left|K^0(+\vec{p})\right\rangle\} = \tag{6}$$

$$= \frac{N}{\sqrt{2}}\{|K_S(+\vec{p})\rangle\,|K_L(-\vec{p})\rangle - |K_L(+\vec{p})\rangle\,|K_S(-\vec{p})\rangle\}, \tag{7}$$

where $N$ is a normalization factor and is close to 1.

Given eq.(7), one can calculate a general formula for the double decay rate. Following QM rules, the decay amplitude of the two kaons forming the state (7) into final states $f_1$ and $f_2$ at times $t_1$ and $t_2$ and directions $+\vec{p}$ and $-\vec{p}$ respectively can be expressed as:

$$\begin{aligned} A\left(f_1,t_1;f_2,t_2\right) &= \frac{N}{\sqrt{2}}\{\left\langle f_1\left|T\right|K_S\left(t_1\right)\right\rangle\left\langle f_2\left|T\right|K_L\left(t_2\right)\right\rangle + \\ &\quad -\left\langle f_1\left|T\right|K_L\left(t_1\right)\right\rangle\left\langle f_2\left|T\right|K_S\left(t_2\right)\right\rangle\} = \\ &= \frac{N}{\sqrt{2}}\{\left\langle f_1\left|T\right|K_S\right\rangle\left\langle f_2\left|T\right|K_L\right\rangle e^{-im_S t_1}e^{-\frac{1}{2}\Gamma_S t_1}e^{-im_L t_2}e^{-\frac{1}{2}\Gamma_L t_2}+ \\ &\quad -\left\langle f_1\left|T\right|K_L\right\rangle\left\langle f_2\left|T\right|K_S\right\rangle e^{-im_L t_1}e^{-\frac{1}{2}\Gamma_L t_1}e^{-im_S t_2}e^{-\frac{1}{2}\Gamma_S t_2}\}, \end{aligned} \tag{8}$$

where $T$ is an operator whose explicit form is unknown, but also not needed here. From (8) one finds the double decay rate into $f_1$, $f_2$ at times $t_1$, $t_2$:

$$\begin{aligned} I\left(f_1,t_1;f_2,t_2\right) &= A\left(f_1,t_1;f_2,t_2\right)A^*\left(f_1,t_1;f_2,t_2\right) = \\ &= C_{12}\{\left|\eta_1\right|^2 e^{-\Gamma_L t_1-\Gamma_S t_2}+\left|\eta_2\right|^2 e^{-\Gamma_S t_1-\Gamma_L t_2}+ \\ &\quad -2\left|\eta_1\right|\left|\eta_2\right| e^{-\frac{\Gamma_S+\Gamma_L}{2}(t_1-t_2)}\cos\left[\Delta m\left(t_1-t_2\right)+\phi_2-\phi_1\right]\}, \end{aligned} \tag{9}$$

where the parameters $\eta_i$ and the constant $C_{12}$ are:

$$\eta_i = \left|\eta_i\right| e^{i\phi_i} \equiv \frac{\left\langle f_i\left|T\right|K_L\right\rangle}{\left\langle f_i\left|T\right|K_S\right\rangle}, \qquad C_{12} = \frac{\left|N\right|^2}{2}\left|\left\langle f_1\left|T\right|K_S\right\rangle\left\langle f_2\left|T\right|K_S\right\rangle\right|^2. \tag{10}$$

The double decay rate may be easier to compare to data when difference $\Delta t = t_1 - t_2$ is used instead of decay times $t_1$ and $t_2$:

$$\begin{aligned} I\left(f_1,f_2,\Delta t\geq 0\right) = \frac{C_{12}}{\Gamma_S+\Gamma_L}\{&\left|\eta_1\right|^2 e^{-\Gamma_L\Delta t}+\left|\eta_2\right|^2 e^{-\Gamma_S\Delta t}+ \\ &-2\left|\eta_1\right|\left|\eta_2\right| e^{-\frac{\Gamma_S+\Gamma_L}{2}\Delta t}\cos\left[\Delta m\Delta t+\phi_2-\phi_1\right]\}, \end{aligned} \tag{11}$$

and for $\Delta t < 0$ we get a similar formula, only with $\Delta t$ replaced by $|\Delta t|$ and subscripts 1 and 2 interchanged.

## 4 Quantum mechanics test

In the case when final states $f_1$ and $f_2$ are the same, eq.(11) is simplified:

$$\begin{aligned} &I\left(f_1=f_2,\Delta t\geq 0\right) = I\left(f_1=f_2,\Delta t\leq 0\right) = \\ &= \frac{C_{12}\left|\eta\right|^2}{\Gamma_S+\Gamma_L}\{e^{-\Gamma_L|\Delta t|}+e^{-\Gamma_S|\Delta t|}-2e^{-\frac{\Gamma_S+\Gamma_L}{2}|\Delta t|}\cos\left(\Delta m\left|\Delta t\right|\right)\}\ , \end{aligned} \tag{12}$$

where eta's subscript is omitted for simplicity. One easily checks that within the scope of quantum mechanics no events are expected in $\Delta t = 0$. This is very counterintuitive, as the two decays at the same time are space-like separated events and one could think that each kaon should behave independently of the other one. A behaviour like that is of the type first mentioned by Einstein *et al.* [5] This motivates an introduction of a decoherence parameter $\zeta$:

$$I\left(f_1,t_1;f_2,t_2\right) = C_{12}\{|\eta_1|^2\, e^{-\Gamma_L t_1-\Gamma_S t_2} + |\eta_2|^2\, e^{-\Gamma_S t_1-\Gamma_L t_2} + \\ - 2\left(1-\zeta\right)|\eta_1|\,|\eta_2|\, e^{-\frac{\Gamma_S+\Gamma_L}{2}(t_1-t_2)}\cos\left[\Delta m\left(t_1-t_2\right)+\phi_2-\phi_1\right]\}. \tag{13}$$

As it turns out, the parameter $\zeta$ is basis-dependent. [6] Current values of $\zeta$ in the two main bases, $\{|K_S\rangle, |K_L\rangle\}$ and $\{|K^0\rangle, |\bar{K}^0\rangle\}$, are: [7]

$$\zeta_{SL} = \left(0.3 \pm 1.8_{\text{stat}} \pm 0.6_{\text{syst}}\right)\cdot 10^{-2},\ \ \zeta_{0\bar{0}} = \left(1.4 \pm 9.5_{\text{stat}} \pm 3.8_{\text{syst}}\right)\cdot 10^{-7}. \tag{14}$$

Fig.1 illustrates the difference between the double decay rates for two values of $\zeta_{SL}$: $\zeta_{SL} = 0$ (QM case) and $\zeta_{SL} = 0.05$. From these plots one concludes that nonzero $\zeta_{SL}$ would manifest itself mainly in the region close to $\Delta t = 0$.

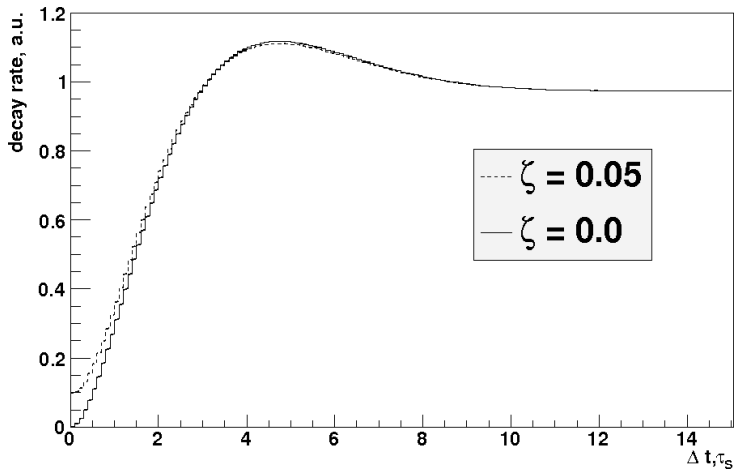


Figure 1: *Decay rate as a function of $\Delta t$ for eq.(13). The solid and dashed lines are for $\zeta_{SL} = 0$ and $\zeta_{SL} = 0.05$, respectively. The biggest discrepancy between these two functions is for $\Delta t$ close to 0.*

## 5 CPT invariance test

Let us now consider final states $f_1 = \pi^- l^+ \nu$ and $f_2 = \pi^+ l^- \bar{\nu}$. We assume that kaons obey a $\Delta S = \Delta Q$ rule, where $\Delta S$ is the difference of strangeness between final and initial states and $\Delta Q$ in this case is the charge of a pion. This assumption is justified, as the violation of this rule is predicted on the level of $10^{-7}$, [8] which is unmeasureable for current experiments. Commonly amplitudes for semileptonic decays (obeying $\Delta S = \Delta Q$) are defined as:

$$\left\langle \pi^- l^+ \nu \left| T \right| K^0 \right\rangle = a + b, \qquad \left\langle \pi^+ l^- \bar{\nu} \left| T \right| \bar{K^0} \right\rangle = a^* - b^*. \tag{15}$$

Combining eqs. (4), (10) and (15) one finds:

$$\eta_{l^+} \approx 1 - 2\delta, \qquad \eta_{l^-} \approx -1 - 2\delta, \tag{16}$$

with $\delta$ defined in eq.(5). The plot of decay intensity for chosen $f_1$ and $f_2$ is shown in Fig.2. The curves are for $\delta = 0$ and $\delta = 5 \cdot 10^{-4} + 0.05i$.

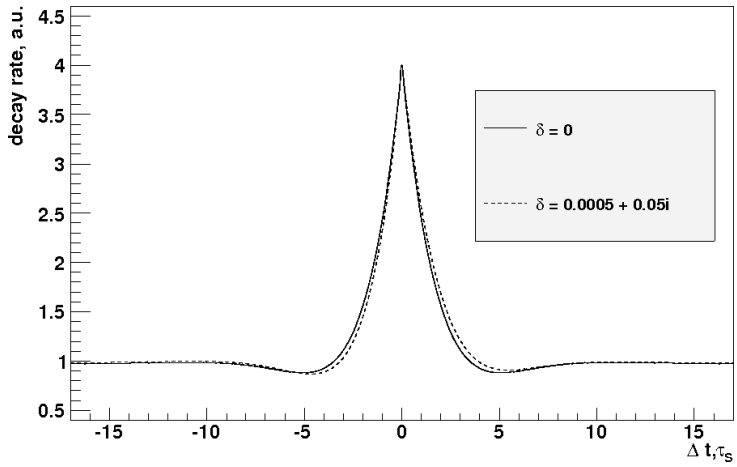


Figure 2: *Double decay rate for semileptonic final states with the choice* $f_1 = \pi^- l^+ \nu$ *and* $f_2 = \pi^+ l^- \bar{\nu}$. *Solid and dashed lines correspond to* $\delta = 0$ *and* $\delta = 5 \cdot 10^{-4} + 0.05i$, *respectively.*

The compilation of $\delta$ measurements from PDG [9] is compatible with no $CPT$ violation:

$$\Re\delta = (2.3 \pm 2.7) \cdot 10^{-4}, \qquad \Im\delta = (0.4 \pm 2.1) \cdot 10^{-5}. \tag{17}$$

## 6 Remarks

Two simple tests, one of quantum mechanics and one of $CPT$ invariance, have been described in this paper. This is just a small fraction of all the tests one can think of for quantum entangled kaons. There are numerous possible sources of this yet unknown physics. Examples are $CPT$ noninvariance due to Lorentz symmetry breaking [10] or simultaneous $CPT$ and QM violation through evolution of pure states into mixed states. [11] A very good review is provided in handbook from ref. 4. A system of quantum entangled kaons proves to be very effective in investigations of these phenomena.

## 7 Acknowledgements

I am indebted to Antonio Di Domenico, Paweł Moskal and Wojciech Wiślicki for the help in broadening my understanding of the physics of kaons. I acknowledge support by Polish Ministry of Science and Higher Education through the Grant No. 0469/B/H03/2009/37.

## References

1. G. Amelino-Camelia *et al.*, ePrint: arXiv:1003.3868[hep-ex].
2. J.H. Christenson *et al.*, Phys. Rev. Lett. **13**, 138 (1964).
3. A. Angelopoulos *et al.* (CPLEAR coll.), Phys. Lett. B **444**, 43 (1998)
4. A. Di Domenico, in *Handbook on neutral kaon interferometry at a* $\Phi$*-factory*, ed. A. Di Domenico, Frascati Physics Series Vol. XLIII, 1 (2007).
5. A. Einstein *et al.*, Phys. Rev. **48**, 73 (1935).
6. R.A. Bertlmann *et al.*, Phys. Rev. D **60**, 114032 (1999).
7. A. Di Domenico *et al.* (KLOE coll.), Found. Phys. **40**, 852 (2010).
8. M. Luke, Phys. Lett. B **256**, 265 (1991).
9. C. Amsler *et al.* (Particle Data Group), Phys. Lett. B **667**, 1 (2008).
10. R. Lehnert, in handbook from ref. 4, p. 131
11. P. Huet, M.E. Peskin, Nucl. Phys. B **434**, 3 (1995) and references therein.

Frascati Physics Series Vol. LI (2010), pp. 49-53
2nd Young Researchers Workshop: Physics Challenges in the LHC Era
Frascati, May 10 and 13, 2010

# MINSIS & MINIMAL FLAVOUR VIOLATION

Rodrigo Alonso de Pablo
*Departamento de Física Teórica*
*Universidad Autónoma de Madrid ,28049 Cantoblanco, Madrid, Spain*

**Abstract**

We explore the reach of future near detectors sensitive to $\nu_\tau$ appearance, such as the recently proposed MINSIS project, to further constrain neutrino mass models. A particularly simple neutrino Minimal Flavour Violation model will be analyzed in detail.

## 1 Short-Baseline Detectors

Neutrino oscillations are the first manifest evidence of physics beyond the Standard Model. The discovery of neutrino oscillations came through long-baseline experiments like Super-Kamiokande, a fact that made the scientific community abandon the short-baseline experiments for, with the measured mass difference, oscillations are unobservable at so short distances. The bounds on a signal from the first generation of short-baseline experiments (NOMAD, CHORUS) were

stablished with a sensitivity $\sim 10^{-4}$, and so they remain to date. The technology for a second generation of improved sensitivity experiments was actually available at the time but, as we said, abandoned.

The reason for this drawback for short-baseline experiments may however turn into its main advantage. In general, extensions of the Standard Model predict flavour violating processes other than oscillations that would appear at such experiments with negligible "oscillation background". In particular we will talk about MINSIS (Main Injector Non Standard Interacions Search), a project for a short-baseline experiment sensitive to $\nu_\mu \rightarrow \nu_\tau$ appearance at Fermilab. MINSIS would improve the sensitivity by two or three orders of magnitude.

## 2 Minimal Flavour Violation Seesaw Model

In our study of processes beyond the standard phenomenology we will use a simple Seesaw Model [1)] that accommodates the neutrino masses and also leads to successful leptogenesis [2)]. It is a Minimal Flavour Violation model for, as we will see, all the flavour violating processes can be traced back to the Yukawa couplings. We will not present it in detail for there is another discussion of it within this volume. Let us remind you the Lagrangian:

$$\mathcal{L} = \mathcal{L}_{SM} + \mathcal{L}_K + \mathcal{L}_I \tag{1}$$

$$\mathcal{L}_K = i\overline{N_R}\not{\partial}N_R + i\overline{N'_R}\not{\partial}N'_R \tag{2}$$

$$\mathcal{L}_I = -([\overline{N_R}Y\tilde{\phi}^\dagger l_L + \overline{N'_R}\epsilon Y'\tilde{\phi}^\dagger l_L + \tfrac{\Lambda}{2}\overline{N_R^c}N'_R] + h.c.) \tag{3}$$

Here the $l_L$ are the lepton weak doublets and $\phi$ is the Higgs doublet. We have omitted the flavour indices in the Lagrangian, each lepton has an index and the Yukawa couplings also carry a flavour index, they are three-component vectors.

In this model we add to the matter content the two heavy right handed neutrinos $N_R, N'_R$ only, with a mass scale $\Lambda$ not necessarily in the GUT scale, but may be as low as the $TeV$ scale. The simultaneous presence of both Yukawa couplings and the majorana mass term breaks global lepton number. The Yukawa $Y'$ interaction is regarded as a small term characterising the breaking of such symmetry and giving rise to neutrino masses.

After integrating out the heavy right handed neutrino fields we obtain

a series of non-renormalizable operators. The first of them is Weinberg's Operator, with flavour structure given by the Yukawas. Such flavour structure determines the mass matrix (up to a constant), and can be related to the $U_{PMNS}$ matrix. One of the most remarkable features of this model is that the connection of high and low energy parameters determines the Yukawa couplings almost (up to a constant again) completely. Explicitly:

$$\begin{pmatrix} Y_e \\ Y_\mu \\ Y_\tau \end{pmatrix} \simeq y \begin{pmatrix} e^{i\delta}s_{13} + e^{-i\alpha}s_{12}r^{1/4} \\ s_{23}(1-\frac{\sqrt{r}}{2}) + e^{-i\alpha}r^{1/4}c_{12}c_{23} \\ c_{23}(1-\frac{\sqrt{r}}{2}) - e^{-i\alpha}r^{1/4}c_{12}s_{23} \end{pmatrix} \tag{4}$$

With $r = \frac{\Delta m^2_{solar}}{\Delta m^2_{atm}}$ and for normal hierarchy. This will be of great use when we study the phenomenology of the theory; our parameter space has reduced to the $\theta_{13}$ angle, the majorana phase $\alpha$, the CP-violating phase $\delta$, and the scale $y/\Lambda$, where $y$ is the undetermined constant in the Yukawa couplings.

## 3 Dimension 6 Operator and Non-Unitarity

But the relevant phenomenology in this study comes from higher dimension operators. The next operator generated is a dimension 6 operator which, after Electro-Weak symmetry breaking, has the form[1]:

$$\delta\mathcal{L}^{d=6} = \frac{v^2}{\Lambda^2} Y_\alpha Y^*_\beta \overline{\nu^\alpha_L} i\not{\partial} \nu^\beta_L \tag{5}$$

This is a correction for the kinetic term of the neutrions for, of course, we already had a kinetic term for them in $\mathcal{L}_{SM}$. To see what it implies let us start from the mass basis ($\nu'$) and make a transformation to the flavour ($\nu$) basis: $\nu_\alpha = N_{\alpha i}\nu'_i$.

$$i\overline{\nu'_L}\not{\partial}\nu'_L \quad \rightarrow \quad i\overline{\nu_L}(N^{-1})^\dagger \not{\partial} N^{-1}\nu_L \tag{6}$$

$$NN^\dagger \simeq \mathbb{1} - \frac{v^2}{\Lambda^2}YY^\dagger \quad \Rightarrow \quad N \simeq U_{PMNS}\left(\mathbb{1} - \frac{v^2}{2\Lambda^2}YY^\dagger\right) \tag{7}$$

The dimension 6 operator induces non-unitarity in the leptonic mixing matrix. But such prediction is constrained because the mixing matrix is unitary as far as we know. The strongest constraint in this regard comes from (the null results on) the rare decay $\mu \rightarrow e\gamma$. This is because non-unitarity prevents the usual G.I.M. cancellation for the amplitude of such process.

[1] $v$ stands for the Higgs vacuum expectation value

## 4 MINSIS

It is straightforward to calculate our model's predictions for an experiment such as MINSIS. If unitarity is no longer preserved the flavour eigenstates are no longer orthogonal, this means that the flavour eigenstate $\mu$ has a small but nonzero projection on the $\tau$ eigenstate. Then a simple algebraic computation gives us the result for $\nu_\mu \to \nu_\tau$ appeareance at zero distance:

$$P_{\mu\tau}(L=0) = \frac{\left|NN^\dagger_{\mu\tau}\right|^2}{\left|NN^\dagger_{\mu\mu}NN^\dagger_{\tau\tau}\right|} \simeq \left|NN^\dagger_{\mu\tau}\right|^2 \tag{8}$$

In our model, non-unitarity is given by the Yukawa couplings, so we can write it in terms of the free parameters: $yv/\Lambda$, $\theta_{13}$ ,$\alpha$, $\delta$. We will look at how MINSIS would restrict the scale $\Lambda/y$ for different values of the other parameters. By doing so we find that there are regions (for $\theta_{13} > 0$) in the parameter space where MINSIS would better constrain the model. This is shown on figure 1 where we plot the upper bounds on the inverse scale $yv/\Lambda$ squared and a region in the $\alpha - \delta$ plane where MINSIS would improve the present data.

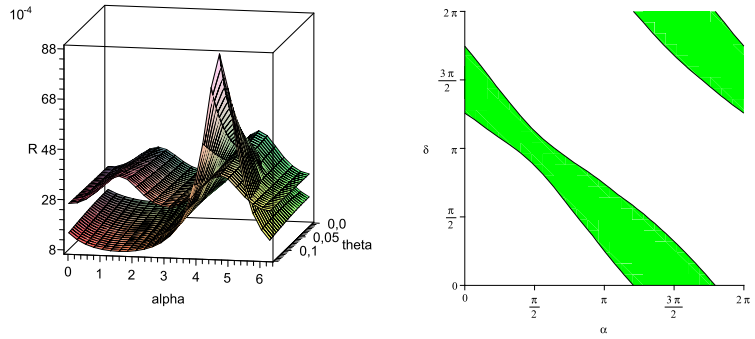


Figure 1: The left figure is a comparison of the bounds on $R = y^2v^2/\Lambda^2$ coming from $\mu \to e\gamma$ (lower sheet in most of the plot) and the expected bound from MINSIS plotted for the allowed values of $\theta_{13}$ and the majorana phase. To the right we see in green the unexplored region in the $\alpha$-$\delta$ plane that MINSIS would reach (for $\theta_{13} = 6.8 \pm 3.6\,^\circ$)

The reason for MINSIS surpassing the strong bounds from the rare decay $\mu \to e\gamma$ is that in these regions there is a vanishing $Y_e$, a fact that restores unitarity for the $e$ leptons, such that any zero distance flavour violating process involving an $e$ lepton is further supressed. This unexpected feature may be strange but showed us that such a setup is an open possibility.

## 5 Conclusion

Our study of the prospects for near detectors, in particular MINSIS, lead us to conclude that they stand as reasonable candidates to discover non standard phenomena. They represent an ideal setup for the appeareance of new flavour violating phenomena, predicted not only in our model but in most of the Standard Model extensions. Within this frame, MINSIS would explore a transition with large room for improvement, lowering two or three orders of magnitude the present measurement's precision. Furthermore, as our study showed us, it may be an accesible window for new physics competitive with other higher sensitivity experiments.

## 6 Acknowledgements

I would like to thank Belén Gavela for introducing me to the subject. I would also like to thank Pilar Hernández and Tracey Li for useful discussions. I am grateful with the organization of the 2nd Young Researchers Workshop for having me.

## References

1. M. B. Gavela, T. Hambye, D. Hernández and P. Hernández, JHEP **0909**, 038 (2009) [arXiv:hep-ph/0906.1461].

2. S. Blanchet, T. Hambye and F. Josse-Michaux JHEP **1004**, 023 (2010)[arXiv:hep-ph/0912.3153].

3. M.C. Gonzalez-García, M. Maltoni and J. Salvado, JHEP **1004**, 056 (2010) [arXiv:hep-ph/1001.4524].

Frascati Physics Series Vol. LI (2010), pp. 55-60
2nd Young Researchers Workshop: Physics Challenges in the LHC Era
Frascati, May 10 and 13, 2010

# THE FLAVOUR OF SEESAW

Daniel Hernandez
*Theoretical Physics Department, Universidad Autnoma de Madrid*

**Abstract**

Minimal Flavour Violation in the lepton sector is presented. It is explored whether it is compatible with a) neutrino mass generation at tree level (Seesaw models) and b) a separation of the scales at which lepton number and flavour violation occur. We present an extremely simple model of neutrino masses, compatible with MFV, in which the full high-energy couplings can be reconstructed from the low energy observables, including CP-violating phases.

## 1 Neutrino masses and Minimal Flavour Violation

Neutrino masses constitute the first evidence of physics beyond the Standard Model (SM) testable in the laboratories. New physics leading to neutrino masses is also necessarily new flavour physics. It is interesting then to assess whether it is possible to predict other types of new flavour physics in the lepton

sector beyond neutrino oscillations. However, new effects are expected to be undetectable if the scale of new physics is orders of magnitude above the TeV, as it is generally required for neutrino mass generation.

In the other hand, it is possible for a theory of new physics to have two different fundamental energy scales: one responsible for the suppression of the dimension five ($d = 5$) Weinberg's effective operator that leads to neutrino masses and a second one suppressing the $d = 6$ operators responsible for exotic flavour processes. This is represented in an effective Lagrangian of the form

$$\mathcal{L} = \mathcal{L}_{SM} + \frac{\alpha^{d=5}}{\Lambda_{LN}}\mathcal{O}^{d=5} + \sum_i \frac{\alpha_i^{d=6}}{\Lambda_{FL}^2}\mathcal{O}_i^{d=6} + ... \qquad (1)$$

where the effective scales $\Lambda_{FL}$ and $\Lambda_{LN}$ take care of the suppressions of each type of contribution and $\Lambda_{LN} \gg \Lambda_{FL}$ is required to obtain simultaneuosly tiny neutrino masses and sizable flavour processes. Since the $d = 5$ operator violates global Lepton Number (LN) symmetry, it is plausible that $\Lambda_{FL}$ is protected from corrections of order $\Lambda_{LN}$.

However, generic $d = 6$ coefficients are very well constrained leading to bounds $\Lambda_{FL} \gtrsim 10^{2-4}$ TeV. This contradicts the fact that the Hierarchy Problem points to new physics around the TeV. This issue can be adressed by adding the so called *Minimal Flavour Violation* hypothesis into the game which effectively lowers the scale of new flavour physics down to the TeV [1]. Minimal Flavour Violation (MFV) is the assumption that all the flavour dynamics in the fundamental theory is carried precisely by the Yukawas of the SM, instead of the latter just being the manifestation of flavour at low energies. The coefficients of any flavour charged effective operator in the low energy theory, such as $\alpha^{d=5}$ and $\alpha^{d=6}$, must then be formed by a combination of those Yukawas. Therefore, we get more than what we asked for. MFV not only lowers the scale of new flavour physics but also implies that relations must exist between neutrino masses and mixings and rare flavour processes.

## 2 MFV in scalar mediated seesaw models

The scalar seesaw mechanism of neutrino mass generation illustrates the MFV separation of scales. This model in its basic form adds only one scalar $\Delta$, triplet of $SU(2)$. The most general Lagrangian that can be written with $\Delta$ and the

SM fields is

$$\mathcal{L}_\Delta = (D_\mu \Delta)^\dagger (D^\mu \Delta) + \left( \widetilde{\overline{L_{\rm L}}} Y_\Delta (\tau \cdot \Delta) L_{\rm L} + \mu_\Delta \widetilde{\phi}^\dagger (\tau \cdot \Delta)^\dagger \phi + \text{h.c.} \right) - \Delta^\dagger {M_\Delta}^2 \Delta$$
$$- \frac{\lambda_2}{2} \left(\Delta^\dagger \Delta\right)^2 - \lambda_3 \left(\phi^\dagger \phi\right) \left(\Delta^\dagger \Delta\right) - \frac{\lambda_4}{2} \left(\Delta^\dagger T^i \Delta\right)^2 - \lambda_5 \left(\Delta^\dagger T^i \Delta\right) \phi^\dagger \tau^i \phi \,, \quad (2)$$

with $\tilde{\phi} \equiv i\tau^2 \phi$, $T_i$ being the three-dimensional representation of the $SU(2)$ generators and $\tau_i$ the Pauli matrices. The coexistence of $Y_\Delta$ and $\mu_\Delta$ explicitly breaks lepton number, inducing at low energies the Weinberg operator:

$$\delta \mathcal{L}^{d=5} = c_{\alpha\beta}^{d=5} \left( \overline{L^c_{L\alpha}} \tilde{\phi}^* \right) \left( \tilde{\phi}^\dagger \, L_{L\beta} \right) + \text{h.c.} \,, \quad (3)$$

with

$$c_{\alpha\beta}^{d=5} = 2 Y_{\Delta\,\alpha\beta} \, \frac{\mu_\Delta}{M_\Delta^2} \,, \quad (4)$$

As for the generated $d = 6$ operators, there is only one at tree level which involves leptons

$$\delta \mathcal{L}^{d=6} = c_{\alpha\beta\gamma\delta}^{d=6} \left( \overline{L_{L\beta}} \gamma_\mu L_{L\delta} \right) \left( \overline{L_{L\alpha}} \gamma_\mu L_\gamma \right) \,, \quad (5)$$

with

$$c_{\alpha\beta\gamma\delta}^{d=6} = - \frac{1}{M_\Delta^2} {Y_\Delta}^\dagger_{\alpha\beta} Y_{\Delta\,\delta\gamma} \,. \quad (6)$$

The scalar seesaw is a concrete model whose low-energy effective theory is such that if we know the flavour structure of the $d = 5$ coefficient, then the $d = 6$ one is completely determined [2]. This is well known.

The flavour breaking scale $\Lambda_{FL}$ is simply the mass of the triplet. The lepton number violating scale $\Lambda_{LN}$ is a bit subtler since it doesn't correspond to the mass of any new particle. The $\Lambda_{LN}$ scale in eq. (1) would correspond instead to the combination $\Lambda_{LN} \sim M_\Delta^2 / \mu_\Delta$. Furthermore, a small value for $\mu_\Delta$ is stable since setting it to zero restores the lepton number symmetry. This allows for $\Lambda_{FL} \sim$ TeV and protects $\Lambda_{LN} \gg \Lambda_{FL}$ as desired.

## 3 MFV in fermionic seesaws. A simple model

If we consider enlarging the SM with fermions then, in order to achieve a model that successfully yields small neutrino masses and sizable flavour processes, it is necessary to introduce two right-handed neutrinos [3]. Consider the mass terms:

$$\mathscr{L}_{mass} = - \begin{pmatrix} \bar{L}_L^\alpha & \bar{N}^c{}_R & \bar{N'}^c{}_R \end{pmatrix} \begin{pmatrix} 0 & Y_N^T v & \epsilon Y_N'^T v \\ Y_N v & \mu' & \Lambda \\ \epsilon Y_N' v & \Lambda & \mu \end{pmatrix} \begin{pmatrix} L_L^{c\alpha} \\ N_R \\ N_R' \end{pmatrix} \,, \quad (7)$$

where $L_L^\alpha$ stands for the three lepton families and $v$ is the vacuum expectation value of the Higgs (vev). $Y_N$ and $Y'_N$ are three dimensional vectors. Also $\epsilon$ is a flavour blind constant; $\epsilon$, $\mu$ and $\mu'$ are "small parameters", that is, the scales in $\mu, \mu'$ are much smaller than those in $\Lambda$ and $v$, and $\epsilon \ll 1$. This ensures an approximate $U(1)_{LN}$ symmetry. The fact that the coupling between $N'$ and the $L_L$s is assumed small changes the phenomenology radically as we will see.

Neglecting terms of second order in $\epsilon$ and $\mu/\Lambda$ we have that the coefficients for the $d = 5$, 6 operators in this mode are given by

$$c_{\alpha\beta}^{d=5} \equiv \epsilon \left( {Y'_N}^T \frac{1}{\Lambda} Y_N + Y_N^T \frac{1}{\Lambda} Y'_N \right)_{\alpha\beta} - \left( Y_N^T \frac{1}{\Lambda} \mu \frac{1}{\Lambda} Y_N \right)_{\alpha\beta} , \tag{8}$$

$$c_{\alpha\beta}^{d=6} \equiv \left( Y_N^\dagger \frac{1}{\Lambda^2} Y_N \right)_{\alpha\beta} + \mathcal{O}(\epsilon) . \tag{9}$$

And with the redefinition $\tilde{Y}_N = Y'_N - \frac{\mu}{2\epsilon\Lambda} Y_N$, we can write $c_{\alpha\beta}^{d=5}$ as

$$c_{\alpha\beta}^{d=5} = \epsilon \left( \frac{\tilde{Y}_N^T Y_N}{\Lambda} + \frac{Y_N^T \tilde{Y}_N}{\Lambda} \right) . \tag{10}$$

The coefficients in Eq. (9) and (10) are characteristic of a model with the mass matrix:

$$M_\nu = \begin{pmatrix} 0 & Y_N^T v & \epsilon \tilde{Y}_N^T v \\ Y_N v & 0 & \Lambda^T \\ \epsilon Y'_N v & \Lambda & 0 \end{pmatrix} , \tag{11}$$

so, up to $d = 6$ and $o(\epsilon, \mu/\Lambda)$, the tree-level phenomenology of the lepton sectors of the two models Eq. (7) and (11) are equivalent.

In the simpler model, Eq. (11), lepton number is broken due to the simultaneous presence of all three types of terms and light neutrino masses are then expected to depend on $Y_N$, $\tilde{Y}_N$ and $\Lambda$. The flavour breaking in this model stems from either $Y_N$ or $\tilde{Y}_N$, and as a consequence there is flavour violation even in the lepton-number conserving $\epsilon \to 0$ limit, since $Y_N$ remains active. Non-trivial leptonic flavour physics can thus affect processes other than neutrino masses.

The structure of the effective Lagrangian in eq. (1) is recovered if one identifies $\Lambda_{FL} \to \Lambda$ and $\Lambda_{LN} \to \Lambda/\sqrt{\epsilon}$. The separation of scales is achieved by having a small $\epsilon$, which is technically natural since $\epsilon = 0$ restores the lepton number symmetry. The $\Lambda_{LN}$ scale does not correspond to any particle mass at this level, while $\Lambda_{FL}$ corresponds to the Dirac heavy right-handed neutrino mass scale, as expected.

As it turns out, the $d = 5$ coefficient in this case has also enough information to reconstruct both Yukawa vectors up to a global renormalization, and therefore, also the flavour structure of $c^{d=6}_{\alpha\beta}$ [3]. Let $U$ be the PMNS matrix, found by diagonalizing $c^{d=5}_{\alpha\beta}$, and let

$$Y_N^T \equiv y\mathbf{u} \quad \tilde{Y}_N^T \equiv \tilde{y}\mathbf{v}, \tag{12}$$

where $y$ and $\tilde{y}$ are real numbers $\langle \mathbf{u}, \mathbf{u}\rangle = \langle \mathbf{v}, \mathbf{v}\rangle = 1$. Then, after choosing a particular hierarchy, normal or inverted, the Yukawa couplings can be reconstructed as linear combinations of the columns of the PMNS matrix. For the normal (inverted) hierarchy we find [3]

$$Y_{N\,i} = \frac{y}{\sqrt{2}}\left[f_1(r)\; U^*_{i3(i2)} + f_2(r)\; U^*_{i2(i1)}\right], \tag{13}$$

$$\tilde{Y}_{N_i} = \frac{\tilde{y}}{\sqrt{2}}\left[f_1(r)\; U^*_{i3(i2)} - f_2(r)\; U^*_{i2(i1)}\right]. \tag{14}$$

where

$$r \equiv \frac{|\Delta m^2_{solar}|}{|\Delta m^2_{atmos}|} = \frac{|\Delta m^2_{12}|}{|\Delta m^2_{23}|}\ . \tag{15}$$

and $f_{1,2}$ are well determined functions [3]. Moreover, since one neutrino is massless, the absolute values of the masses can also be determined from $\Delta m^2_{solar}$ and $\Delta m^2_{atmos}$. Finally, using all low energy observables we can find the value of the combination

$$\left|\frac{\epsilon y \tilde{y}}{\Lambda}\right| \sim 4.9(8.1) \times 10^{-13}\,\mathrm{TeV}^{-1}. \tag{16}$$

From Eq. (13) we obtain the coefficient $c^{d=6}$ and hence, predictions for the rare decays. We show in Fig. 1 the result for the ratios $B_{e\mu}/B_{e\tau}$, $B_{e\mu}/B_{\mu\tau}$, etc, as a function of $\theta_{13}$. One feature to be noted about these ratios for this particular model is the strong dependence on the Majorana phase $\alpha$ as well as on the CP phase for higher values of $\theta_{13}$ [3].

## 4 Conclusions

In this work we identified an extremely simple model of neutrino masses that requires only 2 heavy neutrinos. The Yukawa couplings of this model can be determined in terms of the light neutrino mass matrix and, therefore, a relation exists between the coefficient of the $d = 5$ Weinberg operatos and the

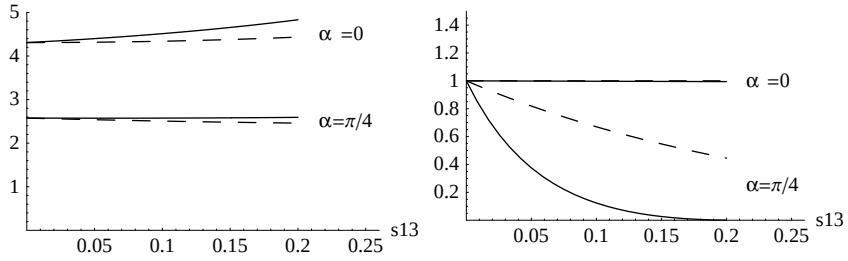


Figure 1: *Ratio $B_{e\mu}/B_{e\tau}$ for different values of the CP phase $\delta = 0$ (solid) and $\delta = \pi/2$ (dashed), with $\alpha = 0, \pi/4$ as denoted. Left: Normal hierarchy. Right: Inverse hierarchy .*

coefficients of the $d = 6$ operators involved in flavour processes. The flavour violating rates induced by the $d = 6$ couplings can be reconstructed - including CP phases - from the parameters in the light neutrino mass matrix.

In general, if new flavour physics in the lepton sector is to be accessible and we stick to the Majorana paradigm of neutrino masses, then two scales must be embedded in the fundamental theory $\Lambda_{FL} \ll \Lambda_{LN}$. This should be regarded as a guiding line for phenomenologically promising MFV models of neutrino masses.

## 5 Acknowledgements

This work was made in collaboration with B. Gavela, T. Hambye and P. Hernandez. D. Hernandez has been partially supported by CICYT through the project FPA2009-09017 and by MEC through FPU grant AP-2005-3603.

## References

1. G. Isidori, Y. Nir and G. Perez, arXiv:1002.0900 [hep-ph].
2. V. Cirigliano, B. Grinstein, G. Isidori and M. B. Wise, Nucl. Phys. B **728** (2005) 121 [arXiv:hep-ph/0507001].
3. M. B. Gavela, T. Hambye, D. Hernandez and P. Hernandez, JHEP **0909** (2009) 038 [arXiv:0906.1461 [hep-ph]].
4. E. J. Chun, K. Y. Lee and S. C. Park, Phys. Lett. B **566** (2003) 142 [arXiv:hep-ph/0304069].

Frascati Physics Series Vol. LI (2010), pp. 61-66
2nd Young Researchers Workshop: Physics Challenges in the LHC Era
Frascati, May 10 and 13, 2010

# NATURAL DIRAC NEUTRINOS FROM WARPED EXTRA DIMENSION

Jackson M. S. Wu
*Albert Einstein Center for Fundamental Physics,*
*Institute for Theoretical Physics, University of Bern,*
*Sidlerstrasse 5, 3012 Bern, Switzerland*

**Abstract**

Dirac neutrinos arising from gauged discrete symmetry à la Krauss-Wilczek are implemented in the minimal custodial Randall-Sundrum model. In the case of a normal hierarchy, all lepton masses and mixing pattern can be naturally reproduced at the TeV scale set by the electroweak constraints, while simultanously satisfy bounds from lepton flavour violation. A nonzero neutrino mixing angle, $\theta_{13}$, is generic in the scenario, as well as the existence of sub-TeV right-handed Kaluza-Klein neutrinos, which may be searched for at the LHC.

## 1 Introduction

Despite that the nature of neutrino remains unknown, most efforts has been directed at Majorana neutrinos. One common reason cited against the Dirac scenario is that it is hard to make realistic without excessive fine-tuning.

Recently, the Randall-Sundrum (RS) extra-dimensional scenario has become a novel and powerful framework to understand flavour. The crucial feature is that the mass hierarchy of the Standard Model (SM) charged fermions can arise naturally from their "geography" in the warped $AdS_5$ bulk [1]. The Yukawa couplings need not be fine-tuned, and can be fully "anarchic" (i.e. all naturally of order one and patternless). It was seen that the observed quark mass and mixing pattern can be accurately reproduced in this approach [2], and it is reasonable to expect the same can for Dirac neutrinos with appropriate bulk localisations, which is indeed found to be the case [3].

## 2 The framework

The setting used is that of the Minimal Custodial RS (MCRS) model [4]. The bulk gauge group is $SU(2)_L \times SU(2)_R \times U(1)_{B-L}$, which incorporates the custodial symmetry protecting the $\rho$ parameter. It is broken down to the SM at the boundaries by the IR-localised SM Higgs, $H_1$, and by UV boundary conditions (BCs) and scalar vaccum expectation value (VEV).

Concentrating on the lepton sector, the leptons are embedded as

$$L_i = \begin{pmatrix} \nu_{iL}\,[+,+] \\ e_{iL}\,[+,+] \end{pmatrix}, \quad E_i = \begin{pmatrix} \tilde{\nu}_{iR}\,[-,+] \\ e_{iR}\,[+,+] \end{pmatrix}, \quad \nu_{iR}\,[+,+]\,, \tag{1}$$

where $i$ is a generation index, $L$, $E$ denote $SU(2)_{L,R}$ doublets respectively, and $\nu_R$ the right-handed (RH) neutrino singlet under $SU(2)_{L,R}$. The parity assignment + (−) denotes Neumann (Dirichlet) BCs applied to the spinors on the boundary branes. Only fields with the [+,+] parity contain zero-modes that are part of the low energy spectrum of the 4D effective theory after the Kaluza-Klein (KK) reduction.

SM lepton masses arise as usual from Yukawa interactions with the SM Higgs. To generate Dirac masses for the neutrinos, a second Higgs doublet, $H_2$, transforming only under the $SU(2)_L$ is introduced on the IR brane. After electroweak symmetry breaking, the lepton mass matrices in the 4D effective theory take the form

$$(M^{RS}_{e,\nu})_{ij} = \frac{v_W}{k r_c \pi} \lambda^{e,\nu}_{5,ij} f^0_L(\pi, c^{e,\nu}_{iL}) f^0_R(\pi, c^{e,\nu}_{jR})\,, \tag{2}$$

where $k r_c \pi \approx 37\pi$ is the warp factor solving the hierarchy problem, the Higgs VEVs, $v_1 = v_2 = v_W = 174/\sqrt{2}$ GeV, are taken equal for simplicity, $\lambda^{e,\nu}_5$

are the complex dimensionless 5D Yukawa matrice for the charged leptons and neutrinos, $f^0_{L,R}$ are the zero-mode wavefunctions, and $c_{L,R}$ are the localisation parameters (see [3] for more details).

## 3 Dirac neutrinos from a gauged discrete $Z_N$

To have Dirac neutrinos, one needs to forbid Majorana mass terms, which can be easily accomplished via a $U(1)$ symmetry. Now if this $U(1)$ is global, it can be violated by quantum gravity effects. But if it is gauged, it has to be broken to avoid any new massless gauge bosons appearing. However, a gauged discrete $Z_N$ symmetry can survive from a gauged $U(1)$ broken at some very high scale [5], which is enough for Dirac neutrinos, as is well-known.

To implement this in the MCRS model, one extends the bulk gauge group by a $U(1)_X$, and add a scalar UV-localised, $\phi$, charged under it:

$$D_\mu \phi = (\partial_\mu - i g_{5X} X_\mu)\, \phi \,, \tag{3}$$

where $X_\mu$ is the $U(1)_X$ gauge field, and $g_{5X}$ the coupling constant. The $U(1)_X$ is spontanously broken when $\phi$ acquires a VEV, $v_\phi$. Parametrising the scalar as $\phi = (v_\phi + \rho) e^{i\eta/v_\phi}$, one sees that the Goldstone field, $\eta$, can be removed by a gauge transformation and a concomitant fermion field redefinition:

$$X_\mu \to X_\mu - \frac{1}{g_{5X}} \frac{\partial_\mu \eta}{v_\phi} \,, \qquad f \to f \exp\left( i \frac{\eta}{v_\phi} Q_X \right) . \tag{4}$$

The $Z_N$ symmetry then emerges if $Q_X$, the fermion charge under the $U(1)_X$, is rational but nonintegral.

## 4 Viability

To see if the Dirac neutrinos thus implemented can be realistic and natural, a parameter space scan is performed searching for configurations that give rise to the observed lepton mass (at a running scale of 1 TeV) and the bi-large mixing pattern while satisfying the current lepton flavour bounds at the same time.

For the search, the KK scale is set to 3 TeV to satisfy electroweak precision test constraints. The 5D Yukawas are taken to be $|\lambda_{5,ij}| \in [0.5, 2.0]$ for perturbativity. It is found that viable configurations compatible with all current data and bounds arise only for the case of neutrino the normal hierarchy.

Displayed in Table 1 are the range of lepton localisation parameters for the viable configurations. In Table 2, the resulting range of neutrino mass and mixing parameters are listed. All viable configurations have charged lepton masses $\{m_e, m_\mu, m_\tau\} = \{0.496, 105, 1780\}$ MeV. Note that $\theta_{13}$ is generically nonzero in all the viable configurations found.

| Lepton species | Parameter range |
|---|---|
| $\{c_{L_1}, c_{L_2}\, c_{L_3}\}$ | {(0.583, 0.588), (0.533, 0.548), (0.500, 0.502)} |
| $\{c_{E_1}, c_{E_2}\, c_{E_3}\}$ | {-0.728, -0.721, (-0.601, -0.588), (-0.520, -0.523)} |
| $\{c_{\nu_{R1}}, c_{\nu_{R2}}\, c_{\nu_{R3}}\}$ | {(-1.33, -1.22), (-1.36, -1.22), (-1.38, -1.22)} |

Table 1: Range of lepton localisation parameters for the viable configurations.

| Lepton parameters | Paramter range |
|---|---|
| $\{m_{\nu_1}, m_{\nu_2}\, m_{\nu_3}\}$ (meV) | {(0.096, 1.4), (8.5, 9.1), (47, 53)} |
| $\{\theta_{12}, \theta_{23}, \theta_{13}\}$ (°) | {(32, 39), (36, 53), (1.9, 12)} |
| $\delta_{CP}$ (rad.) | $[0, 2\pi)$ |

Table 2: Range of neutrino mass and mixing parameters from the viable configurations.

## 5 Phenomenology

### 5.1 Light KK neutrinos

KK excitations are characteristic in the extra-dimensional scenarios. But with the KK scale at 3 TeV, they are already hard to produce and thus detect at the LHC. However, depending on their localisations, the RH $(-+)$ KK neutrinos, $\tilde{\nu}_{iR}$, can be much lighter in comparison. For the viable range of $c_E$, one has for $\tilde{\nu}_{iR}$ the first KK masses (determined from their BCs [3])

$$m_{\tilde{\nu}_1} : 175 - 222\,\text{MeV}\,, \quad m_{\tilde{\nu}_2} : 16 - 24\,\text{GeV}\,, \quad m_{\tilde{\nu}_3} : 168 - 180\,\text{GeV}\,. \qquad (5)$$

### 5.2 Low energy constraints

The RH $(-+)$ KK neutrinos couple to the SM W and Z primarily through gauge mode mixings arising from SM Higgs interactions on the IR brane. These couplings can be parametrised as

$$W\tilde{\nu}_{iR}e_{iR} : \frac{g_L}{\sqrt{2}}\, r_i(c_{E_i})\,, \quad Z\bar{\tilde{\nu}}_{iR}\tilde{\nu}_{iR} : \frac{g_L}{\cos\theta_W}\gamma^\mu\Big[z_{Li}(c_{E_i})\hat{L} + z_{Ri}(c_{E_i})\hat{R}\Big]\,, \quad (6)$$

where $g_L \equiv e/\sin\theta_W$, $\theta_W$ the Weinberg angle, and $\hat{L}$, $\hat{R}$ the usual chiral projectors. The quantities $r_i$, $z_{Li}$ and $z_{Ri}$ involve gauge couplings and products of wavefunction overlap integrals. For simplicity $g_L = g_R$ is assumed.

With $m_{\tilde{\nu}_1} > m_\pi$, the charged kaon decay $K^+ \to e^+\tilde{\nu}_1$ sets the most stringent limit with the bound $|r_1|^2 < 10^{-6}$ for a 160 to 220 MeV neutrino [6]. Another limit comes from the LEP invisible Z decay measurement, which gives $N_\nu = \Gamma_{inv}/\Gamma_\nu^{SM} = 2.9840 \pm 0.0082$ [7]. Since only $\tilde{\nu}_1$ is light enough to escape the detector without leaving tracks, this sets a bound on $\Gamma(Z \to \bar{\tilde{\nu}}_1\tilde{\nu}_1)$ and thus $z_{L1}^2 + z_{R1}^2 \leq 0.096$ (95% CL). For the viable range of $c_E$, these constraints turns out to be very weak, as $r_1 \sim O(10^{-6})$, while $z_{L1} \sim z_{R1} \sim O(10^{-2})$.

### 5.3 Decay modes and LHC production

The decay modes of the RH $(-+)$ KK neutrinos depends crucially on their masses. For the heaviest $O(100)$ GeV $\tilde{\nu}_3$, a decay predominantly into $\tau\, W$ is expected with a width $\Gamma_{\tilde{\nu}_3} \sim 1.5 \times 10^{-6}$ GeV for the viable range of $c_E$.

For the (much) lighter $\tilde{\nu}_{1,2}$, three body decays are dominant. For $\tilde{\nu}_1$, the dominant decay channel is the charged current (CC) decay $\tilde{\nu}_1 \to e e^+ \nu_e$ [1] with a width $\Gamma_1^{\rm CC} \sim 0.73 \times 10^{-17}|r_1|^2$ GeV, corresponding to a lifetime of $\tau_{\tilde{\nu}_1} \sim 2.3 \times 10^4$ s for the viable range of $c_E$. For $\tilde{\nu}_2$, the main decays channels are $\tilde{\nu}_2 \to \mu\bar{l}\nu_l$, $\mu\bar{u}d$, $\mu\bar{c}s$. The total width is estimated to be $\Gamma_2^{\rm CC} \sim 0.027|r_2|^2$ GeV, and so a lifetime $\tau_{\tilde{\nu}_2} \sim 1.2 \times 10^{-15}$ s for the viable range of $c_E$.

At the LHC, due to the large background $\tilde{\nu}_1$ is not expected to be seen given that $m_{\tilde{\nu}_1} \ll 1$ GeV. For $\tilde{\nu}_2$, it can be detected via the process $u\bar{d} \to \tilde{\nu}_2\mu^+ \to \mu^+\mu^- e(\tau)\bar{\nu}$. The final state will involve apparent lepton flavor violation plus missing energy with the $\mu^+\mu^-$ pair not in resonance, characteristic of heavy neutrino signatures. Similarly, $\tilde{\nu_3}$ can be detected via the process $u\bar{d} \to \tau^+\tilde{\nu}_3 \to \tau^+\tau^- W$, where a $W$ jet plus $\tau$ jets are expected with the $\tau$ jets not in resonance. For the viable range of $c_E$, the total production cross section at $\sqrt{s} = 14$ TeV is estimated to be $\sim 0.3$ fb and $\sim 10^{-3}$ fb for $\tilde{\nu}_{2,3}$ respectively.

[1] The $\tilde{\nu}_1 \to e\mu^+\nu_\mu$ contribution is phase space suppressed, the $e\,\pi$ mode is negligible, while the virtual $Z$ mediated amplitudes are unimportant.

## 6 Conclusion

It is shown that Dirac neutrinos can be naturally implemented in the MCRS setting with a $SU(2)_L \times SU(2)_R \times U(1)_{B-L} \times U(1)_X$ bulk gauge symmetry group à la Krauss-Wilczek. For normal neutrino hierarchy only, lepton masses and mixing patterns can be successfully reproduced with just the RS anarchic 5D flavour structure, at the TeV scale, and at the same time still satisfy the lepton flavour bounds.

In the Dirac neutrino scenario presented, $\theta_{13}$ is generially neither zero nor small, which can be tested at the upcoming long-baseline experiments. There are also light KK neutrinos in the spectrum, of which the $O(200)$ MeV $\tilde{\nu}_1$ is too light to be picked out at the LHC but has a long life time of $O(10^4)$ s, the heavy $O(200)$ GeV $\tilde{\nu}_3$ has to small a production rate, leaving only the $O(20)$ GeV $\tilde{\nu}_2$ possible to be searched for at the LHC.

## 7 Acknowledgements

JW thank LNF for the hospitality and support provided during the 2nd Young Researchers Workshop.

## References

1. N. Arkani-Hamed and M. Schmaltz, Phys. Rev. D **61**, 033005 (2000), Y. Grossman and M. Neubert, Phys. Lett. B **474**, 361 (2000).

2. W. F. Chang, J. N. Ng and J. M. S. Wu, Phys. Rev. D **78**, 096003 (2008); **79**, 056007 (2009).

3. W. F. Chang, J. N. Ng and J. M. S. Wu, Phys. Rev. D **80**, 113013 (2009).

4. K. Agashe, A. Degado, M. J. May and R. Sundrum, JHEP **0308**, 050 (2003).

5. L. M. Krauss and F. Wilczek, Phys. Rev. Lett. **62**, 1221 (1989).

6. C. Amsler et al., Phys. Lett. B **667** (2008) 1.

7. ALEPH Collaboration *et al.*, Phys. Rept. **427**, 257 (2006).

Frascati Physics Series Vol. LI (2010), pp. 67-72
2nd Young Researchers Workshop: Physics Challenges in the LHC Era
Frascati, May 10 and 13, 2010

# FLAVOUR IN SOFT LEPTOGENESIS*

Chee Sheng Fong
*C. N. Yang Institute for Theoretical Physics, Stony Brook University*

**Abstract**

Successful Soft Leptogenesis (SL) requires a relatively low mass scale for the SU(2) singlet neutrinos of $10^5 - 10^8$ GeV. However, conventional SL (unflavoured) requires an unnaturally small soft supersymmetry(SUSY)-breaking bilinear $B \ll \mathcal{O}(\text{TeV})$ coupling for successful leptogenesis. On the other hand, in this regime, the interactions mediated by $\tau$, $\mu$ (and even $e$) charged lepton Yukawa interactions are in equilibrium, making the lepton number asymmetries and the washouts flavour dependent. Hence, it is crucial to take into account the flavour effects. Considering a general soft SUSY-breaking trilinear $A$ couplings, it is possible to enhance the efficiency up to $\mathcal{O}(1000)$ compared to the unflavoured case. With the enhanced efficiency, we can raise the $B$ up to TeV scale for successful leptogenesis. Taking into account the low energy constraints, we verify that the fast lepton flavour violation processes induced by the soft SUSY-breaking slepton masses would not destroy the enhancement.

* Work done in collaboration with M. C. Gonzalez-Garcia, Enrico Nardi and Juan Racker. Based on hep-ph/1004.5125.

## 1 Soft Leptogenesis Lagrangian and CP Asymmetries

The type-I SUSY seesaw model can be described by the superpotential:

$$W = W_{\rm MSSM} + \frac{1}{2} M_{ij} \hat{N}_i \hat{N}_j + Y_{ik} \epsilon_{\alpha\beta} \hat{N}_i \hat{L}_k^\alpha \hat{H}^\beta, \tag{1}$$

where $W_{\rm MSSM}$ is the superpotential for the Minimal Supersymmetric Standard Model (MSSM), $k = 1, 2, 3$ are the lepton flavour indices, $M_{ij}$ are the Majorana masses of the right-handed singlet neutrinos with generation indices $i, j$, and $\hat{N}_i$, $\hat{L}_k$, $\hat{H}$ are the chiral superfields for the right-handed singlet neutrinos, the left-handed lepton doublets and the Higgs doublets, with $\epsilon_{\alpha\beta} = -\epsilon_{\beta\alpha}$ and $\epsilon_{12} = +1$.

The relevant soft SUSY-breaking terms are given by

$$-\mathcal{L}_{soft} \;=\; A Z_{ik} \epsilon_{\alpha\beta} \widetilde{N}_i \tilde{\ell}_k^\alpha h^\beta + \frac{1}{2} B_{ij} M_{ij} \widetilde{N}_i \widetilde{N}_j + m^2_{\widetilde{\ell}_{kl}} \widetilde{\ell}_k \widetilde{\ell}_l + \text{h.c.} \tag{2}$$

The singlet sneutrino and anti-sneutrino states mix, giving rise to the mass eigenstates:

$$\begin{aligned} \widetilde{N}_{+i} &= \frac{1}{\sqrt{2}} (e^{i\Phi/2} \widetilde{N}_i + e^{-i\Phi/2} \widetilde{N}_i^*), \\ \widetilde{N}_{-i} &= \frac{-i}{\sqrt{2}} (e^{i\Phi/2} \widetilde{N}_i - e^{-i\Phi/2} \widetilde{N}_i^*), \end{aligned} \tag{3}$$

where $\Phi \equiv \arg(BM)$, that correspond to the mass eigenvalues

$$M^2_{ii\pm} \;=\; M^2_{ii} \pm |B_{ii} M_{ii}|. \tag{4}$$

For simplicity, we will concentrate on SL arising from a single sneutrino generation $i = 1$ and in what follows we will drop that index. After superfield phase rotations, we have three independent physical phases, they are

$$\phi_{Ak} \;=\; \arg(Z_k Y_k^* A B^*), \qquad (k = 1, 2, 3) \tag{5}$$

Eq. (2) leads to CP asymmetries $\epsilon_k(T)$ arising from self-energy diagrams induced by the bilinear $B$ term,

$$\epsilon_k(T) \;=\; -P_k \frac{Z_k}{Y_k} \sin\phi_{Ak} \frac{A}{M} \frac{4B\Gamma}{4B^2 + \Gamma^2} \Delta_{BF}(T), \quad P_k \equiv \frac{Y_k^2}{\sum_j Y_j^2}, \tag{6}$$

where

$$\Delta_{BF}(T) \quad = \quad \frac{c^s(T) - c^f(T)}{c^s(T) + c^f(T)}, \tag{7}$$

is the thermal factor associated to the difference between the phase-space, Bose-enhancement and Fermi-blocking factors for the scalar and fermionic channels, that vanishes in the zero temperature limit $\Delta_{BF}(T=0) = 0$ [2, 3].

## 2 Flavour Structure

Regarding the flavour structure of the soft terms relevant for flavoured SL, we can distinguish two general possibilities:

1. *Universal soft SUSY-breaking terms.* This case is realized in supergravity and gauge mediated SUSY-breaking models (neglecting the renormalization group running of the parameters), in our notations corresponds to

$$Z_k = Y_k. \tag{8}$$

In this case the only flavour structure arises from the Yukawa couplings and both the CP asymmetries $\epsilon^k$ and the corresponding washout terms are proportional to the same $P_k$, resulting in mild enhancement of $\mathcal{O}(30)$ in efficiency from one-flavour approximation [4]. We refer to this case as *Universal Trilinear Scenario* (UTS).

2. *General soft SUSY-breaking terms.* The most general form for the soft-SUSY breaking terms is allowed, only subject to the phenomenological constraints from limits on flavour changing neutral currents (FCNC) and from lepton flavour violating (LFV) processes. To simplify the analysis while still capture some of the main features of the general case, we choose

$$Z_k = \frac{\sum_j |Y_j|^2}{3Y_k^*} \ , \tag{9}$$

such that the CP asymmetries become flavour independent, $\epsilon^k = \epsilon/3$ for each flavour. In what follows we will refer to this case as the *Simplified Misaligned Scenario* (SMS). With this choice, since it is possible to reduce the washout in a particular flavour direction while keeping the corresponding CP asymmetry fixed, a much greater enhancement than the UTS becomes possible.

In both the UTS and SMS, from (5), we see that we only have one unique phase $\phi_A = \arg(AB^*)$.

## 3 Results

We numerically solved the relevant Boltzmann Equations [1] to obtain the final amount of $B-L$ asymmetry generated in the decay of the singlet sneutrinos (assuming no pre-existing asymmetry) which can be parametrized as:

$$Y_{B-L}(z\to\infty) = -2\eta\,\bar{\epsilon}\,Y^{\rm eq}_{\widetilde{N}}(T\gg M), \quad \eta\equiv\sum_k \eta_k. \tag{10}$$

After conversion by the sphaleron transitions, the final baryon asymmetry is related to the $B-L$ asymmetry by

$$Y_B = \frac{8}{23}\,Y_{B-L}(z\to\infty). \tag{11}$$

We also define the $\tilde{N}_\pm$ decay parameter, $m_{\rm eff}\equiv\sum_k Y_k^2 v_u^2/M$ which is related to the washout parameter $K$ as $K=\Gamma_{\widetilde{N}}/H(M)=m_{\rm eff}/m_*$ where $\Gamma_{\widetilde{N}}$ is the total singlet sneutrino decay width, $v_u = v\sin\beta$ (with $v=174$ GeV), $m_* = \sqrt{\frac{\pi g^*}{45}}\times\frac{8\pi^2 v_u^2}{m_P}\sim 10^{-3}$ eV with $g_s^*$ the total number of relativistic degrees of freedom ($g^*=228.75$ in the MSSM) and $m_P$ the Planck mass.

In the left panel of Fig. (1), we plot the efficiencies as a function of $m_{\rm eff}$ for both the scenarios UTS and SMS. Deviating from the flavour equipartition case $P_1=P_2=P_3=1/3$, in the SMS, we can obtain an enhancement up to $\mathcal{O}(1000)$ compared to the one-flavoured approximation. With this enhancement, it is possible to push the values of $B$ up to natural values at TeV scale for successful leptogenesis as shown in the right panel of Fig. (1).

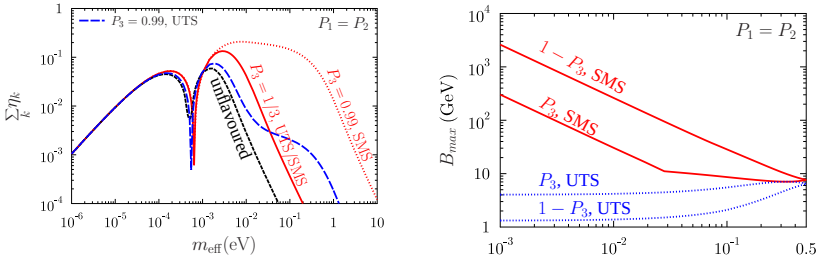


Figure 1: Left: The dependence of the efficiencies on $m_{\rm eff}$. Right: Maximum values of $B$ which can lead to successful leptogenesis as a function of $P_3$ and $1-P_3$. The figures correspond to $A\sin\phi_A$=1 TeV and $\tan\beta=30$.

[1] For more details, please refer to Ref. [1)]

## 4 Low Energy Constraints

As has been highlighted in Ref. [5], at sufficiently low temperatures the off-diagonal soft-SUSY breaking slepton masses can give rise to lepton flavour equilibration (LFE), effectively damping all dynamical flavour effects. In the left panel of Fig. (2), we show the dependence of the efficiencies (normalized to the flavour equipartition case) on the off-diagonal soft slepton mass parameter $m_{od}$ which for simplicity, we assume to be flavour independent. We see that there is a cut-off value of $\widetilde{m}_{od}$ for each $M$ such that the enhancement is totally damped out. In the right panel of Fig. (2), we show that in most part of the SUSY parameter space that is relevant for SL, subjecting to low energy constraints, the large flavour enhancements can survive the LFE effects.

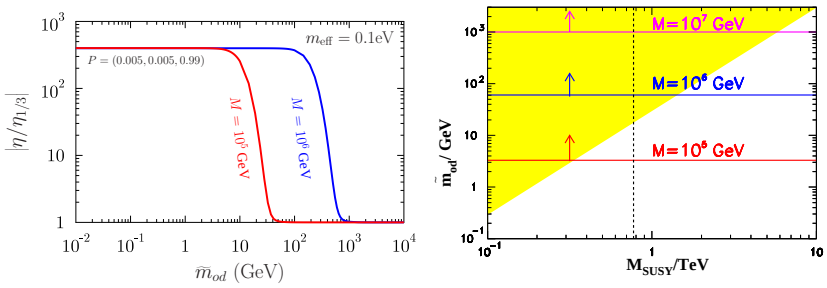


Figure 2: Left: The dependence of the efficiencies (normalized to the flavour equipartition case) on the off-diagonal soft slepton mass parameter $\widetilde{m}_{od}$. Right: Excluded region (shaded in yellow) of $\widetilde{m}_{od}$ versus $m_{\rm SUSY}$ arising from the present bound of $BR(\mu \to e\gamma) \leq 1.2 \times 10^{-11}$, together with the minimum value of $\widetilde{m}_{od}$ for which LFE effects start damping out flavour effects. Three lines shown corresponds to $M = 10^5\,$GeV, $M = 10^6\,$GeV and $M = 10^7\,$GeV. The vertical dashed line represents the value of $m_{\rm SUSY}/(30)^{\frac{1}{2}}$ required to explain the discrepancy between the Standard Model (SM) prediction and the measured value of muon anomalous magectic moment $a_\mu$ [6]. In the plots, we assume $\tan\beta = 30$.

## 5 Acknowledgements

The speaker thanks Concha Gonzalez-Garcia, Enrico Nardi and Juan Racker with whom he collaborated with in this work. He is also grateful to the 2$^{\rm nd}$

Young Researchers Workshop (in conjuction with XV Frascati Spring School "Bruno Touschek") organizing committee for the hospitality during his stay in beautiful Frascati.

**References**

1. C. S. Fong, M. C. Gonzalez-Garcia, Enrico Nardi, and J. Racker, To appear [arXiv:1004.5125 [hep-ph]].
2. Y. Grossman, T. Kashti, Y. Nir and E. Roulet, Phys. Rev. Lett. **91** (2003) 251801 [arXiv:hep-ph/0307081].
3. G. D'Ambrosio, G. F. Giudice and M. Raidal, Phys. Lett. B **575**, 75 (2003) [arXiv:hep-ph/0308031].
4. C. S. Fong and M. C. Gonzalez-Garcia, JHEP **0806** (2008) 076 [arXiv:0804.4471 [hep-ph]].
5. D. Aristizabal Sierra, M. Losada and E. Nardi, JCAP **0912**, 015 (2009) [arXiv:0905.0662 [hep-ph]].
6. S. Davidson, J. Garayoa, F. Palorini and N. Rius, JHEP **0809**, 053 (2008) [arXiv:0806.2832 [hep-ph]].

Frascati Physics Series Vol. LI (2010), pp. 73-78
2nd Young Researchers Workshop: Physics Challenges in the LHC Era
Frascati, May 10 and 13, 2010

# MODEL INDEPENDENT AND GENUINE FIRST OBSERVATION OF TIME REVERSAL VIOLATION

José Bernabéu
*Department of Theoretical Physics, University of Valencia*
*IFIC Joint Center Univ.Valencia-CSIC*
*TH Unit, CERN, Geneva*

Fernando Martínez-Vidal
*IFIC (Valencia University)*

Pablo Villanueva-Pérez
*IFIC (Valencia University)*

**Abstract**

This document discusses the proposal and feasibility studies to perform for the first time a separate and independent experimental test of Tviolation using B-factory data.

## 1 Theoretical Motivation

The violation of CP invariance has been observed in the $K^0 - \bar{K}^0$ and $B^0 - \bar{B}^0$ systems. Up to now, the experimental results are in agreement with the Cabibbo-Cobayashi-Maskawa (CKM) mechanism. On the other hand, CPT invariance imposed by any local quantum field theory with Lorentz invariance, is confirmed by all avaliable data. A direct evidence for time-reversal violation (TRV) in a single experiment, independent of CP violation and CPT invariance, would be of great interest. There is no existing result [1)] that clearly

demonstrates TRV in this sense. Sometimes the Kabir asymmetry $K^0 \to \bar{K}^0$ vs. $\bar{K}^0 \to K^0$ has been presented [2] as a proof for TRV. This process has, however, besides the drawbacks discussed in [1], the feature that $K^0 \to \bar{K}^0$ is a CPT-even transition, so that it is impossible to separate T violation from CP violation.

There are effects in particle physics that are odd under time $t$, but they are not genuine T-violating, because do not correspond to an interchange of "in" into "out" states. In fact, the $t$-asymmetry can only be connected [4] to T-asymmetry under the assumptions of CPT invariance plus the absence of an absorptive part difference between the initial and final states of the transition. As a consequence, we have to disregard these $t$-asymmetries as direct evidence for T violation.

As shown in Refs. [4, 5], B-factories offer a unique opportunity to show separate evidence for T violation (and CP violation) and measure the corresponding effects. The proposal has been scrutinized by Lincoln Wolfenstein [1] and Helen Quinn [3] with the conclusion that it appears to be a true TRV-effect. The crucial role played by B-factories is the EPR entanglement [6] between the neutral B-mesons produced by the $\Upsilon(4S)$ decay.

Although this coherence imposed by Bose statistics has only been used for flavor tagging up to now, one has to emphasize, following what quantum mechanics dictates, that the individual state of the neutral meson is not defined before its collapse as a filter imposed by the observation of the decay process of its companion. Similarly to the writing of the physical state of the two particles in terms of Bose-correlated orthogonal $B^0$ and $\bar{B}^0$, which allows to infer the flavor of the still alive meson by observing the specific flavor decay of the other (and first decaying) meson, one can rewrite the two particle state in terms of any pair of orthogonal states of individual neutral B-mesons. In particular, let us consider the pair of orthogonal states $B_+$ and $B_-$ of neutral B-mesons, where $B_-$ is the state that decays to $J/\psi K_+$, $K_+$ being the neutral $K_+ \to \pi\pi$, and $B_+$ is the orthogonal state to $B_-$, i.e., not connected to $J/\psi K_+$. We may call the filter imposed by a first observation of one of these decays a "CP-tag" [6], because $B_+$ and $B_-$ are approximately, up to terms of $Re(\epsilon_K)$ giving the non-orthogonality of $K_L$ and $K_S$ , the neutral B-mesons associated with final states of their decays which are CP-eigenstates, with the identification of $K_+ \equiv K_S$. As we are going to discuss much larger expected effects, one is authorized to

use the language of identifying $B_-$ by $J/\psi K_S$ , and $B_+$ by $J/\psi K_L$. To clarify the point, $B_-$ and $B_+$ should not be associated with CP-eigenstates of the neutral $B$ mesons themselves.

The theoretical ingredient to be used for this proposal is the EPR entanglement. Let us consider the two particle state of the neutral B-mesons produced by the $\Upsilon(4S)$ decay:

$$|i>= \frac{1}{\sqrt{2}}[B^0(t_1)\bar{B}^0(t_2) - \bar{B}^0(t_1)B^0(t_2)] = \frac{1}{\sqrt{2}}[B_+(t_1)B_-(t_2) - B_-(t_1)B_+(t_2)], \tag{1}$$

where the states 1 and 2 are defined by the time of their decay with $t_1 < t_2$. We may proceed to a partition of the complete set of events into four categories, defined by the tag in the first decay as $B_+$ , $B_-$ , $B^0$ or $\bar{B}^0$. Let us take as process I $B^0 \to B_+$, through the observation of a negatively charged lepton $l^-$ first (produced by the semileptonic decay of the opposite $\bar{B}^0$ meson) and $J/\psi K_L$ later, denoted as ($l^-$,$J/\psi K_L$), and consider:

- I.i) Its CP transformed $\bar{B}^0 \to B_+$ ($l^+$,$J/\psi K_L$), so that $B^0 \to B_+$ and $\bar{B}^0 \to B_+$, as a function of $\Delta t = t_2 - t_1$, provide a genuine CP-violating asymmetry.

- I.ii) Its T transformed $B_+ \to B^0$ ($J/\psi K_S, l^+$), so that $B^0 \to B_+$ and $B_+ \to B^0$, as a function of $\Delta t = t_2 - t_1$, provide a genuine T-violating asymmetry.

- I.iii) Its CPT transformed $B_+ \to \bar{B}^0$ ($J/\psi K_S, l^-$), so that $B^0 \to B_+$and $B_+ \to \bar{B}^0$, as a function of $\Delta = t_2 - t_1$, provide a genuine CPT-violating asymmetry.

One may check, a fortiori, that the events used for the asymmetries I.i), I.ii) and I.iii) are completely independent. Furthermore, the expectation is that the asymmetry described by I.ii) will prove and measure, for the first time, T violation with a large significance. Similarly, one may take as reference processes II ($B^0 \to B_-$), III ($\bar{B}^0 \to B_+$) and IV ($\bar{B}^0 \to B_-$).

On purpose, up to now there is no reference to the results expected for all these genuine asymmetries in the Weisskopf-Wigner effective Hamiltonian approach for the time evolution of the $B^0 - \bar{B}^0$ system, as well as within the standard CKM mechanism for CP violation [4, 5]. We proceed in this way

since our goal is to demonstrate and measure the violation of time reversal invariance without using the procedure of fitting parameters in a given theory. The outcome will be a model-independent observation of T violation.

## 2 Monte Carlo Study

In this section we describe the procedure we have followed to generate the simulated samples of the required decays, as discussed previously. In the second part, we estimate the T violation asymmetry and its expected significance with the size of currently available B-factory data samples.

Concerning to the Monte Carlo simulation, it has been done using an standard probability density function (PDF) which contains effects of T, CP and CPT violation and is based on the Wigner-Weiskopff formalism [8]. Neglecting effects from mistags, CPT violation (complex parameter $z$ set to zero), and taking $\Delta\Gamma = 0$, $|q/p| = 1$, the decay rate $g_{\pm}$ from a neutral $B$ meson to a CP eigenstate $(B_+, B_-)$ is given by equation 2 taken from [8, 9] [8, 7]. To generate our samples we have set the parameter $Im(\lambda_f)$ (i.e. the well known CP-violating parameters $\sin 2\beta$) to 0.672 and $|\lambda_f| = 1$, so $S_f = 0.672$ and $C_f = 0$ (i.e. no direct CP violation in the $B_+$, $B_-$ decays), taken from [9]:

$$g_{\pm}(\Delta t) = \frac{e^{\frac{-|\Delta t|}{\tau_{B^0}}}}{4\tau_{B^0}}\{1 \pm [S_f sin(\Delta m_d \Delta t) - C_f cos(\Delta m_d \Delta t)]\} \qquad (2)$$

With this PDF we generate the eight subsamples, from which we evaluate our asymmetries.

The T asymmetry ($A_T(\Delta t)$) is built counting the number of entries in each generated subsample ($N_a$) and its T transformed ($N_b$). Then we subtract bin by bin in $\Delta t$ the entries from the two subsamples, correcting by efficiency effects. Taking as example the BaBar experiment, we consider 3255 $J/\psi K_L$ and 7750 $J/\psi K_S$ signal events, obtaining the data points in the T asymmetry plots (figure 1). The red dotted curves are obtained after setting $Im(\lambda_{CP}) = 0$, which in practice correspond to the integration over the bin size of the curve without T violation. These curves have been produced generating 1 million events (i.e. a virtually infinite statistics). We perform this comparison since our final goal is to compare the asymmetries with T violation and the corresponding ones without T violation with all the experimental effects included. This comparison will be done through a $\chi^2$ test.

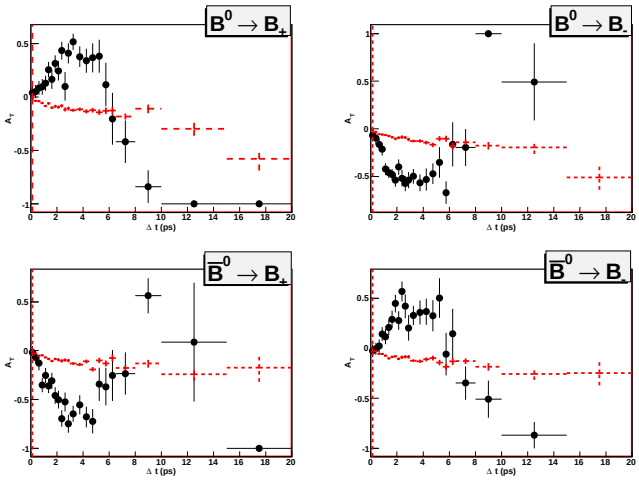


Figure 1: *T asymmetries for each reference process with proper-time resolution, mistags, efficiency effects (black dots) and curves without T violation (red dashed curves)*

In our exercise we have included approximate $\Delta t$ resolution, mistags and reconstruction efficiencies as observed at the B factories.

Finally, we perform a $\chi^2$ test for each of the four statistically independent T asymmetries, using the $\chi^2$ ansatz given by

$$\chi^2_0 = \sum_{\Delta t_i} \frac{(A_T^{exp}(\Delta t_i) - A_T^{NoT-Violation}(\Delta t_i))^2}{\sigma^2_{A_T^{exp}}(\Delta t_i) + \sigma^2_{A_T^{NoT-Violation}}(\Delta t_i)}, \tag{3}$$

from which a confidence level (or equivalently a significance of the T violation effect) can be computed. For this study we assume a $\chi^2$-distributed variable, although in the experimental analysis a careful study of the true distribution will have to be pursued.

Assuming a $\chi^2$ distribution, the results of the $\chi^2$ test for T asymmetry with proper-time resolution, mistags, and efficiency effects for our simulated samples are summarized in Table 1. We can compute that $\chi^2/dof \approx 14$ for the TRV test, so we can anticipate to establish directly for the first time T violation with a significance above 10 standard deviations.

Table 1: $\chi^2$ *test of the T asymmetries.*

| T asymmetries Test | $B^0 \to B_+$ | $B^0 \to B_-$ | $\bar{B}^0 \to B_+$ | $\bar{B}^0 \to B_-$ |
|---|---|---|---|---|
| $\chi^2_0$ | 326.7, 21 bins | 361.0, 21 bins | 327.9, 22 bins | 278.8, 22 bins |
| Prob($\chi^2 > \chi^2_0$) | $1.12 \cdot 10^{-56}$ | $1.04 \cdot 10^{-63}$ | $2.55 \cdot 10^{-56}$ | $2.32 \cdot 10^{-46}$ |

## 3 Acknowledgments

This research has been supported in part by the MICINN, Grant FPA 2008-02878 and the Generatitat Valenciana Grant PROMETEO 2008/004.

## References

1. L. Wolfenstein, Int. J. Mod. Phys. E **8**, 501 (1999).
2. T. Nakada, Discrete'08 Conference, Valencia 2008, J. Phys. Conf. Ser. **171**, 011001 (2009).
3. H. R. Quinn, Discrete'08 Conference, Valencia 2008, J. Phys. Conf. Ser. **171**, 011001 (2009).
4. M. C. Bañuls and J. Bernabeu, Phys. Lett. B **464**, 117 (1999), [arXiv:hep-ph/9908353].
5. M. C. Bañuls, J. Bernabeu, Nucl. Phys. B **590**, 19 (2000), [arXiv:hep-ph/0005323].
6. M. C. Bañuls, J. Bernabeu, JHEP **032**, 9906 (1999), [arXiv:hep-ph/9807430].
7. B. Aubert *et al.* (BaBar Collaboration), Phys. Rev. D **66**, 032003 (2002); K. Abe *et al.* (Belle Collaboration), Phys. Rev. D **66**, 032007 (2002).
8. B. Aubert *et al.* (BaBar Collaboration), Phys. Rev. Lett. **92**, 181801 (2004); Phys. Rev. D **70**, 012007 (2004).
9. B. Aubert *et al.* (BaBar Collaboration), Phys. Rev. D **79**, 072009 (2009); K.F. Chen *et al.* (Belle Collaboration), Phys. Rev. Lett. **98**, 031802 (2007).

Frascati Physics Series Vol. LI (2010), pp. 79-84
2nd Young Researchers Workshop: Physics Challenges in the LHC Era
Frascati, May 10 and 13, 2010

# MEASURING $\sin\phi_s$ FROM NEW PHYSICS POLLUTED $B$ DECAYS

Marc Ramon
*Unitat de Física Teòrica, Universitat Autònoma de Barcelona*
*Edifici Cn., 08193 Bellaterra (Barcelona), Spain.*

**Abstract**

We discuss an alternative approach to measure the weak mixing angle $\phi_s$ of the $B_s^0 - \bar{B}_s^0$ system, using a theoretical input which is short-distance dominated in QCD factorisation and thus free of IR-divergencies at $O(\alpha_s)$. We also present a new expression that allow to obtain directly $\sin\phi_s^{NP}$ if there is only a significant contribution of New Physics in the mixing.

## 1 Introduction

An intensive research has been performed on the phenomenology of hadronic $B_d$ decays for the past 20 years, mainly at the $B$-factories BaBar and Belle working around the $\Upsilon$ ressonance. The analysis of the data collected has proven that the CKM mechanism is accurate enough to describe most of CP and flavour violation phenomena observed in the energy range explored so far. Only the D0

and CDF experiments at Fermilab have been able to make some measurements on the $B_s$ system, namely the mass difference $\Delta M_s$, other mixing parameters and some decay modes. However, this situation is going to change with the starting of LHCb, the upgrade of Belle and the future building of a Super-$B$ factory, so the list of observables measured for $B_s$ decays will grow to constitute a good place to look for New Physics (NP).

From a theoretical point of view, the study of non-leptonic $B$-decays is rather involved, due to the presence of important long-distance strong interaction effects. Having them under control is crucial to be able to resolve small NP contributions. Two methods have been used in the literature to handle these low-energy effects: *flavour symmetries* and *direct computations from QCD*. Flavour symmetries suffer from big uncertainties, mainly due to poorly estimated $SU(3)$ breaking, while the direct computations from QCD, appearing for instance in QCD factorisation (QCDf), are based on factorisation and the $1/m_b$ expansion, and may suffer from uncertainties due to non-factorisable chirally enhanced $1/m_b$ corrections and long distance charm loops.

## 2 Theoretical inputs from QCDf

### 2.1 The amplitudes

If there is no NP entering the amplitude, the unitarity of the CKM matrix

$$\lambda_u^{*(s)} + \lambda_c^{*(s)} + \lambda_t^{*(s)} = 0, \tag{1}$$

allows us to write the amplitude of a $B$ meson decaying into two light mesons as

$$A(B_s \to M_1 M_2) = \lambda_u^{*(s)} T^{(s)}_{M_1 M_2} + \lambda_c^{*(s)} P^{(s)}_{M_1 M_2}, \tag{2}$$

where $\lambda_q^{(s)} = V_{qs}^* V_{qb}$. Using QCDf for $B \to PP$ decays, the amplitudes can be rewritten as

$$A(B_s \to M_1 M_2) = A_{M_1 M_2} f_1(a_i^{(p)}) + B_{M_1 M_2} f_2(b_j), \tag{3}$$

where $p = u, c$ quarks, $f_1$ ($f_2$) denotes a linear combination of $a_i^{(p)}$ ($b_j$) and

$$a_i^{(p)} = \left(C_i + \frac{C_{i\pm1}}{N_C}\right) N_i(M_2) + \frac{C_{i\pm1}}{N_C}\frac{C_F \alpha_s}{4\pi}\left[V_i(M_2) + \frac{4\pi^2}{N_C} H_i(M_1, M_2)\right] + P_i^{(p)}(M_2), \tag{4}$$

$$b_j \;\propto\; f_3(C_j \Phi_j \otimes T_j). \tag{5}$$

Eq. 3 gives the structure of the amplitude in QCDf, while the exact expressions can be found in [1]. $C_{i,j}$ are the Wilson coefficients of the effective Hamiltonian associated to these processes. The meson functions appearing in $a_i^{(p)}$ correspond, respectively, to the single leading order diagram ($N_i(M_2)$), to the four hard-vertex correction diagrams ($V_i(M_2)$), to the two hard-spectator scattering (HSS) diagrams ($H_i(M_1, M_2)$) and to the two penguin diagrams ($P_i^{(p)}(M_2)$) appearing in the $B$ decays into light mesons. The $b_j$ terms, are given by linear combinations of light-cone distribution amplitudes ($\Phi_j$) convoluted with hard-scattering kernels ($T_j$), and are related to the four weak annihilation (WA) diagrams.

### 2.2 The divergencies

The HSS terms are proportional to [1]

$$H_i(M_1M_2) \propto \frac{A_{M_1M_2}}{B_{M_1M_2}} \int_0^1 dx \int_0^1 dy \left[ \frac{\Phi_{M_2}(x)\Phi_{M_1}(y)}{\bar{x}\bar{y}} + r_\chi^{M_1} \frac{\Phi_{M_2}(x)\Phi_{m_1}(y)}{x\bar{y}} \right], \tag{6}$$

where $x$ and $y$ are the quark momentum fractions inside the mesons and $r_\chi^{M1} \sim \Lambda_{\rm QCD}/m_b$. The $y$ part of the second term in eq. 6 can be expressed [1]

$$\int_0^1 \frac{dy}{\bar{y}} \Phi_{m_1}(y) = \Phi_{m_1}(1) \int_0^1 \frac{dy}{\bar{y}} + \int_0^1 \frac{dy}{\bar{y}} \left[ \Phi_{m_1}(y) - \Phi_{m_1}(1) \right] \tag{7}$$

and, since the first integral is divergent as $\bar{y} \to 0$, an IR-divergence arises in $H_i(M_1, M_2)$; the same kind of divergent integrals come from the WA contributions around the regions $\bar{x}$, $y \sim 1$. Each divergent contribution have been parametrised in the literature [1] introducing a model-dependent parameter $X_k^{M_l} = (1 + \rho_k e^{i\psi_l}) ln(m_b/\Lambda_{\rm QCD})$, where $k = H, A$ accounts for the origin of the divergency (HSS or WA) and $l$ for the final-state meson involved.

## 3 Construction of a theoretically clean input

### 3.1 A nice example: the decay $B \to K^0 \bar{K}^0$

The $T$ and $P$ contributions for this exclusive process can be computed in QCDf, obtaining [1]

$$T_s^0 = A_{KK}[\alpha_4^{(u)} - (1/2)\alpha_{4,EW}^{(u)} + \beta_3 + 2\beta_4 - (1/2)\beta_{3,EW} - \beta_{4,EW}], \tag{8}$$

$$P_s^0 = A_{KK}[\alpha_4^{(c)} - (1/2)\alpha_{4,EW}^{(c)} + \beta_3 + 2\beta_4 - (1/2)\beta_{3,EW} - \beta_{4,EW}], \tag{9}$$

with $\alpha_4^{(p)} = a_4^{(p)} + r_\chi^{M_2} a_6^{(p)}$ and $\beta_k \propto b_k$. It is straightforward to see that in the quantity $\Delta \equiv T - P$ [2], all $\beta$ terms cancel and, with them, the IR-divergencies coming from the weak annhilition terms. As the only term in eq. 4 that actually depends on the final up-type quark ($u$ or $c$) is $P_i^{(p)}(M_2)$, which can be computed perturbatively, we get (neglecting the EW penguins)

$$\Delta = T_s^0 - P_s^0 \simeq \left[P_4^{(u)}(\bar{K}^0) - P_4^{(c)}(\bar{K}^0)\right] + r_\chi^{\bar{K}^0}\left[P_6^{(u)}(\bar{K}^0) - P_6^{(c)}(\bar{K}^0)\right], \quad (10)$$

so we have also gotten rid of the IR-divergencies coming from the HSS terms.

Thus, in some kinds of penguin mediated decays $\Delta$ is free from IR-divergencies at $O(\alpha_s)$ in QCDf. This will lead to smaller uncertainties and safer predictions than the full amplitude computed directly using QCDf.

### 3.2 The vectorial partner: $B_s \to K^{*0}\bar{K}^{*0}$

The magnitude $\Delta$ has been derived for $B \to PP$, but can also be applied to the *longitudinal component of the polarisation of final vector mesons* in $B \to VV$ decays. The advantages of doing so are the following: (1) larger branching ratios, $Br(B_s \to K^{*0}\bar{K}^{*0}) \sim O(10^{-6})$, make them easier to measure in hadronic machines; (2) the final decay products are charged ($K^{*0} \to K^+\pi^-$ and $\bar{K}^{*0} \to K^-\pi^+$) and thus easier to identify, and have $CP$-eigenstates in the final state; (3) the longitudinal observables are better behaved ($H_0$ is not suppressed, while $H_-$ is suppressed by $1/m_b$ and $H_+$ by $1/m_b^2$ [3]).

## 4 The sum rule

### 4.1 The building blocks

The longitudinal $CP$-asymmetries can be defined as [2, 4]

$$\begin{aligned}
\mathcal{A}_{dir}^{long} &\equiv \frac{|A_0|^2 - |\bar{A}_0|^2}{|A_0|^2 + |\bar{A}_0|^2}, \quad \mathcal{A}_{mix}^{long} \equiv -2\eta_f \frac{\mathrm{Im}\left(e^{-i\phi_s} A_0^* \bar{A}_0\right)}{|A_0|^2 + |\bar{A}_0|^2}, \\
\mathcal{A}_{\Delta\Gamma}^{long} &\equiv -2\eta_f \frac{\mathrm{Re}\left(e^{-i\phi_s} A_0^* \bar{A}_0\right)}{|A_0|^2 + |\bar{A}_0|^2},
\end{aligned} \quad (11)$$

fulfilling $|\mathcal{A}_{dir}^{long}|^2 + |\mathcal{A}_{mix}^{long}|^2 + |\mathcal{A}_{\Delta\Gamma}^{long}|^2 = 1$, and the $CP$-averaged longitudinal branching ratio

$$Br^{long} = \frac{<\Gamma_i^{long}>_{CP}}{\sum_i \Gamma_i} = \tau_B \frac{\Gamma_{B^0\to f}^{long} + \Gamma_{\bar{B}^0\to \bar{f}}^{long}}{2} = g_{PS} \frac{|A_0|^2 + |\bar{A}_0|^2}{2}. \quad (12)$$

where $A_0$ labels the longitudinally polarised $V$ amplitude, $\eta_f = \pm 1$ is the $CP$-eigenvalue of the final state $f$ and $g_{PS}$ contains the phase-space factors. From now on the superscript "*long*" will be dropped to simplify the notation, although we will keep dealing with longitudinal observables.

### 4.2 Derivation of the sum rule

From the longitudinal component of eq. 2 and its $CP$-conjugated partner it can be found

$$\Delta_s = \frac{(\lambda_u^{(s)} + \lambda_c^{(s)})A_0 - (\lambda_u^{*(s)} + \lambda_c^{*(s)})\bar{A}_0}{\lambda_u^{*(s)}\lambda_c^{(s)} - \lambda_u^{(s)}\lambda_c^{*(s)}}. \tag{13}$$

Taking its modulus squared and substituting the building blocks (eqs. 11 and 12), it can be obtained [2)]

$$|\Delta_s|^2 = \frac{2Br}{g_{PS}} \left\{ x_1 + [x_2 \sin\phi_s - x_3 \cos\phi_s] \frac{\mathcal{A}_{mix}}{\eta_f} - [x_2 \cos\phi_s + x_3 \sin\phi_s] \frac{\mathcal{A}_{\Delta\Gamma}}{\eta_f} \right\}, \tag{14}$$

here $x_1$, $x_2$ and $x_3$ are functions of just $|\lambda_u^{(s)}|$, $|\lambda_c^{(s)}|$ and $\gamma$.

## 5 Consistency test of the Standard Model

In the SM, eq. 1 can be rearranged into $(|\lambda_u^{(s)}|/|\lambda_c^{(s)}|)e^{i\gamma} - (|\lambda_t^{(s)}|/|\lambda_c^{(s)}|)e^{-i\beta_s^{SM}} = -1$ and the $B_s^0 - \bar{B}_s^0$ mixing angle $\phi_s^{SM} = 2\beta_s^{SM} + O(\lambda^6)$. These two conditions make $x_2 \sin\phi_s - x_3 \cos\phi_s = 0$, which cancels the second term in eq. 14.

Now, transforming $|\Delta_s|^2$ conveniently one can get [4)]

$$\sin(\beta_s^{SM}) = \frac{Br/g_{PS}}{2|\lambda_c^{(s)}|^2|\Delta_s|^2} \left[ 1 - \frac{1}{\eta_f} \sqrt{1 - (\mathcal{A}_{dir})^2 - (\mathcal{A}_{mix})^2} \right]. \tag{15}$$

This is a *consistency test of the SM*: measuring the $Br$, $\mathcal{A}_{dir}$ and $\mathcal{A}_{mix}$ and computing $|\Delta_s|$, the value of $\beta_s^{SM}$ can be predicted. Therefore, if a value of $\beta_s$ incompatible with $\beta_s^{SM}$ is measured, it would constitute a signal of NP. Alternatively, and since $\mathcal{A}_{\Delta\Gamma} = \sqrt{1 - (\mathcal{A}_{dir})^2 - (\mathcal{A}_{mix})^2}$, if $\mathcal{A}_{\Delta\Gamma}$ can be determined experimentally, the $Br$ will be the only other observable needed to extract $\beta_s$. This can be done measuring the time-dependent longitudinal untagged rate $\Gamma(B_s(t) \to VV) + \Gamma(\bar{B}_s(t) \to VV) \propto R_H e^{-\Gamma_s^H t} + R_L e^{-\Gamma_s^L t}$, from where $\mathcal{A}_{\Delta\Gamma}$ can be obtained:

$$\mathcal{A}_{\Delta\Gamma}(B_s \to VV) = \frac{R_H - R_L}{R_H + R_L}. \tag{16}$$

## 6 Extraction of $\sin\phi_s$ in presence of New Physics in the mixing

If NP enters only the $B_s^0 - \bar{B}_s^0$ mixing, then $\phi_s = 2\beta_s^{SM} + \phi_s^{NP}$, and the sum rule can be written as

$$\sin\phi_s^{NP} = \frac{1}{\eta_f}\frac{\mathcal{A}_{mix}(1-C) - \mathrm{sign}(\mathcal{A}_{mix})|\mathcal{A}_{\Delta\Gamma}|\sqrt{1-(\mathcal{A}_{dir})^2-(1-C)^2}}{1-(\mathcal{A}_{dir})^2}, \quad (17)$$

where $C \equiv 2|\lambda_c^{(s)}|^2 \sin^2\beta_s^{SM} g_{PS}|\Delta|^2/Br$ and, given that NP enters only via the mixing angle, $\mathcal{A}_{dir} = \mathcal{A}_{dir}^{SM}$. The interpretation of eq. 17 is simple: computing two theoretical inputs ($|\Delta_s|$ and $|\lambda_c^{(s)}|$) and measuring three observables ($\mathcal{A}_{dir}$, $\mathcal{A}_{mix}$ and $Br$) a value for $\sin\phi_s^{NP}$ can be obtained. Of course, if there is no NP $1 - C = |\mathcal{A}_{\Delta\Gamma}^{SM}|$ and $\sin\phi_s^{NP} = 0$.

## 7 Conclusion

To conclude, we would like to add a few comments about the method proposed. It can only be applied to those processes for which $\Delta$ does not receive contributions from HSS or WA diagrams (like $B \to K^{(*)}\bar{K}^{(*)}$), but in these situations $\Delta$ is the most reliable theoretical input that can be built using QCDf for B decaying into two light mesons.

We are currently working to get a $\sin\phi_s$ formula for the more general case where there is NP both in the mixing and in the amplitude, and show the size of the uncertainties one would have when applying it to a particular NP model.

## 8 Acknowledgments

I would like to thank the organisers of the XV LNF Spring School "Bruno Touschek" at Frascati for their hospitality. This work has been supported by Universitat Autònoma de Barcelona.

## References

1. M. Beneke and M. Neubert, Nucl. Phys. B **675** (2003) 333.
2. S. Descotes-Genon, J. Matias, J. Virto, Phys. Rev. Lett. **97** (2006) 061801.
3. M. Suzuki, Phys. Rev. D **65** (2002) 097501.
4. S. Descotes-Genon, J. Matias, J. Virto, Phys. Rev. D **76** (2007) 074005.

**FRASCATI PHYSICS SERIES VOLUMES**

**Volume I**
*Heavy Quarks at Fixed Target*
Eds.: S. Bianco and F.L. Fabbri
Frascati, May 31–June 2, 1993
ISBN—88–86409–00–1

**Volume II – Special Issue**
*Les Rencontres de Physique de la Vallée d'Aoste – Results and Perspectives in Particle Physics*
Ed.: M. Greco
La Thuile, Aosta Valley, March 5 –11, 1995
ISBN—88–86409–03–6

**Volume III**
*Heavy Quarks at Fixed Target*
Ed.: B. Cox
University of Virginia, Charlottesville
October 7–10, 1994, 11
ISBN—88–86409–04–4

**Volume IV**
*Workshop on Physics and Detectors for DAΦNE*
Eds.: R. Baldini, F. Bossi, G. Capon, G. Pancheri
Frascati, April 4–7, 1995
ISBN—88–86409–05–2

**Volume V – Special Issue**
*Les Rencontres de Physique de la Vallée d'Aoste – Results and Perspectives in Particle Physics*
Ed.: M. Greco
La Thuile, Aosta Valley, March 3–9, 1996
ISBN—88–86409–07–9

**Volume VI**
*Calorimetry in High Energy Physics*
Eds.: A. Antonelli, S. Bianco, A. Calcaterra, F.L. Fabbri
Frascati, June 8–14, 1996
ISBN—88–86409–10–9

**Volume VII**
*Heavy Quarks at Fixed Target*
Ed.: L. Kőpke
Rhinefels Castle, St. Goar, October 3–6, 1996
ISBN—88–86409–11–7

**Volume VIII**
*ADONE a milestone on the particle way*
Ed.: V. Valente 1997
ISBN—88–86409–12–5

**Volume IX – Special Issue**
*Les Rencontres de Physique de la Vallée d'Aoste – Results and Perspectives in Particle Physics*
Ed.: M. Greco
La Thuile, Aosta Valley, March 2–8, 1997
ISBN–88–86409–13–3

**Volume X**
*Advanced ICFA Beam Dynamics*
*Workshop on Beam Dynamics Issue for $e^+e^-$ Factories*
Eds.: L. Palumbo, G. Vignola
Frascati, October 20–25, 1997
ISBN—88–86409–14–1

**Volume XI**
*Proceedings of the XVIII International Conference on Physics in Collision*
Eds.: S. Bianco, A. Calcaterra, P. De Simone, F. L. Fabbri
Frascati, June 17–19, 1998
ISBN—88–86409–15–X

**Volume XII – Special Issue**
*Les Rencontres de Physique de la Vallée d'Aoste – Results and Perspectives in Particle Physics*
Ed.: M. Greco
La Thuile, Aosta Valley, March 1–7, 1998
ISBN—88–86409–16–8

**Volume XIII**
*Bruno Touschek and the Birth of thee$^+ e^-$*
Ed.: G. Isidori
Frascati, 16 November, 1998
ISBN—88–86409–17–6

**Volume XIV – Special Issue**
*Les Rencontres de Physique de la Vallée d'Aoste – Results and Perspectives in Particle Physics*
Ed.: M. Greco
La Thuile, Aosta Valley, February 28–March 6, 1999
ISBN—88–86409–18–4

**Volume XV**
*Workshop on Hadron Spectroscopy*
Eds.: T. Bressani, A. Feliciello, A. Filippi
Frascati, March 8 2 1999
ISBN—88–86409–19–2

**Volume XVI**
*Physics and Detectors for DA$\Phi$NE*
Eds.: S. Bianco, F. Bossi, G. Capon, F.L. Fabbri, P. Gianotti, G. Isidori, F. Murtas
Frascati, November 16 –19, 1999
ISBN—88–86409–21–4

**Volume XVII – Special Issue**
*Les Rencontres de Physique de la Vallée d'Aoste – Results and Perspectives in Particle Physics*
Ed.: M. Greco
La Thuile, Aosta Valley, February 27 March 4, 2000
ISBN—88–86409–23–0

**Volume XVIII**
*LNF Spring School*
Ed.: G. Pancheri
Frascati, 15–20 May, 2000
ISBN—88–86409–24–9

**Volume XIX**
*XX Physics in Collision*
Ed.: G. Barreira
Lisbon June 29–July1st. 2000
ISBN—88–86409–25–7

**Volume XX**
*Heavy Quarks at Fixed Target*
Eds.: I. Bediaga, J. Miranda, A. Reis
Rio de Janeiro, Brasil, October 9–12, 2000
ISBN—88–86409–26–5

**Volume XXI**
*IX International Conference on Calorimetry in High Energy Physics*
Eds.: B. Aubert, J. Colas, P. Nédélec, L. Poggioli
Annecy Le Vieux Cedex, France, October 9–14, 2000
ISBN—88–86409–27–3

**Volume XXII – Special Issue**
*Les Rencontres de Physique de la Vallée d'Aoste – Results and Perspectives in Particle Physics*
Ed.: M. Greco
La Thuile, Aosta Valley, March 4–10, 2001
ISBN—88–86409–28–1

**Volume XXIII**
*XXI Physics in Collision*
Ed.: Soo–Bong Kim
Seoul, Korea, June 28 30, 2001
ISBN—88–86409–30–3

**Volume XXIV**
*International School of Space Science – 2001 Course on: Astroparticle and Gamma–ray Physics in Space*
Eds.: A. Morselli, P. Picozza
L'Aquila, Italy, August 30 September 7, 2000
ISBN—88–86409–31–1

**Volume XXV**
*TRDs for the 3rd Millennium Workshop on Advanced Transition Radiation Detectors for Accelerator and Space Applications*
Eds. N. Giglietto, P. Spinelli
Bari, Italy, September 20–23, 2001
ISBN—88–86409–32–X

**Volume XXVI**
*KAON 2001* International Conference on CP Violation
Eds.: F. Costantini, G. Isidori, M. Sozzi
Pisa Italy, June 12th 17th, 2001
ISBN—88–86409–33–8

**Volume XXVII – Special Issue**
*Les Rencontres de Physique de la Vallée d'Aoste – Results and Perspectives in Particle Physics*
Ed.: M. Greco
La Thuile, Aosta Valley, March 3–9, 2002
ISBN—88–86409–34–6

**Volume XXVIII**
*Heavy Quarks at Leptons 2002*
Eds.: G. Cataldi, F. Grancagnolo, R. Perrino, S. Spagnolo
Vietri sul mare (Italy), May 27th June 1st, 2002
ISBN—88–86409–35–4

**Volume XXIX**
*Workshop on Radiation Dosimetry: Basic Technologies, Medical Applications, Environmental Applications*
Ed.: A. Zanini
Rome, Italy, February 56, 2002
ISBN—88–86409–36–2

**Volume XXIX – Suppl.**
*Workshop on Radiation Dosimetry: Basic Technologies, Medical Applications, Environmental Applications*
Ed.: A. Zanini
Rome, Italy, February 56, 2002
ISBN—88–86409–36–2

**Volume XXX – Special Issue**
*Les Rencontres de Physique de la Vallée d'Aoste –*
*Results and Perspectives in Particle Physics*
Ed.: M. Greco
La Thuile, Aosta Valley, March 9–15, 2003
ISBN—88–86409–39–9

**Volume XXXI**
*Frontier Science 2002 – Charm, Beauty and CP,*
*First International Workshop on Frontier Science*
Eds.: L. Benussi, R. de Sangro, F.L. Fabbri, P. Valente
Frascati, October 6–11, 2002
ISBN—88–86409–37–0

**Volume XXXII**
*19th International Conference on x–ray and Inner–Shell Processes*
Eds.: A. Bianconi, A. Marcelli, N.L. Saini
Universitá di Roma La Sapienza June 24–28, 2002
ISBN—88–86409–39–07

**Volume XXXIII**
*Bruno Touschek Memorial Lectures*
Ed.: M. Greco, G. Pancheri
Frascati, May 11, 1987
ISBN—88–86409–40–0

**Volume XXXIV – Special Issue**
*Les Rencontres de Physique de la Vallée d'Aoste –*
*Results and Perspectives in Particle Physics*
Ed.: M. Greco
La Thuile, Aosta Valley, February 29 – March 6, 2004
ISBN—88–86409–42–7

**Volume XXXV**
*Heavy Quarks And Leptons 2004*
Ed.: A. López
San Juan, Puerto Rico, 1–5 June 2004
ISBN—88–86409–43–5

**Volume XXXVI**
*DAΦNE 2004: Physics At Meson Factories*
Eds.: F. Anulli, M. Bertani, G. Capon, C. Curceanu–Petrascu,
F.L. Fabbri, S. Miscetti
Frascati, June 7–11, 2004
ISBN—88–86409–53–2

**Volume XXXVII**
*Frontier Science 2004, Physics and Astrophysics in Space*
Eds.: A. Morselli, P. Picozza, M. Ricci
Frascati, 14–19 June, 2004
ISBN—88–86409–52–4

**Volume XXXVIII**
*II Workshop Italiano sulla Fisica di ATLAS e CMS*
Eds.: Gianpaolo Carlino and Pierluigi Paolucci
Napoli, October 13 – 15, 2004
ISBN—88–86409–44–3

**Volume XXXIX – Special Issue**
*Les Rencontres de Physique de la Vallée d'Aoste –*
*Results and Perspectives in Particle Physics*
Ed.: M. Greco
La Thuile, Aosta Valley, February 27 – March 5, 2005
ISBN—88–86409–45–1

**Volume XL**
*Frontier Science 2005 – New Frontiers in Subnuclear Physics*
Eds.: A. Pullia, M. Paganoni
Milano, September 12 - 17, 2005
ISBN—88–86409–46–X

**Volume XLI**
*Discoveries in Flavour Physics at $e^+e^-$ Colliders*
Eds.: L. Benussi, S. Bianco, C. Bloise, R. de Sangro, C. Gatti,
G. Isidori, M. Martini, F. Mescia, S. Miscetti
Frascati, February 28th - March 3rd, 2006
ISBN—88–86409–51–6

**Volume XLII – Special Issue**
*Les Rencontres de Physique de la Vallée d'Aoste –*
*Results and Perspectives in Particle Physics*
Ed.: M. Greco
La Thuile, Aosta Valley, March 5 March 11, 2006
ISBN—88–86409–47–8

**Volume XLIII – Special Issue**
*Neutral Kaon Interferometry at A Phi-Factory: from Quantum Mechanics to Quantum Gravity*
Ed.: A. Di Domenico
Frascati, March 24th 2006
ISBN 978—88–86409–50–8

**Volume XLIV– Special Issue**
*Les Rencontres de Physique de la Vallée d'Aoste –*
*Results and Perspectives in Particle Physics*
Ed.: M. Greco
La Thuile, Aosta Valley, February 28, 2 March 5, 2007
ISBN 978—88–86409–49–4

**Volume XLV** *Frontier Science – Science with the New Generation*
*High Energy Gamma-ray Experiments*
Eds.: A. Lionetto, A. Morselli
Villa Mondragone, Monteporzio, Italy, June 18 -20, 2007
ISBN–978—88–86409–54–0

**Volume XLVI**
*XII International Conference on Hadron Spectroscopy*
Eds.: L. Benussi, M. Bertani, S. Bianco, C. Bloise, R. de Sangro, P. de Simone, P. di Nezza, P. Giannotti, S. Giovanella, M.P. Lombardo, S. Pacetti
Laboratori Nazionali di Frascati, October 713, 2007
ISBN—978–88–86409–55–1

**Volume XLVII – Special Issue**
*Les Rencontres de Physique de la Vallée d'Aoste –*
*Results and Perspectives in Particle Physics*
Ed.: M. Greco
La Thuile, Aosta Valley, February 24, 2 March $1^{st}$, 2008
ISBN 978–88–86409–56–8

**Volume XLVIII**
*The XIV LNF Spring School "Bruno Touschek" in Nuclear, Subnuclear and Astroparticle Physics*
*Young Researchers Workshop "Physics Challenges in the LHC Era"*
Ed. E. Nardi
Laboratori Nazionali di Frascati, Frascati, May 11th - May 14th, 2009
ISBN 978–88–86409–57-5

**Volume XLIX**
*Workshop on Monte Carlo's, Physics and Simulations at the LHC*
Ed. P. Nason
Laboratori Nazionali di Frascati, Frascati, February 27-28, 2006
ISBN 978–88–86409–58-2

**Volume L – Special Issue**
*Les Rencontres de Physique de la Vallée d'Aoste – Results and Perspectives in Particle Physics*
Ed.: M. Greco
La Thuile, Aosta Valley, March 1 7, 2009
ISBN 978–88–7438–053–4

**FRASCATI PHYSICS SERIES VOLUMES – Italian Collection**

*Collana: Scienza Aperta Vol. I (2006) - ComunicareFisica2005*
Atti 1 Convegno "Comunicare Fisica e altre Scienze",
Frascati, 24-27 Ottobre, 2005
Eds: Franco L. Fabbri, Piero Patteri
ISBN – 88-86-409-48-6